Reaching top precision in top quark property measurements using the ATLAS detector

—

Marco Vanadia,
on behalf of the ATLAS collaboration
CERN LHC SEMINAR 1/10/2019

Outline

- Brief introduction on top physics
- Reconstruction of top events in the ATLAS detector
- Measurement of the ttbar production cross-section and lepton differential distributions in eμ dilepton events from pp collisions at $\sqrt{s}$=13 TeV with the ATLAS detector ATLAS-CONF-2019-041
- Measurement of the top quark mass using a dileptonic invariant mass in pp collisions at $\sqrt{s} = 13$ TeV with the ATLAS detector ATLAS-CONF-2019-046
- Inclusive and differential measurement of the charge asymmetry in ttbar events at 13 TeV with the ATLAS detector ATLAS-CONF-2019-026

Physics of the top quark

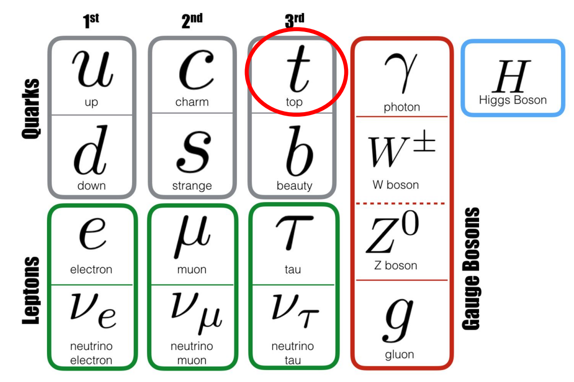

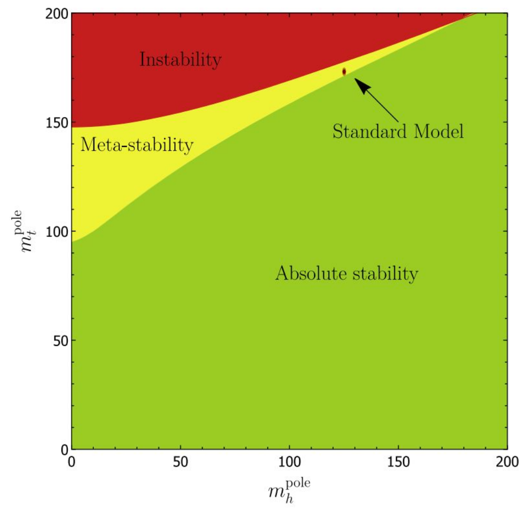

- <u>Heaviest</u> elementary particle in the SM
  - $m_t \sim 173$ GeV
- High mass → special properties
  - only quark decaying before hadronization
  - m_t crucial input for EW precision tests
- Special interplay with the <u>Higgs boson</u>
  - Yukawa coupling O(1)
  - naturalness, vacuum stability, quartic coupling…
- <u>Cosmological</u> consequences
  - e.g. Universe lifetime, see [PhysRevD.97.056006]
- <u>Challenging</u> for experiments AND theory
- Top physics → new physics?

Top pairs production at hadron colliders

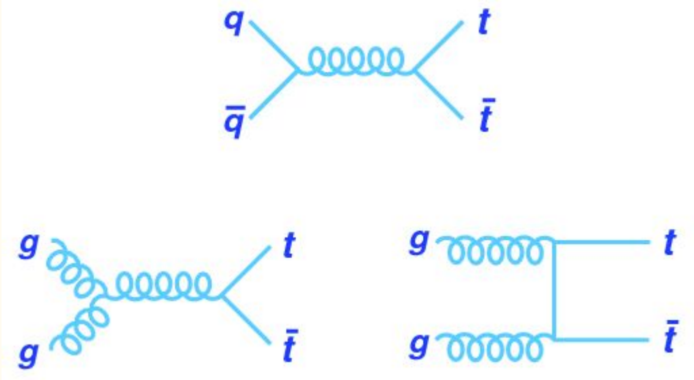

- Production at Tevatron
  - 90% qqbar, σ(ppbar→ttbar @ 1.96 TeV)~7 pb
- Production at LHC
  - 90% gg, σ(pp→ttbar @ 13 TeV)~830 pb
  - $O(10^{34} cm^{-2} s^{-1}) \rightarrow O(10$ ttbar/s)

pile-up

- Decay: t→Wb

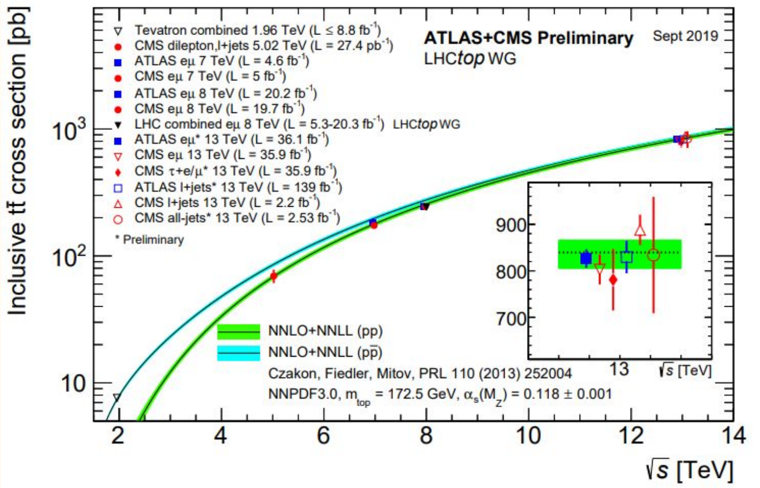

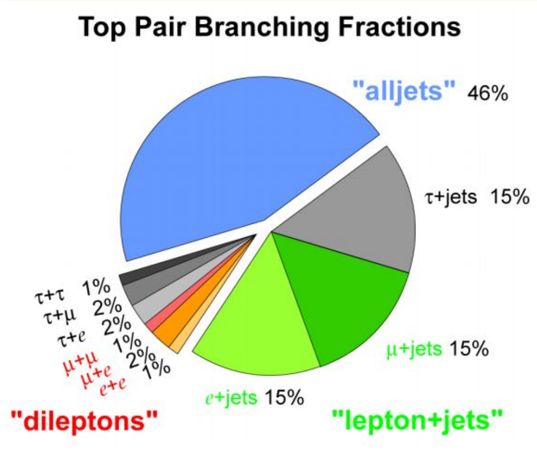

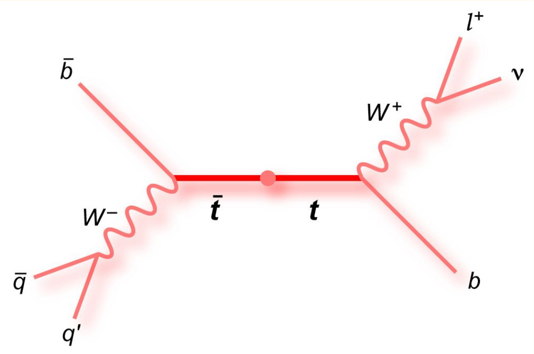

Diagram of a l+jets decay

The ATLAS detector

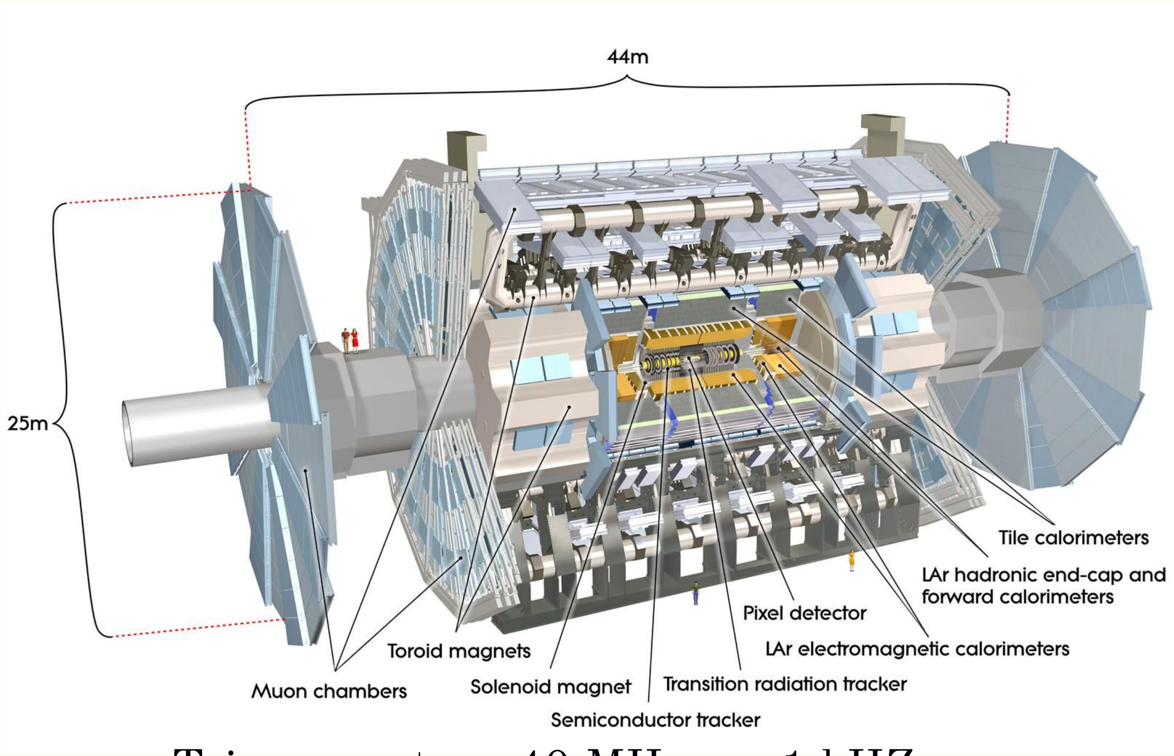

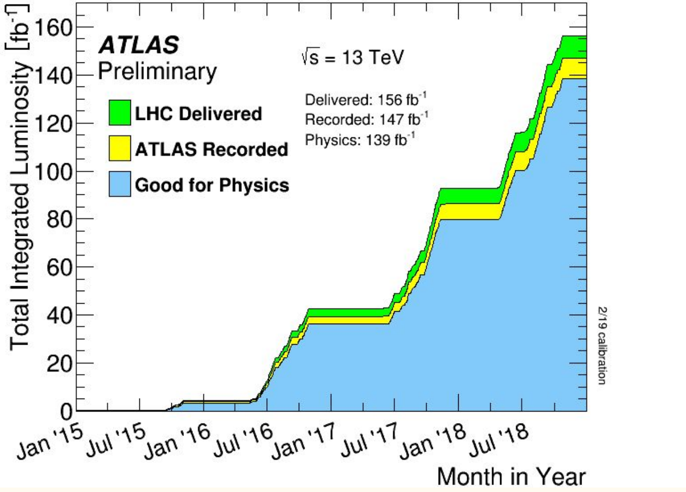

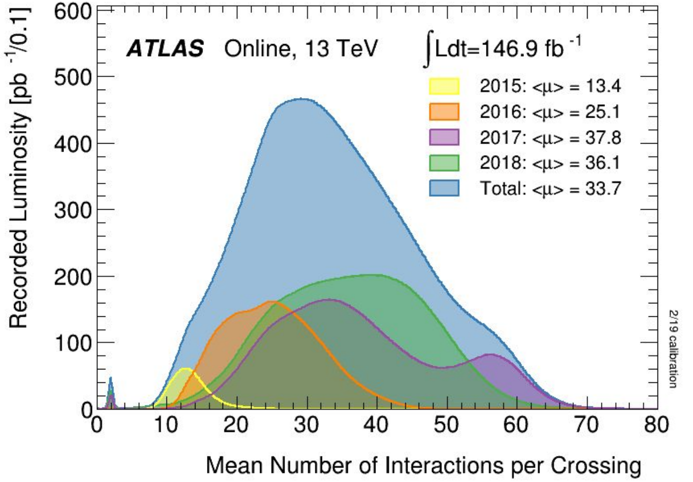

Trigger system: 40 MHz → ~1 kHZ

~139/fb of 13 TeV data available for analyses,
~1.7% uncertainty on luminosity ATLAS-CONF-2019-021

ttbar events in the ATLAS detector: jets

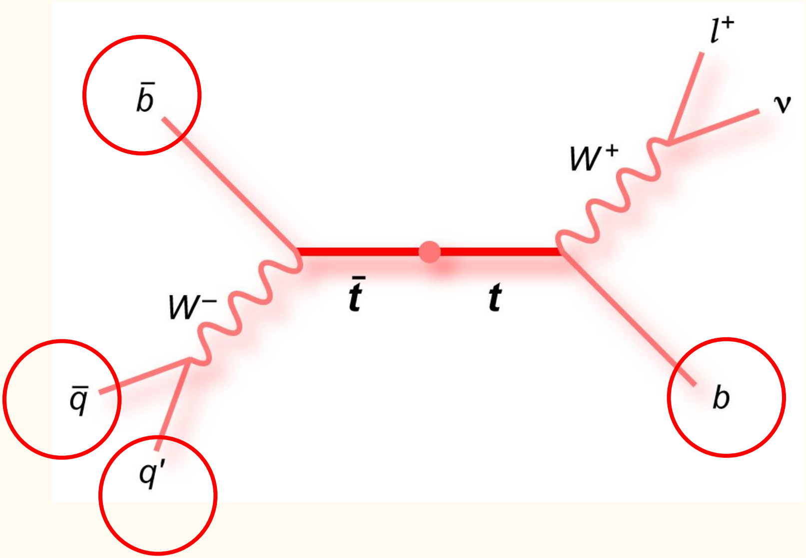

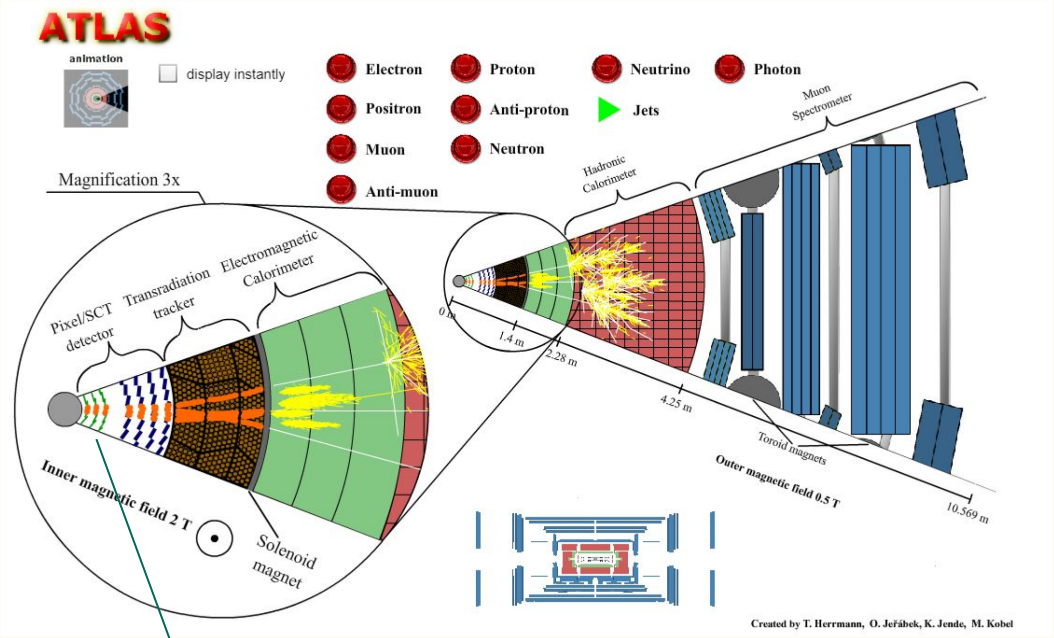

Signature: shower of hadrons in Inner Detector + Calorimeters (+ Muon Spectrometer punch-through…)

b-jet tagging: secondary vertices, impact parameter of tracks associated to jets…

ID is crucial, in run-2 added Inner B-layer @ 3.3 cm from beams

Jet reconstruction in ATLAS

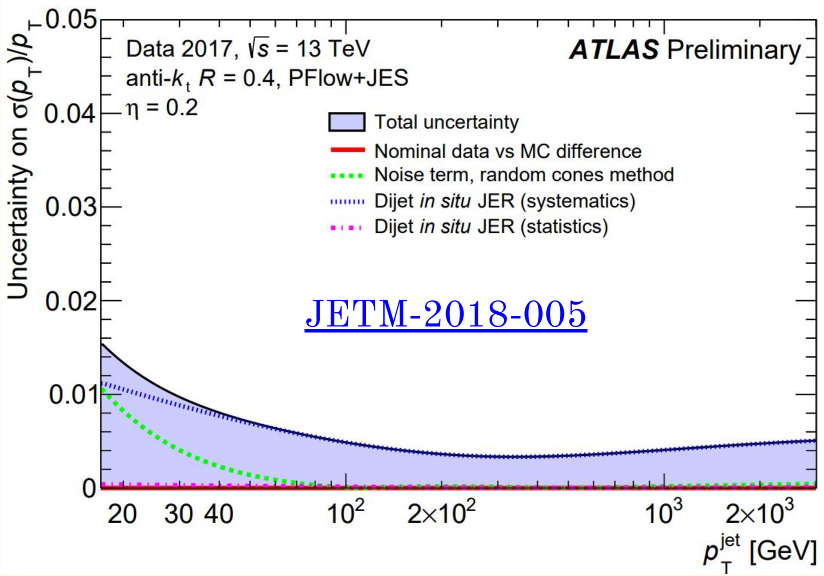

boosted objects →

overlapping jets →

R=1.0 "Large" jets

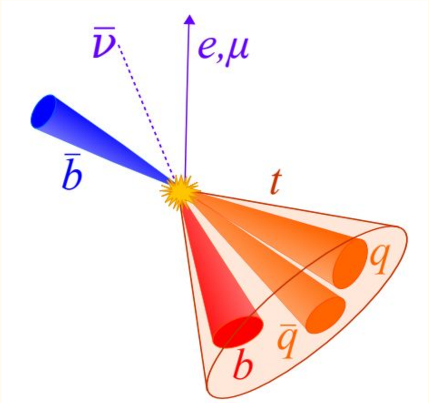

Hadronic jets:

1-4%-level unc. on jet energy scale (JES)

1-2%-level resolution (JER)

1%-level uncertainty on JER

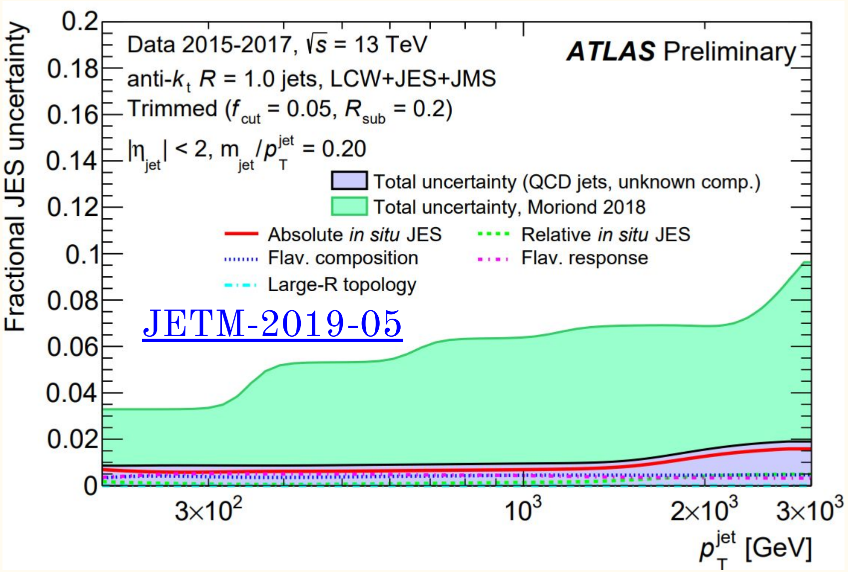

b-jet identification in ATLAS

b→μ+X decays can also be used, see later in the talk

- Low-level taggers: secondary vert., impact parameter of tracks, kinematics...
- Several low-level taggers → (multivariate/neural network) → high-level taggers
- Performance calibrated in data
- E.g. MV2c10 working point with 70% efficiency on b-jets
    - rejection of factor 12 for c-jets, ~400 for light/gluon-jets

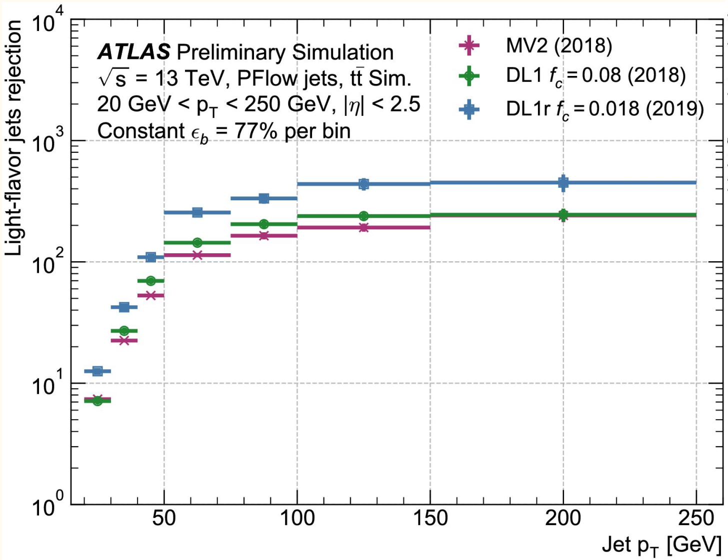

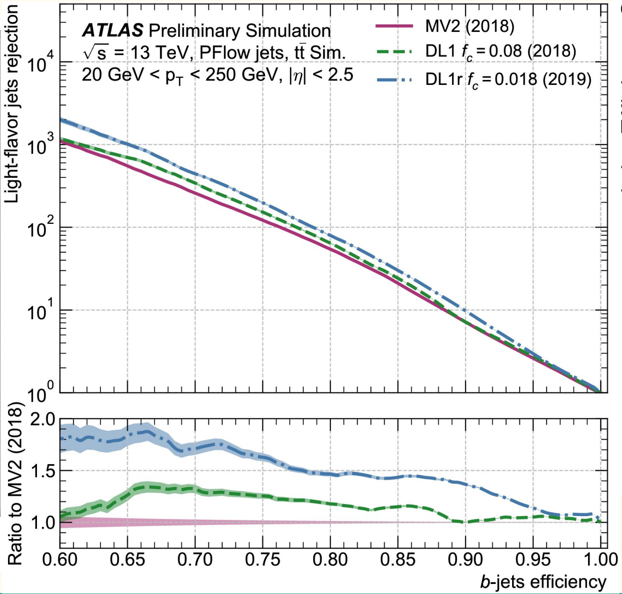

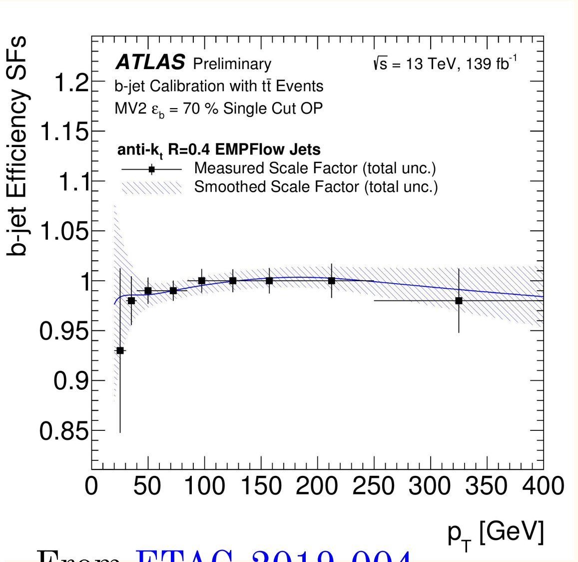

From FTAG-2019-004 and FTAG-2019-005

ttbar events in the ATLAS detector: e/μ

used also for trigger

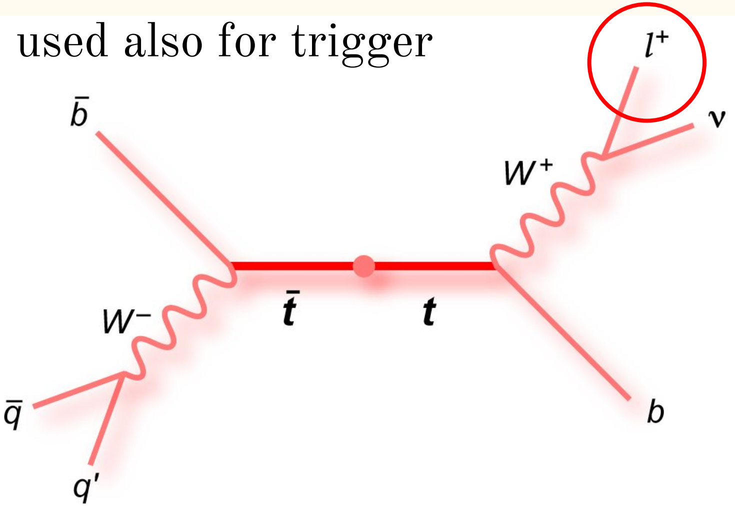

e

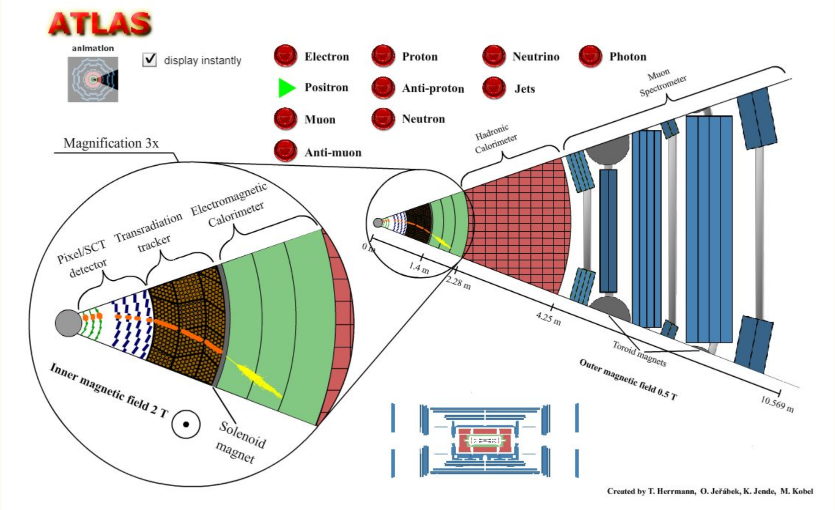

μ

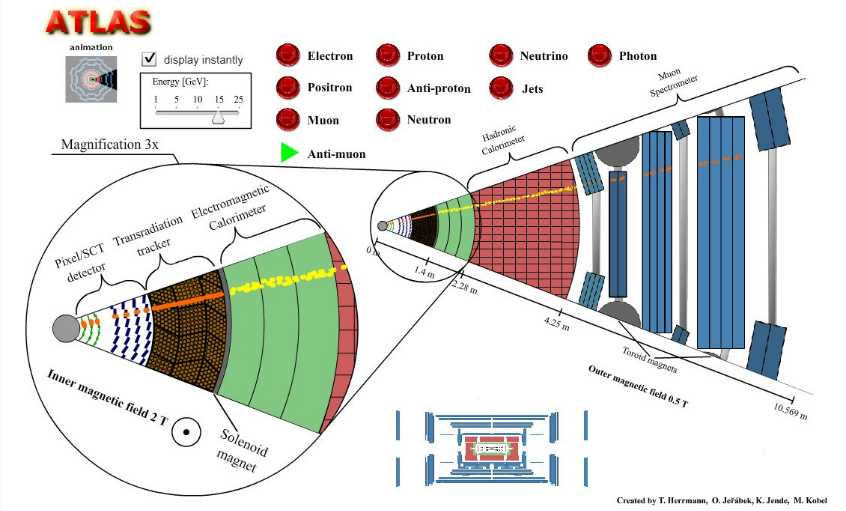

Signature: isolated track in Inner Detector + deposits in Calorimeters (e) or track in Muon Spectrometer (μ)

Reconstructed with high efficiency and O(1%)-level resolution

ttbar events in the ATLAS detector: ν

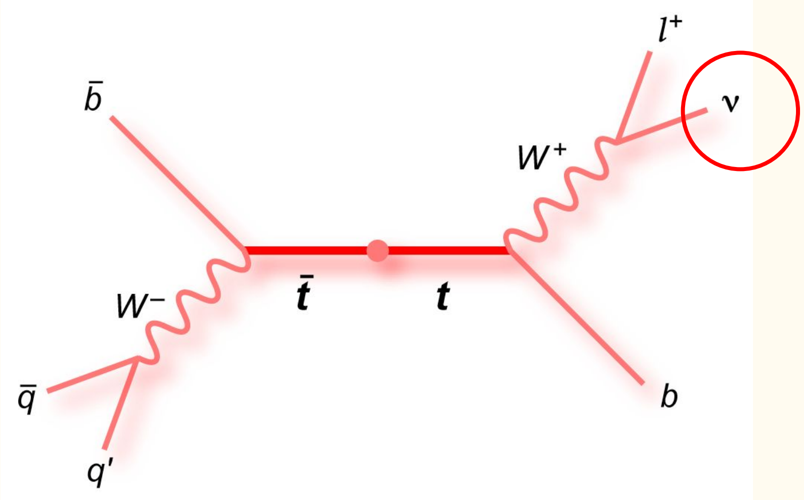

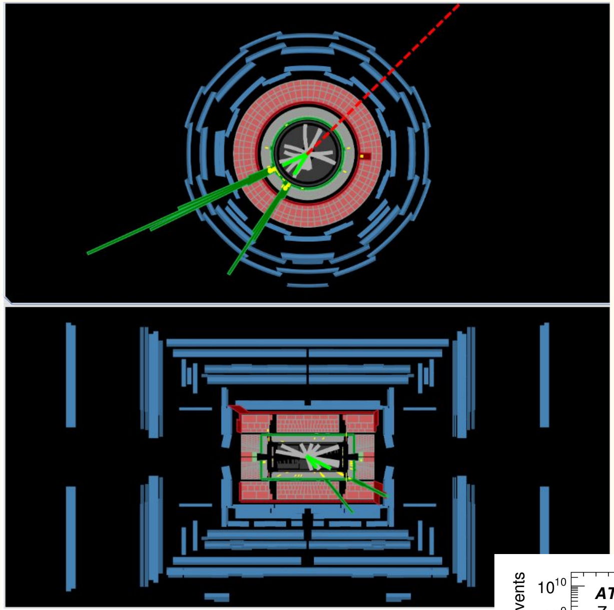

Signature: transverse momentum imbalance

pp collisions

$$\mathbf{E}_{\mathrm{T}}^{\mathrm{miss}} = - \sum \mathbf{p}_{\mathrm{T}}^{e} - \sum \mathbf{p}_{\mathrm{T}}^{\gamma} - \sum \mathbf{p}_{\mathrm{T}}^{\tau_{\mathrm{had}}} - \sum \mathbf{p}_{\mathrm{T}}^{\mu} - \sum \mathbf{p}_{\mathrm{T}}^{\mathrm{jet}} - \sum \mathbf{p}_{\mathrm{T}}^{\mathrm{track}}$$

Eur. Phys. J. C (2018) 78: 903

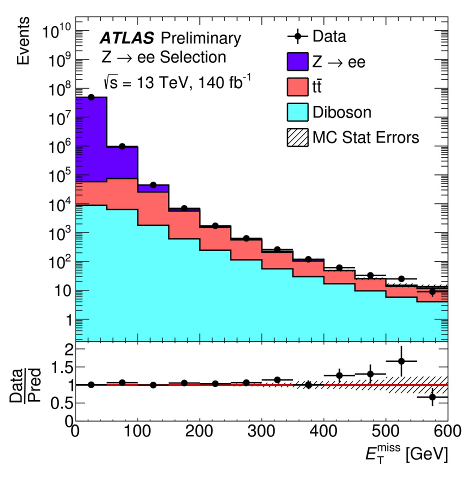

ttbar cross section measurement in dilepton events with Run-2 data ATLAS-CONF-2019-041

36/fb @ 13 TeV

Measuring σ(ttbar): motivations

NNLO+NNLL σ(pp→ttbar @ 13 TeV)=

$$832 \pm 35^{+20}_{-29}\,\mathrm{pb}$$ [Top++ 2.0]

$m_t = 172.5$ GeV

PDF + α_s uncertainty

QCD scale variations

- Test of predictions (5.5% uncertainty!)
  - $R^{tt}_{13/7}$=σ(tt @ 13 TeV)/σ(tt @ 7 TeV), double ratios vs Z+jets → reduced uncertainties (theor. and exp.)
- Sensitive to top mass: 2.7% change for 1 GeV shift on m_t^{pole}
- Differential: do we describe top quark kinematics well?

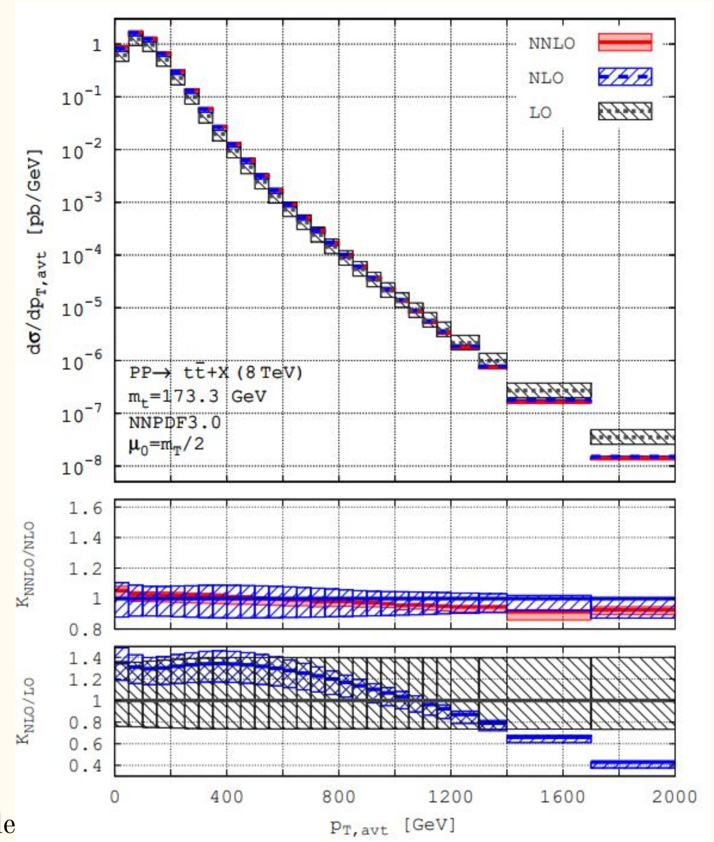

dσ(ttbar)/dp_T^{top} @ 8 TeV from [JHEP04(2017)071]

Measuring σ(ttbar): selection

- OR of single e and μ triggers
- One isolated e and one isolated μ
  - $p_T > 20$ GeV
  - opposite charge used for main analysis
- anti-k_t $R=0.4$ jets
  - $p_T > 25$ GeV and $|\eta| < 2.5$
- MV2c10 tagging @ 70% ε_b
  - events classified depending on $N_{b\text{-tag}}$

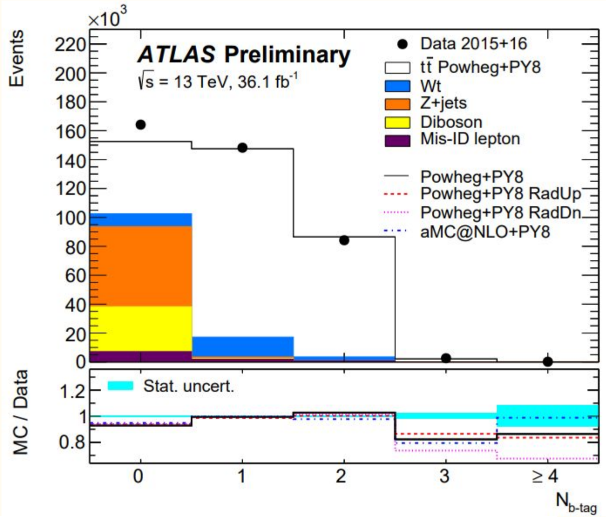

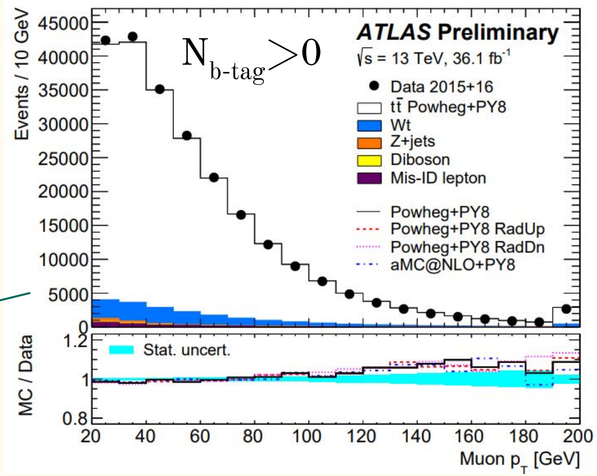

MC harder than data in lepton p_T

Measuring σ(ttbar): the idea

$\varepsilon_{e\mu}$: efficiency for ttbar event to pass Opposite Sign dilepton selection ~0.9%

N_i:
events with 1/2 b-tagged jets (measured)

$$N_1 = L\sigma_{t\bar{t}}\epsilon_{e\mu}2\epsilon_b(1 - C_b\epsilon_b) + N_1^{bkg}$$
$$N_2 = L\sigma_{t\bar{t}}\epsilon_{e\mu}C_b\epsilon_b^2 + N_2^{bkg}$$

ε_b: b-tagging efficiency x acceptance

C_b: correlation correction on b-tagging 2 jets ~1.007

σ_{ttbar} and ε_b are measured in data using these equations

Measuring σ(ttbar): backgrounds

- Wt, dominant bkg, MC
- Z+jets, MC with data-driven normalization from Z→ee/μμ+1/2 b-jets
- Diboson, MC
- Bkg with mis-id lepton from Same-Sign events

Sample	2015		2016	
Event counts	N_1	N_2	N_1	N_2
Data	14239	8351	133977	75853
Wt single top	1329 ± 92	261 ± 86	12490 ± 870	2430 ± 810
$Z(\to \tau\tau \to e\mu)$+jets	123 ± 15	7 ± 2	910 ± 110	37 ± 9
Diboson	42 ± 5	1 ± 0	481 ± 58	21 ± 7
Misidentified leptons	164 ± 54	58 ± 37	1720 ± 520	670 ± 390
Total background	1660 ± 110	327 ± 94	15600 ± 1000	3160 ± 890

$$N_j^{\text{mis-id}} = R_j(N_j^{\text{data,SS}} - N_j^{\text{sim,prompt,SS}})$$
$$R_j = \frac{N_j^{\text{sim,mis-id,OS}}}{N_j^{\text{sim,mis-id,SS}}},$$

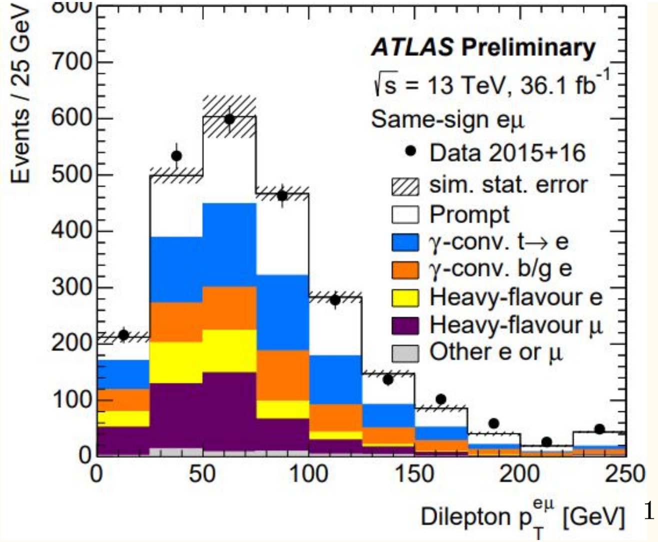

Measuring σ(ttbar): uncertainties

- Luminosity uncertainty dominating inclusive measurement
- 0.1% uncertainty on beam energy → paper
- ttbar modelling:
  - hadronisation: Powheg+Pythia8 vs Powheg+Herwig7
  - ISR/FSR: changes of μ_R, μ_F, h_{damp}, Pythia8 tune
  - generator: Powheg+Pythia8 vs aMCatNLO+Pythia8
  - PDF: 100 NNPDF variations
  - ttbar + HF: reweight MC events to match data fraction of events with $N_{b\text{-tag}}>2$

	Uncertainty source	$\Delta\sigma_{t\bar{t}}/\sigma_{t\bar{t}}$ (%)	$\Delta\sigma^{\text{fid}}_{t\bar{t}}/\sigma^{\text{fid}}_{t\bar{t}}$ (%)
	Data statistics	0.44	0.44
$t\bar{t}$ mod.	$t\bar{t}$ generator	0.43	0.10
	$t\bar{t}$ hadronisation	0.49	0.67
	Initial/final state radiation	0.45	0.41
	$t\bar{t}$ heavy-flavour production	0.26	0.26
	Parton distribution functions	0.45	0.07
	Simulation statistics	0.22	0.18
Lept.	Electron energy scale	0.06	0.06
	Electron energy resolution	0.01	0.01
	Electron identification	0.37	0.37
	Electron charge mis-id	0.10	0.10
	Electron isolation	0.24	0.24
	Muon momentum scale	0.03	0.03
	Muon momentum resolution	0.01	0.01
	Muon identification	0.30	0.30
	Muon isolation	0.18	0.18
	Lepton trigger	0.14	0.14
Jet/b	Jet energy scale	0.03	0.03
	Jet energy resolution	0.01	0.01
	Pileup jet veto	0.02	0.02
	b-tagging efficiency	0.20	0.20
	b-tag mistagging	0.06	0.06
Bkg.	Single top cross-section	0.52	0.52
	Single-top/$t\bar{t}$ interference	0.15	0.15
	Single top modelling	0.34	0.34
	Z+jets extrapolation	0.09	0.09
	Diboson cross-sections	0.02	0.02
	Diboson modelling	0.03	0.03
	Misidentified leptons	0.43	0.43
	Analysis systematics	1.39	1.31
L/E_b	Integrated luminosity	1.90	1.90
	Beam energy	0.23	0.23
	Total uncertainty	2.40	2.36

Measuring σ(ttbar): inclusive results

$$\sigma_{t\bar{t}} = 826.4 \pm 3.6 \pm 11.5 \pm 15.7 \pm 1.9 \text{ pb}$$

Total uncertainty 2.4%

data stat

syst

luminosity

beam energy

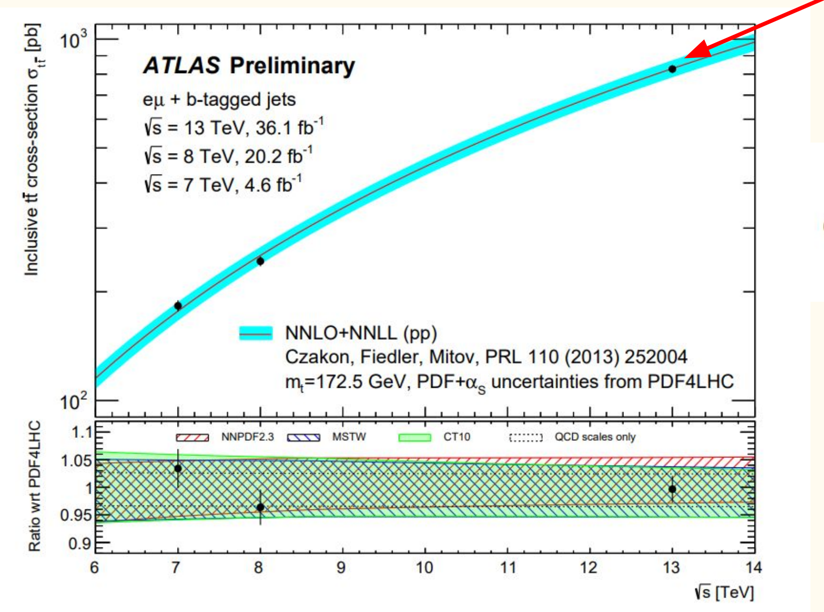

Extraction of top mass:

from here

$$\sigma_{t\bar{t}}^{\text{theo}}(m_t^{\text{pole}}) = \sigma(m_t^{\text{ref}}) \left(\frac{m_t^{\text{ref}}}{m_t^{\text{pole}}}\right)^4 (1 + a_1 x + a_2 x^2)$$

$x = (m_t^{\text{pole}} - m_t^{\text{ref}})/m_t^{\text{ref}}$

m_t^{ref}=173.3 GeV

PDF set	m_t^{pole} [GeV]
CT14	$173.1^{+2.0}_{-2.1}$
CT10	$172.1^{+2.0}_{-2.0}$
MSTW	$172.3^{+2.0}_{-2.1}$
NNPDF2.3	$173.4^{+1.9}_{-1.9}$
PDF4LHC	$172.1^{+3.1}_{-2.0}$

Uncertainty source	Δm_t^{pole} [GeV]
Experimental	1.0
PDF+α_S	$^{+1.5}_{-1.4}$
QCD scales	$^{+1.0}_{-1.5}$
Total uncertainty	$^{+2.0}_{-2.1}$

Measuring σ(ttbar): ratios

With double-ratios wrt Z+jets luminosity uncertainty cancels out

luminosity uncertainties mostly uncorrelated between run-1 and run-2

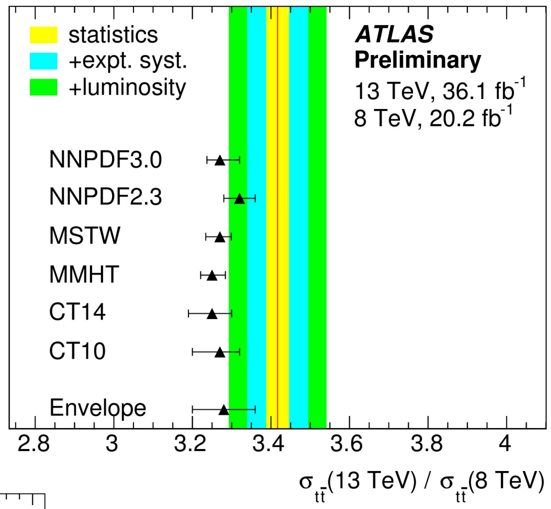

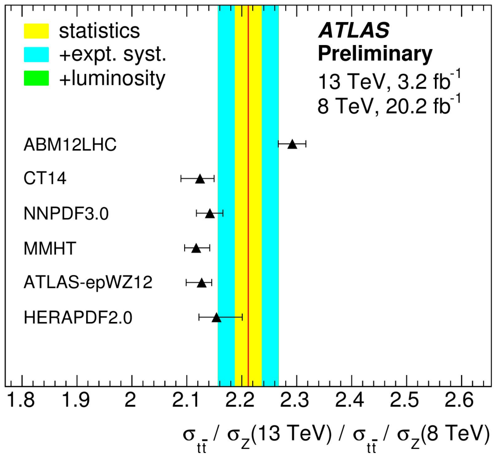

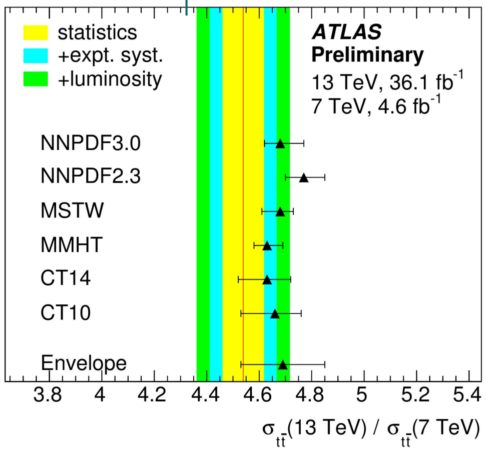

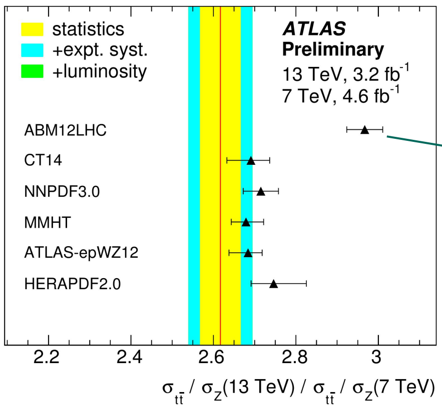

lower gluon density at high x → larger increase of σ vs √s

Measuring dσ(ttbar)/dx: results

$(1/\sigma)d\sigma/dx$ measured for:

- p_T^{ℓ}, $|\eta^{\ell}|$
- $p_T^{e\mu}$, $m^{e\mu}$, $|y^{e\mu}|$, $\Delta\phi^{e\mu}$
- $p_T^{e}+p_T^{\mu}$, $E^{e}+E^{\mu}$
- $|\eta^{\ell}|\times m^{e\mu}$, $|y^{e\mu}|\times m^{e\mu}$, $|\Delta\phi^{\ell}|\times m^{e\mu}$

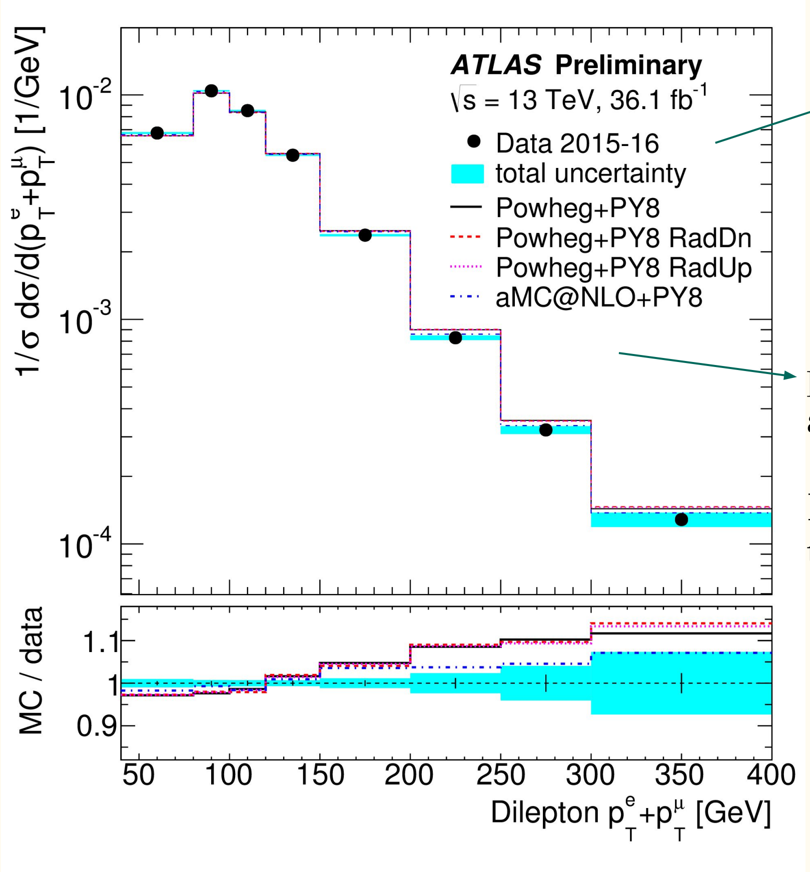

here comparing with NLO MC

$p(\chi^2)$~9% for aMCatNLO+Pythia8, 10^{-4}-10^{-5} for the Powheg+Pythia8 tunings shown in the plot

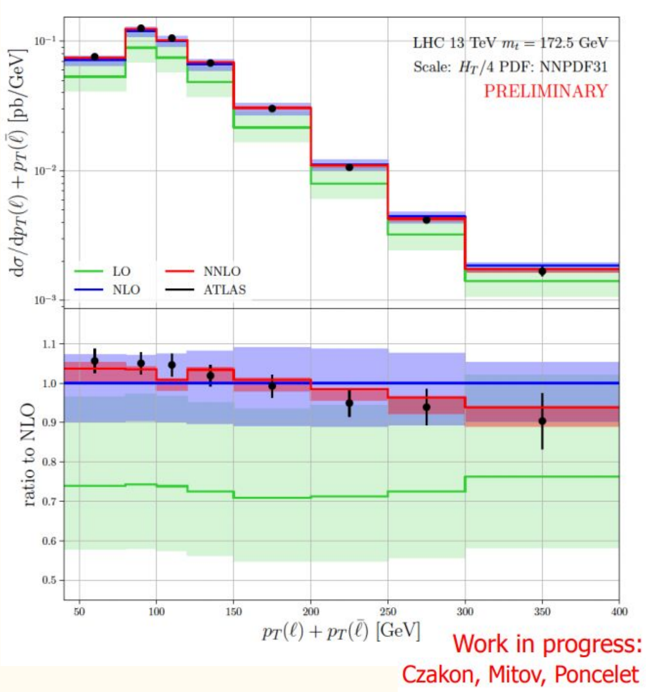

From talk @ TOP2019

Measuring dσ(ttbar)/dx: results

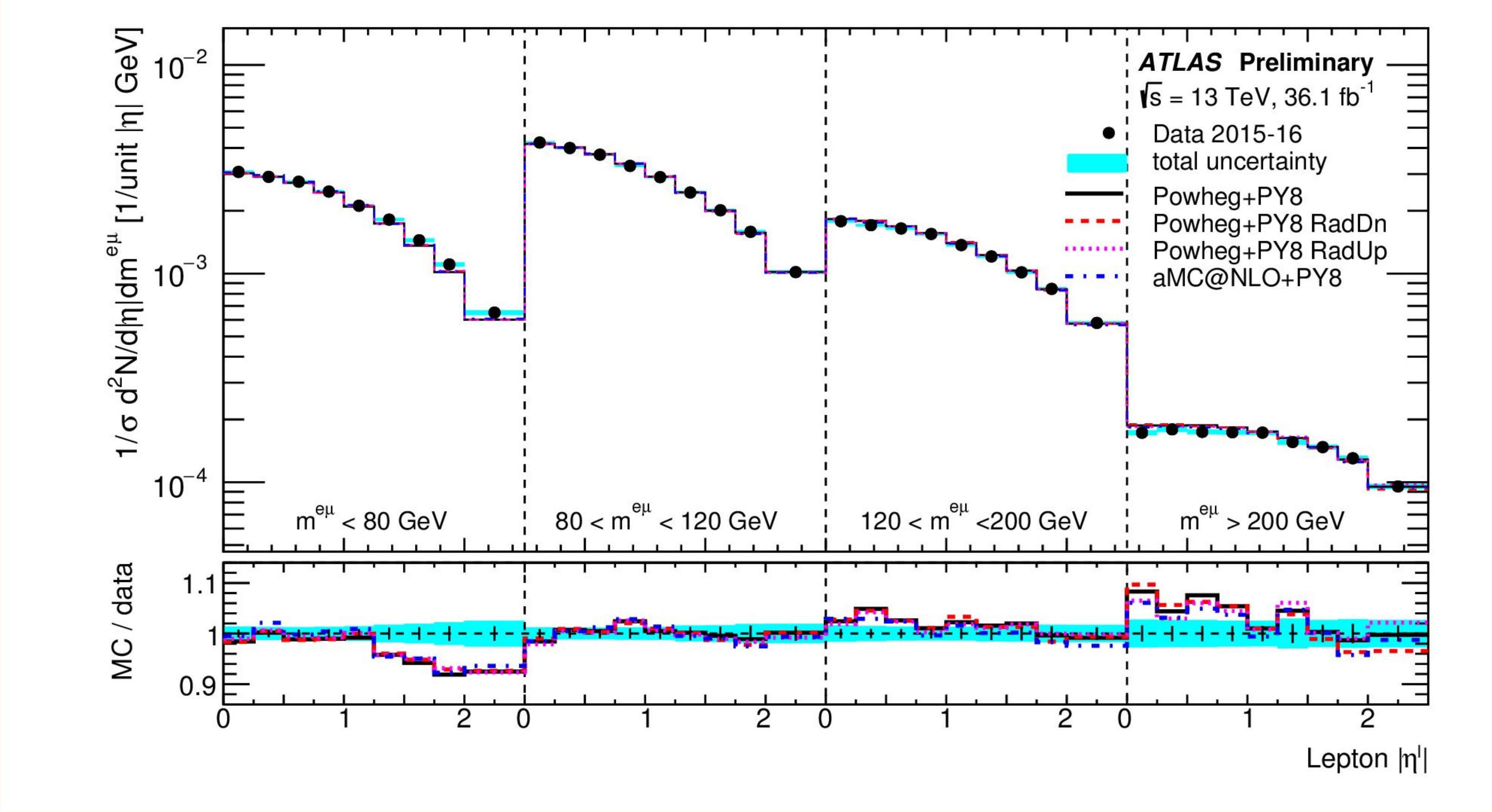

$p(\chi^2)$~2-4% for the MC generators shown in the plot

Measuring dσ (ttbar)/dx: comparing with different MC

Powheg+ various PS generators

Powheg+ Pythia8 with different amounts of radiation

Powheg+ Pythia8 with different PDF sets

aMC@NLO+ Pythia8 with different PDF sets

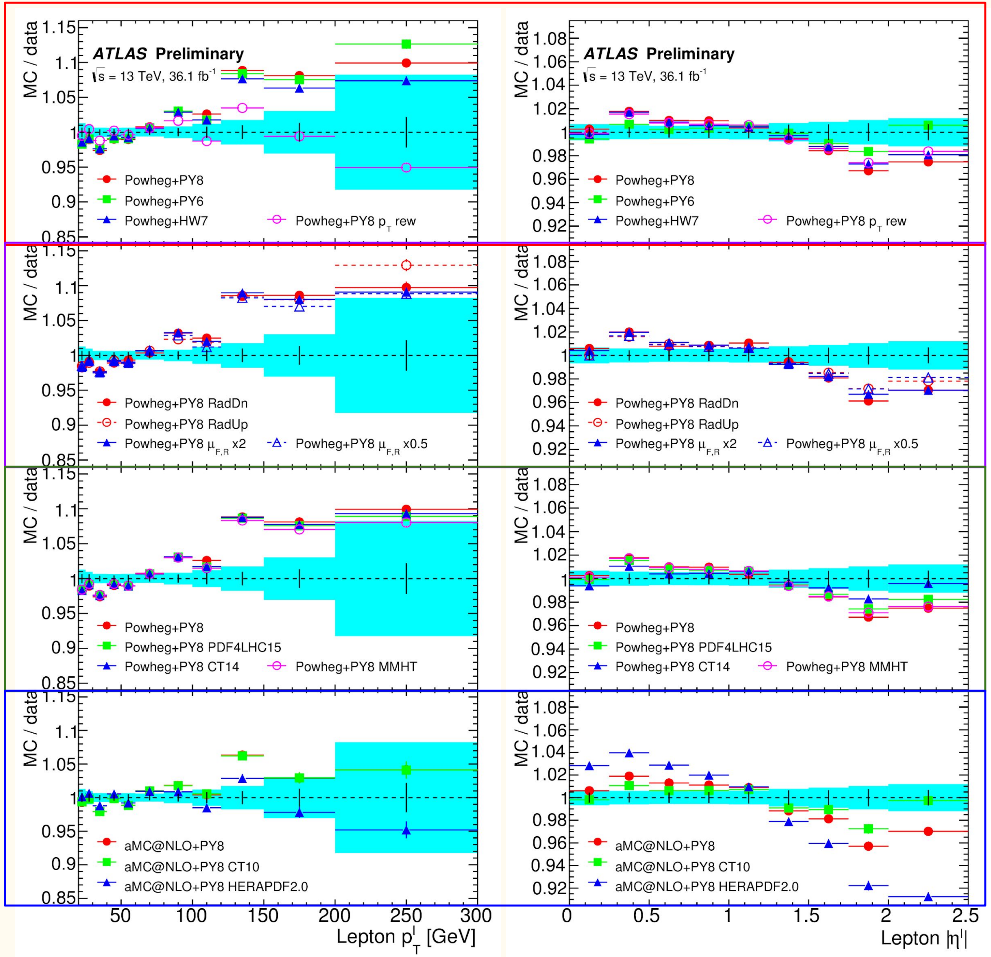

Results compared with NLO MC samples (variations in generators, tuning, PDFs)

$p(\chi^2)$~0 for describing all 1D-distributions <u>simultaneously</u> for all MC settings considered

Experimental precision at <1% level in some bins!

σ(ttbar) vs state of the art

- ATLAS, dilepton, 36/fb:
  - 2.4% unc. (8 TeV result → 3.2% uncertainty)
  - now hitting the luminosity wall...
  - also differential and double differential results
- A lot of information in ttbar σ
  - differential → inputs for modelling
  - sensitive to top mass, e.g.

    ATLAS (tt+1 jet), ATLAS (diff cross section @ 8 TeV), CMS (triple diff.), CMS (top mass running)
  - Measurement of Yukawa coupling, CMS
  - tt+V, tt+γ
- Do not forget single-top, tZq, ...

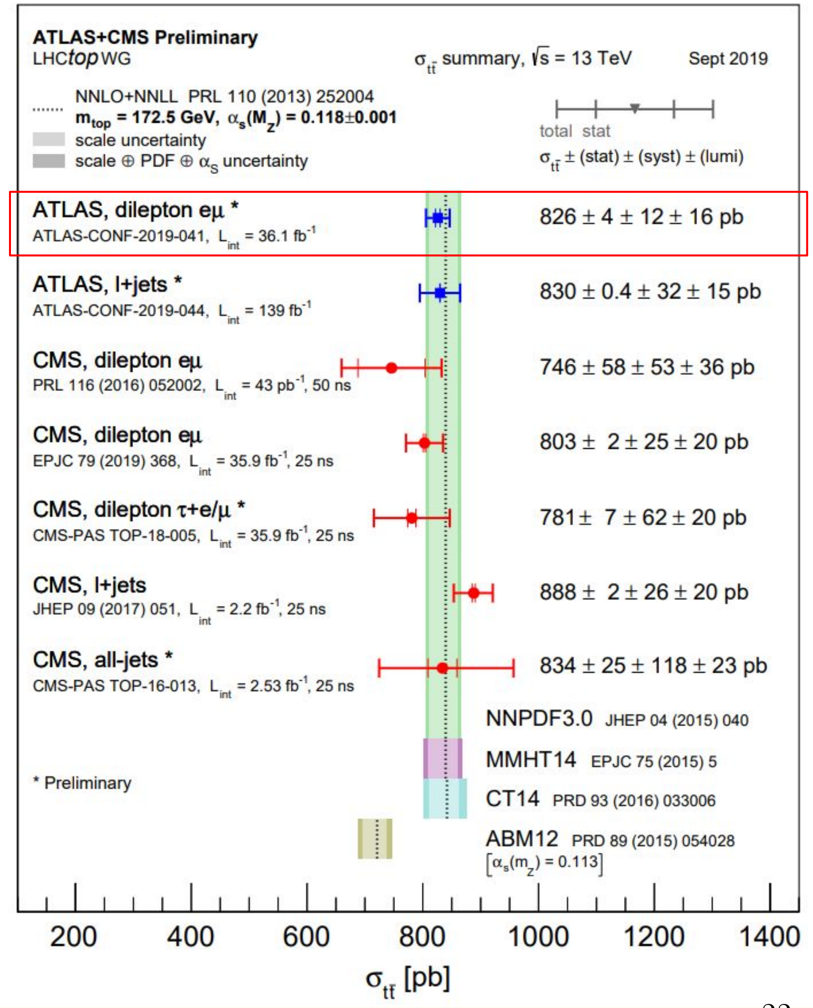

Summary of 13 TeV results from LHC

Measurement of the top quark mass using a dileptonic invariant mass in pp collisions at $\sqrt{s} = 13$ TeV with the ATLAS detector

[ATLAS-CONF-2019-046]

36/fb @ 13 TeV

Top mass: what are we measuring (and why)?

- m_t fundamental parameter of SM
  - EW precision test, Higgs interplay, vacuum stability, cosmological consequences (e.g. Higgs inflation model PRL 108 (2012) 191302) …

- Measurement from direct reconstruction:
  - decay products → m_t
  - problem: measurement of "m_t^{MC}" due to color

Scheme not well defined, e.g. due to Parton Shower

- Measurement from production properties:
  - property $f(m_t^{pole})$ (e.g. cross section) + theory → m_t(scheme)
  - but: uncertainties in fixed-order calculations due to soft radiation, NP effects, …

recent review top mass definitions

No full consensus on uncertainties on $m_t^{MC} \leftrightarrow m_t^{pole}$, ~few hundreds MeV

Top mass is not a physical mass, but a scheme dependent parameter

Top mass: the idea

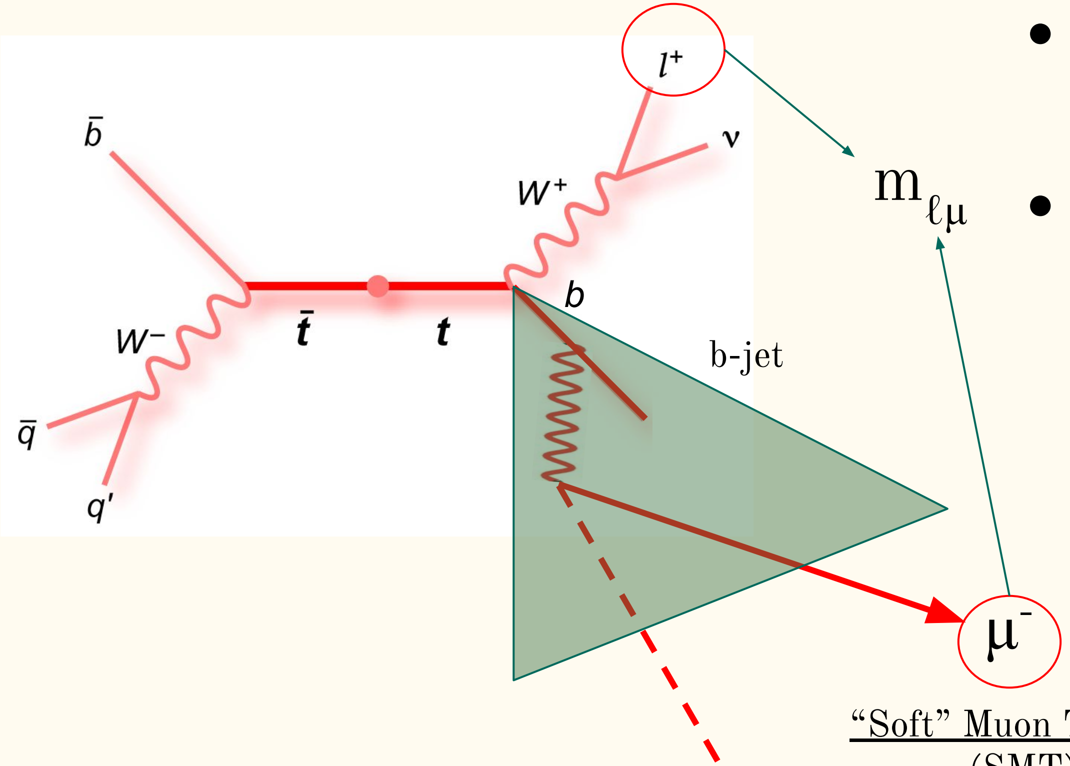

"Soft" Muon Tagging
(SMT)

- "Standard": e.g. $m_{\ell b} \to m_t$
- Here: semi-lept. decay of B-hadrons
  - BR=20% for B→...→μ+X
- Invariant mass $m_{\ell\mu} \to m_t$
  - purely leptonic,
    less sensitive to jets unc.
  - more direct impact from b→B
    fragmentation modelling

1st proof of principle: CDF Phys. Rev. D80 (2009) 051104, m_t=180.5 ± 12.5 GeV
Similar idea: with J/Ψ→μμ from CMS JHEP 12 (2016) 123, m_t=173.5 ± 3.1 GeV

Top mass: baseline selection

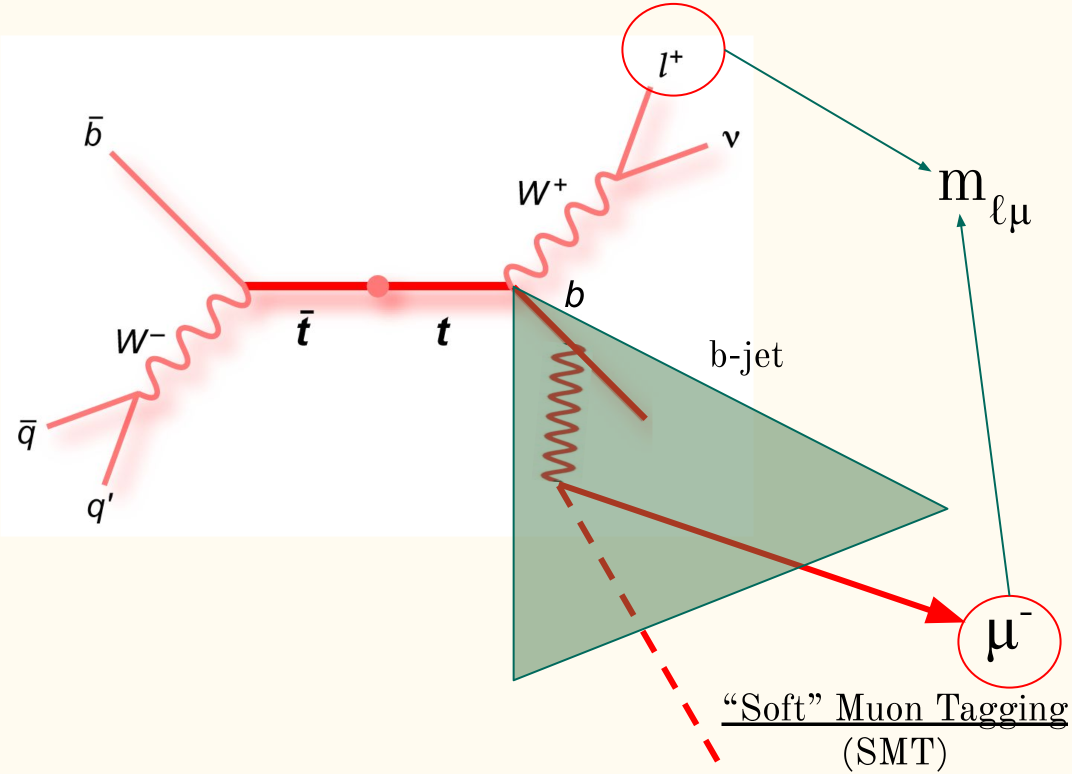

- =1 isolated e/μ
- Cuts on E_T^{miss} and M_T^W
- ≥4 jets
- ≥1 jet MV2c10 tagged
- ≥1 SMT jet
  - i.e. μ with p_T>8 GeV found within ΔR<0.4 of a jet

SMT calibrated in data:

- efficiency from $J/\Psi \to \mu\mu$
- fake rate from W+1 jet

Top mass: signal composition

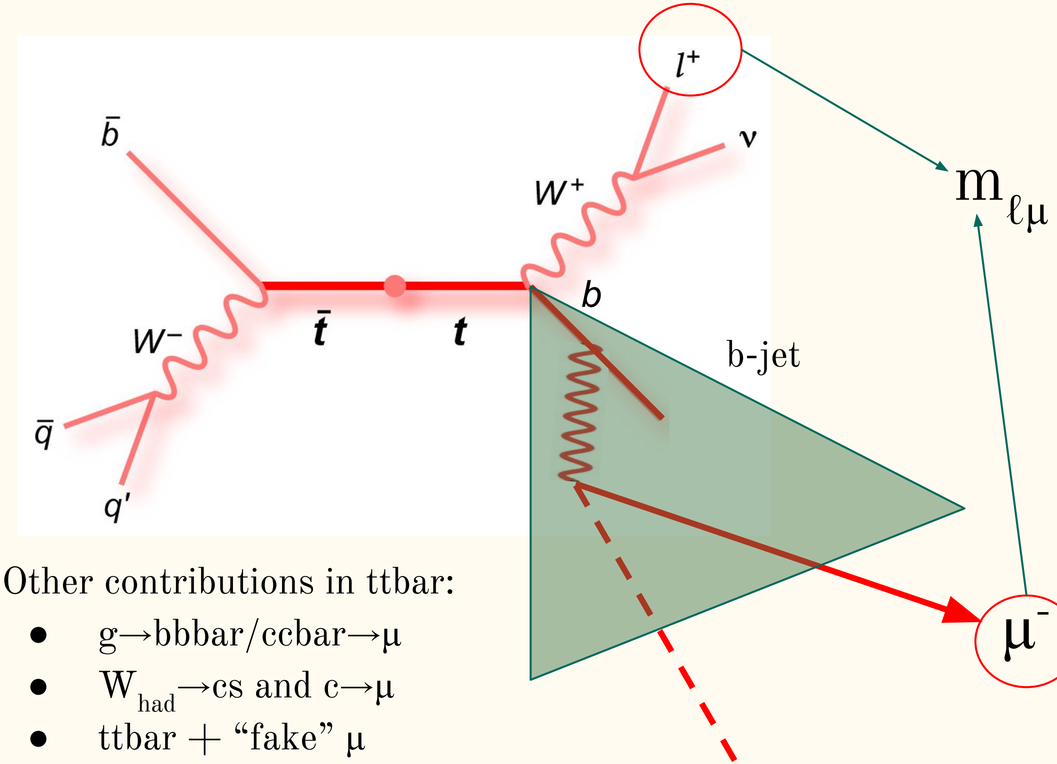

Other contributions in ttbar:

- g→bbbar/ccbar→μ
- W_{had}→cs and c→μ
- ttbar + “fake” μ (from light hadron or detector bkg.)
- dilepton ttbar, one prompt μ inside real/pile-up jet

Soft-μ in jets have different origins in ttbar:

- direct b-hadron decay: most sensitive to m_t!
- B→D→μ and B→DDbar→μ (rarer)

More sensitivity to m_t if leptons from

SAME Top→ ΔR(W-lep, soft-μ)<2

OS

($q_{lep}q_{soft\ \mu}$<0 → more direct b→μ, more same top)

SS

($q_{lep}q_{soft\ \mu}$>0 → more b→c→μ, more different top)

Top mass: signal modelling

Reweighted MC → PDG for:

- Production Fractions

  (change muon kinematics)

- inclusive BRs to μ

  (change signal composition)

Crucial to control fragmentation, i.e.

b-quark→B-hadron momentum transfer

- used Lund-Bowler model in Pythia8
- used e^+e^- data to tune r_b parameter for the standard ATLAS A14 tune

  $r_b = 0.855 \rightarrow r_b = 1.05 \pm 0.02$

Hadron	PDG (%)	Powheg+Pythia8	Scale Factor
B^0	0.404±0.006	0.429	0.941
B^+	0.404±0.006	0.429	0.942
B_s^0	0.103±0.005	0.095	1.088
b-baryon	0.088±0.012	0.047	1.874
D^+	0.226±0.008	0.290	0.780
D^0	0.564±0.015	0.553	1.020
D_s^0	0.080±0.005	0.093	0.857
c-baryon	0.109±0.009	0.038	2.898

Hadron	PDG	Powheg+Pythia8	Scale Factor
$b \rightarrow \mu$	$0.1095^{+0.0029}_{-0.0025}$	0.106	1.032
$b \rightarrow \tau$	0.0042 ± 0.0004	0.0064	0.661
$b \rightarrow c \rightarrow \mu$	0.0802 ± 0.0019	0.085	0.946
$b \rightarrow c\bar{c} \rightarrow \mu$	$0.016^{+0.003}_{-0.003}$	0.018	0.888
$c \rightarrow \mu$	0.082 ± 0.005	0.084	0.976

$z = E_{B\text{-had}}/E_{b\text{-quark}}$

$$f(z) = \frac{1}{z^{1+br_b m_b^2}}(1-z)^a \exp(-bm_T^2/z).$$

a,b fitted to data sensitive to light-quark fragmentation, universal for light/heavy quarks

Top mass: backgrounds and yields

- Multi-jet from data-driven matrix method
- W+jets from MC, normalized in data using W^+/W^- asymmetry; flavor composition also data-driven
- Z+jets from MC, validated in data
- SMT fake from MC, validated in data
- Other from MC

Process	Yield (OS)	Yield (SS)
$t\bar{t}$ (SMT from b- or c-hadron)	56 000 ± 4000	34 800 ± 2800
$t\bar{t}$ (SMT from $W \to \mu\nu$)	2190 ± 320	4.9 ± 3.6
$t\bar{t}$ (SMT fake)	1490 ± 210	1240 ± 170
Single top t-chan	770 ± 70	490 ± 40
Single top s-chan	63 ± 6	49 ± 4
Single top Wt	1840 ± 140	1260 ± 100
W+jets	1600 ± 400	1080 ± 240
Z+light jets	210 ± 80	15 ± 6
Z+HF jets	550 ± 170	310 ± 100
Diboson	17.2 ± 2.9	6.3 ± 1.4
Multi-jet	530 ± 140	480 ± 130
Total Expected	65 000 ± 5000	39 800 ± 3000
Data	66 891	42 087

Break-up of ttbar
(SMT from b- or c-hadron)

	OS [%]	SS [%]
Processes involving a μ from a t or $\bar{t}$		
$t \to B \to \mu$	73.6	51.2
$t \to B \to D \to \mu$	16.7	44.2
$t \to B \to \tau \to \mu$	2.0	1.3
$t \to B \to D \to \tau \to \mu$	0.8	0.8
Processes involving a μ not from a t or $\bar{t}$		
$B \to \mu$	0.6	0.9
$D \to \mu$	5.8	1.4
$\tau \to \mu$	0.5	0.1

Top mass: backgrounds and yields

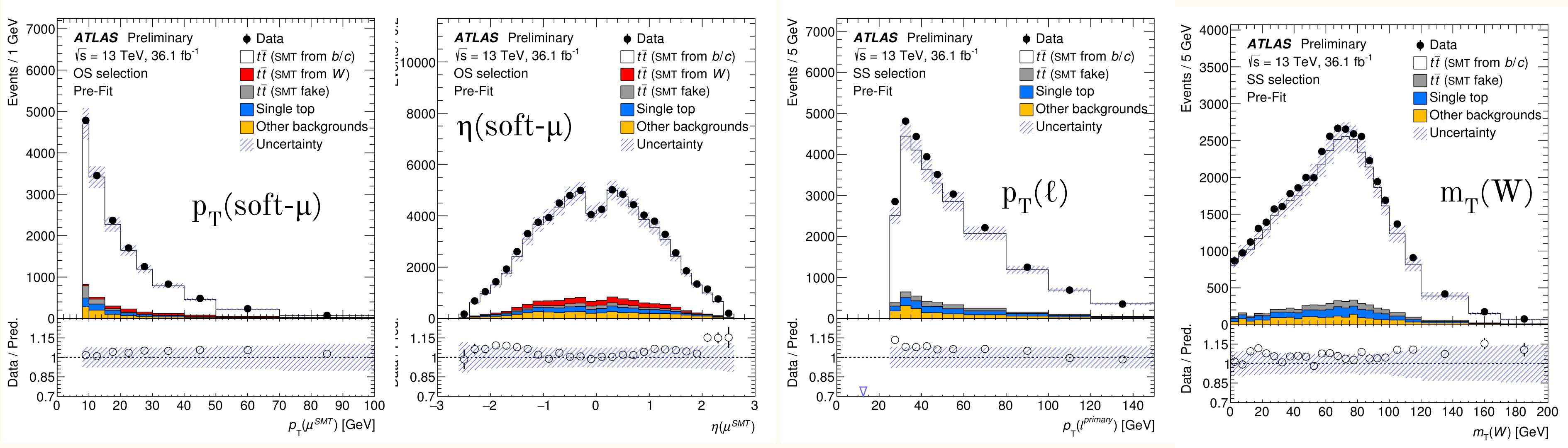

Control plots for few kinematic variables

- in the final analysis ttbar normalization fitted from data
- W-lepton p_T data/MC slope well known from many other analyses, no significant impact on m_t measurement

Top mass: extraction

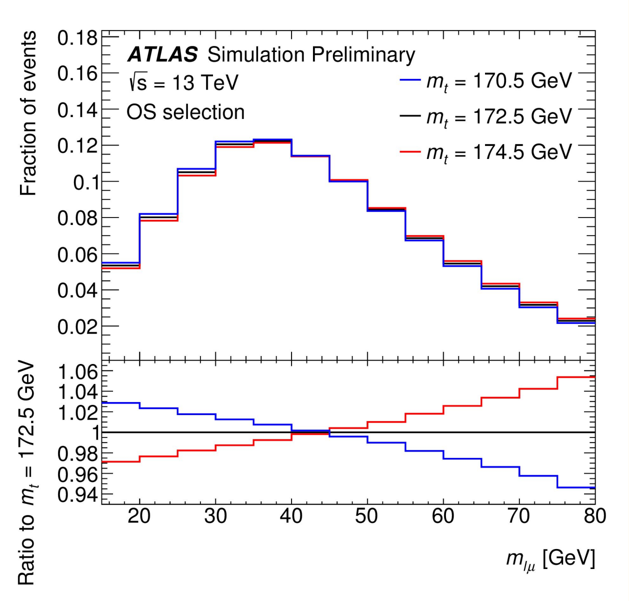

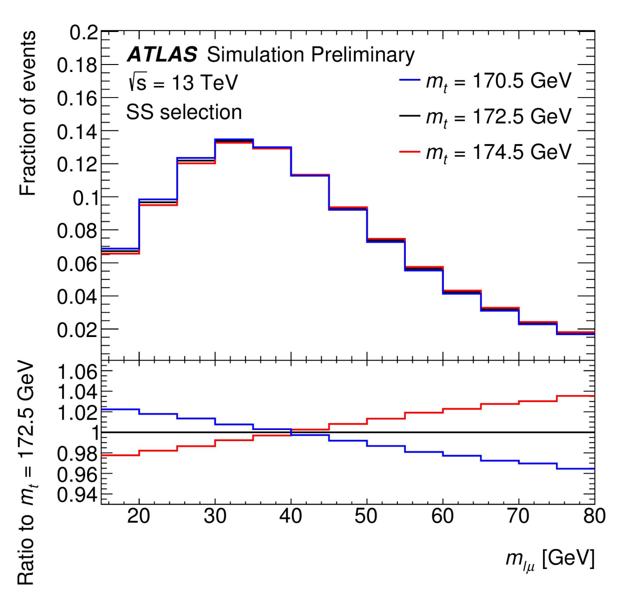

- Profiled Binned likelihood template fit in the 15-80 GeV region of $m_{\ell\mu}$
  - systematic uncertainties used as nuisance parameters
- Higher sensitivity of OS region to m_t well visible

Top mass: systematic uncertainties

- BR b→ccbar→μ
  - 20% uncertainty from direct meas.
- Pile-up
  - ttbar, Z→μμ with prompt-μ overlapping with pile-up jet
- BR b→μ: affects composition
- r_b: impacts fragmentation

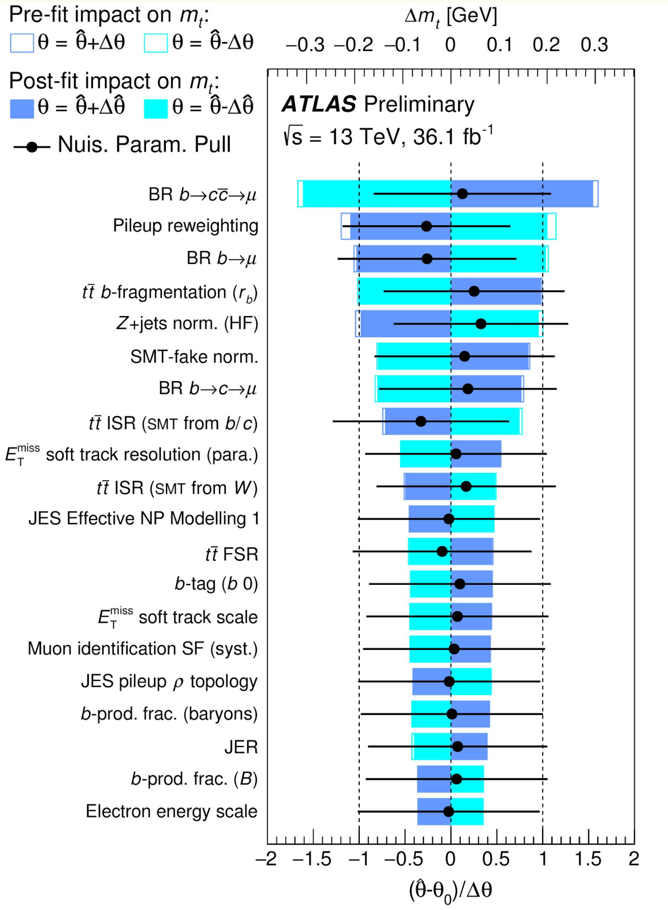

Top mass: results

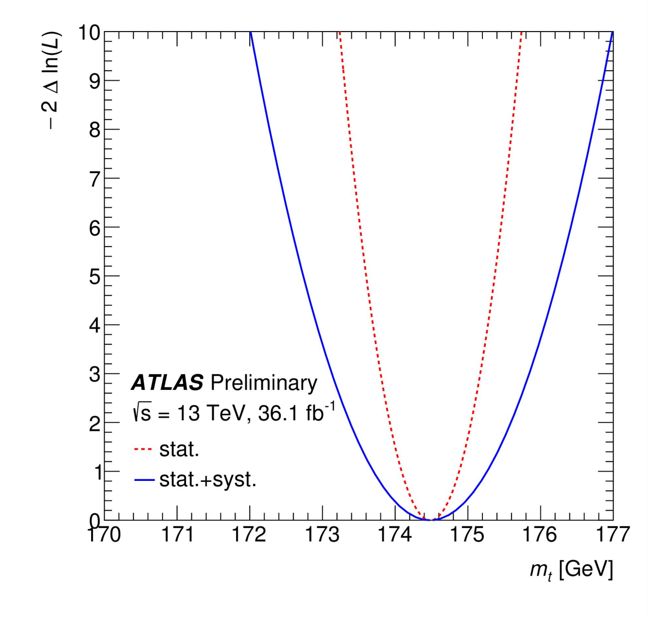

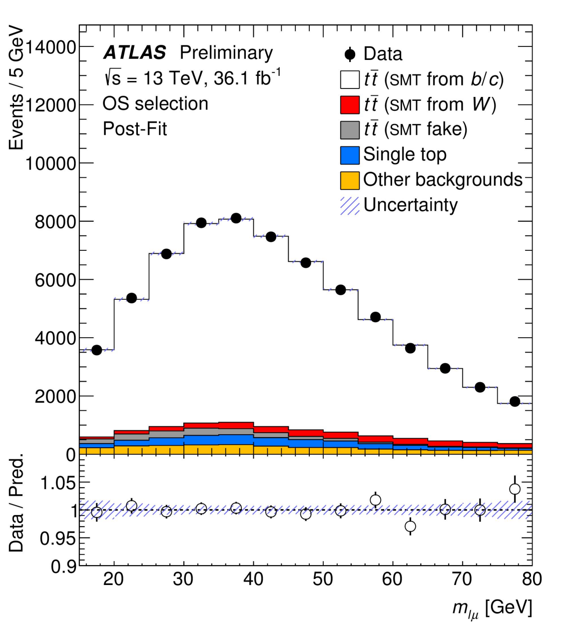

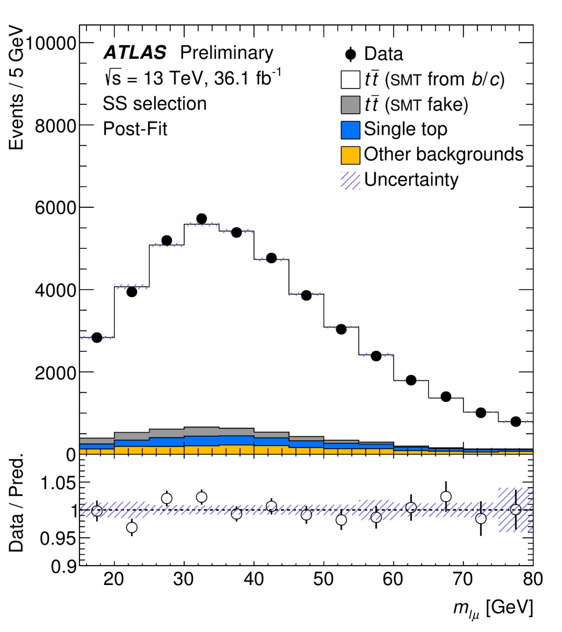

$$m_t = 174.48 \pm 0.40\,(\mathrm{stat}) \pm 0.67\,(\mathrm{syst})\ \mathrm{GeV} = 174.48 \pm 0.78\ \mathrm{GeV}$$

Precision measurement, competitive with "standard" techniques!

Top mass with SMT vs state of the art

$$m_t = 174.48 \pm 0.40\,(\text{stat}) \pm 0.67\,(\text{syst})\text{ GeV} = 174.48 \pm 0.78\text{ GeV}$$

0.45% of uncertainty
Compatibility with other ATLAS measurements at 2.2σ level, systematic uncertainties largely uncorrelated

- ATLAS
  - "standard" l+jets: 172.08 ± 0.91 GeV (0.52% unc.) [8 TeV]
    - combined: 172.69 ± 0.48 GeV (0.28% unc.) [7-8 TeV, l+jets, dilepton, all-had]
- CMS
  - "standard" l+jets: 172.35 ± 0.51 GeV (0.30% unc.) [8 TeV]
    - combined: 172.44 ± 0.49 GeV (0.28% unc.) [7-8 TeV, l+jets, dilepton, all-had]
  - "standard" l+jets: 172.25 ± 0.63 GeV (0.37% unc.) [13 TeV]
    - combined: 172.26 ± 0.61 GeV (0.35% unc.) [13 TeV, l+jets, all-had]

Top mass with SMT vs state of the art (2)

- Direct measurements are @ ~500 MeV level
  - ambiguities on m_t^{MC} definition cannot be hidden under the carpet anymore…
  - modelling uncertainties will need a rigorous, systematic approach to improve
- Non-standard techniques can be competitive
  - sensitivity to different systematics → useful in combinations,
    “independent” checks, orthogonal information on ttbar modelling
- m_t^{pole} (“indirect”) measurements also reaching impressive uncertainty
  - ATLAS results on ttbar+1 jet and from differential cross section [8 TeV]:

$$171.1 \pm 0.4\,(\text{stat}) \pm 0.9\,(\text{syst})^{+0.7}_{-0.3}\,(\text{theo})\ \text{GeV}$$

$$173.2 \pm 0.9\,(\text{stat}) \pm 0.8\,(\text{syst}) \pm 1.2\,(\text{theo})\ \text{GeV}$$

  - CMS from σ+PDF+α_s fit [13 TeV]:

$$170.5 \pm 0.7\,(\text{fit}) \pm 0.1\,(\text{model})^{+0.0}_{-0.1}\,(\text{param}) \pm 0.3\,(\text{scale})\ \text{GeV}$$

    - also direct/indirect “mixed” method, first experimental study of running of m_t, …

Inclusive and differential measurement of the charge asymmetry in ttbar events ATLAS-CONF-2019-026

139/fb @ 13 TeV

Charge asymmetry: motivation

- ttbar symmetric at LO
- higher-order → interference of *qqbar* @ LO/NLO
  - t prefers direction of q
  - small effect also from *qg*,10-20% EW contribu.
- ppbar collider → q prefers direction of p → direct measurement of A_{FB}
- LHC is *pp* → this is not possible
- BUT PDF(q) != PDF(*qbar*)

$$A_C = \frac{N(\Delta|y| > 0) - N(\Delta|y| < 0)}{N(\Delta|y| > 0) + N(\Delta|y| < 0)}$$

LHC: dominant process (90%) is gg → symmetric
asymmetry from qqbar and qg contributions diluted

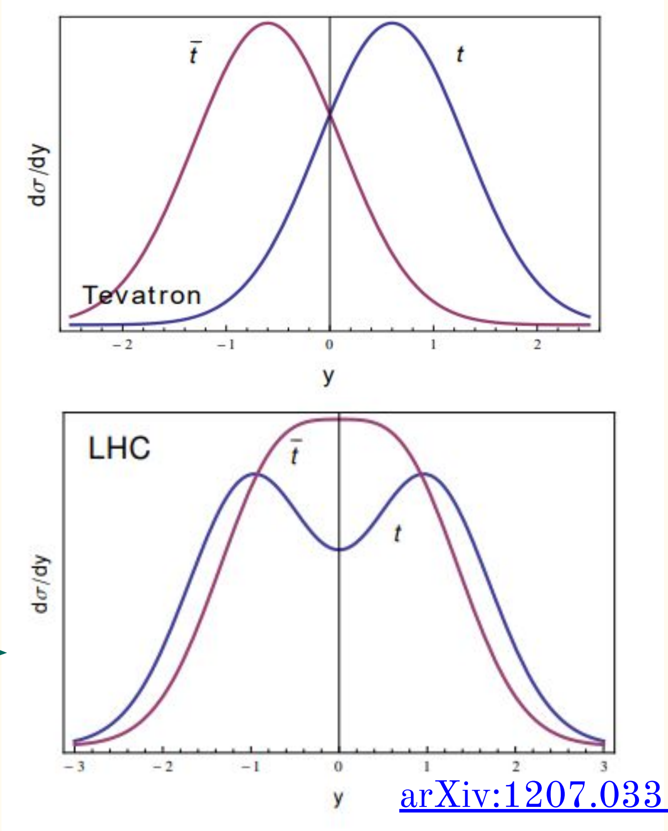

arXiv:1207.0331

BSM can alter expected A_c

Charge asymmetry: BSM effects

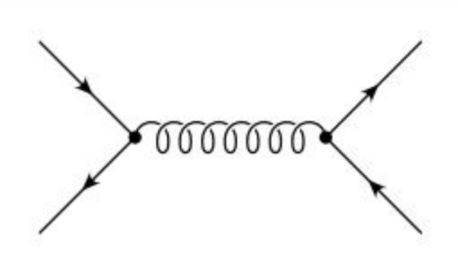

interference

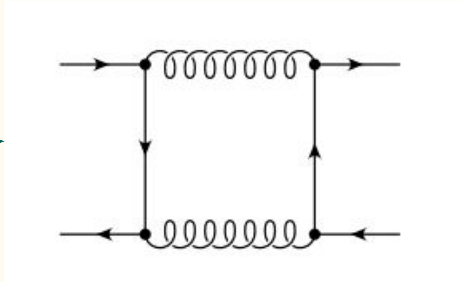

SM asymmetry
$A_c \sim 0.5\%$

New BSM particles → New amplitude terms → Changes in asymmetry

The enhancement can be more significant in <u>specific kinematic regions</u>
[PLB 707 (2012) 92]

$\beta_{ttbar,z}$ = boost of ttbar system along z-axis

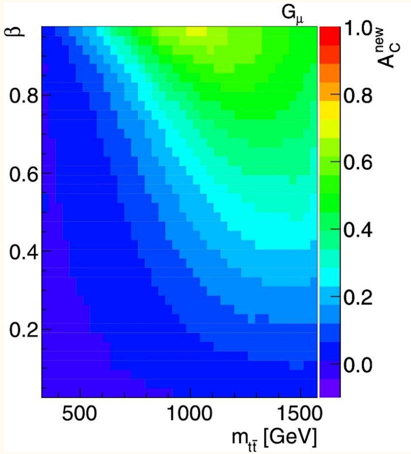

axigluon, s-chan.

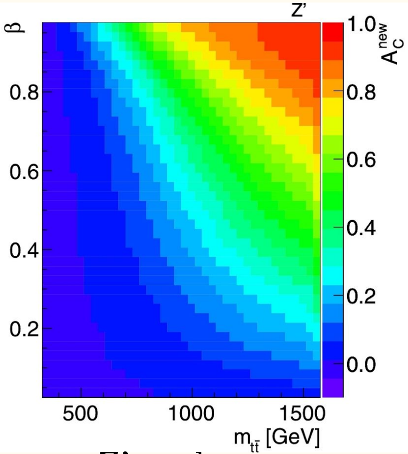

Z', t-chan.

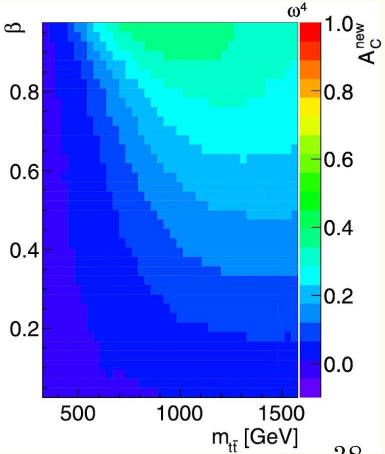

coloured triplet, u-chan.

Charge asymmetry: a little bit of history

- A_{FB} is ~10% at Tevatron
- First measurements A_{FB} from CDF, D0 higher than SM predictions
    - not significant, but there was hope for signs of new physics
- Push for more precise calculations
    - α_s^4-order calculations higher by 10% wrt previous NLO, less tension with exp.
    - CDF+D0 combined resulted in A_{FB}=(12.8±2.5)% vs new pred. (9.5±0.7)%
- A_C at LHC is predicted to be only ~0.5%: challenge!
- ATLAS results at 8 TeV: l+jets, l+jets boosted and dilepton channels standalone
- New ATLAS analysis:

  l+jets resolved and boosted simultaneously measured within a single measurement!

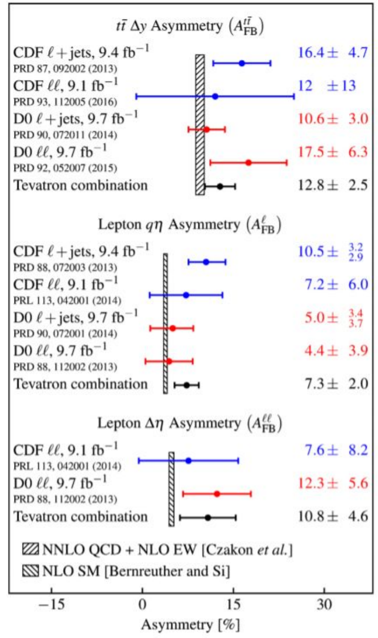

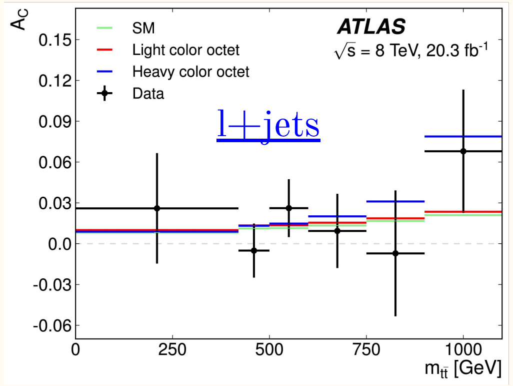

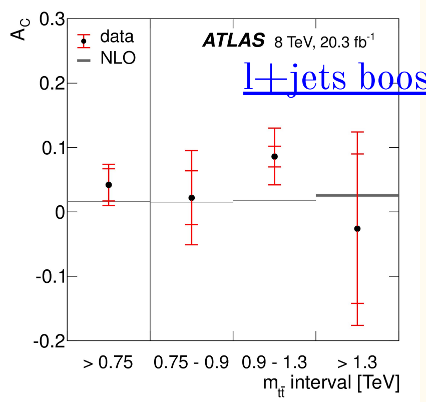

Charge asymmetry: selection

- Single e/μ trigger
- =1 isolated e/μ
- Cuts on E_T^{miss}, M_T^W
- "small-R" jets (R=0.4)
  - $\geq$1 b-tagged by MV2c10 @ 77% ε_b
- "large-R" jets (R=1.0)

  (for boosted topology selection)

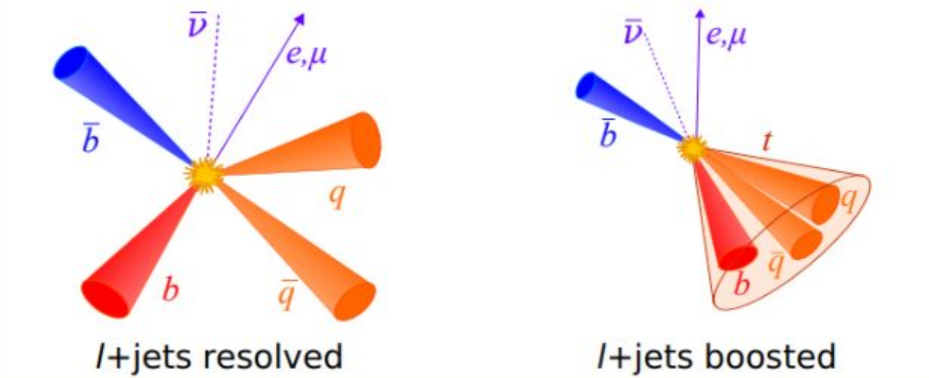

Events passing both selections are only used for boosted

trimming: R=0.2 subjets
p_T^{subjet}/p_T^{jet}<5% removed

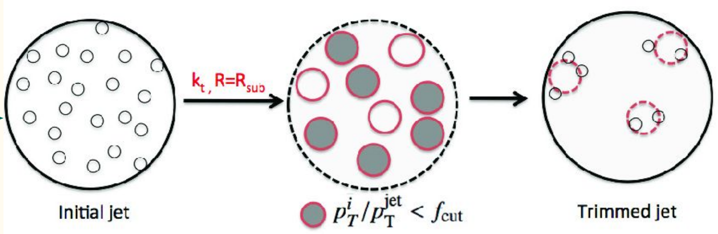

Charge asymmetry: resolved selection

- $\geq$4 small-R jets
- topology reconstruction: assign jets → partons
- Boosted Decision Tree
  - likelihood from KLFitter + 12 other variables
    - KLF= likelihood-based reconstruction algorithm
  - tries all permutations of $\leq$ 5 jets
  - trained on ttbar MC
- Highest BDT-score permutation used
- BDT_{score}>0.3 cut applied
  - S/B improves factor 2
  - expect 75% ttbar events correctly assigned

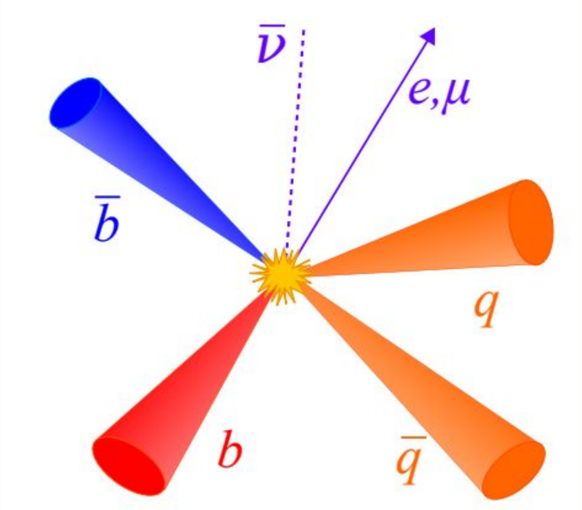

Charge asymmetry: boosted topology

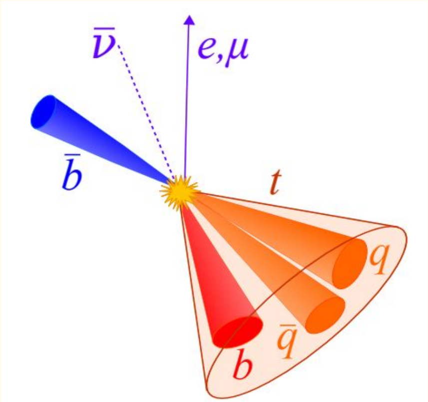

- $\geq$1 small-R jet, $\Delta R(lep,jet)<1.5$
- 1 large-R jet: $p_T>350$ GeV, $|\eta|<2$
- Top tagger algorithm, cut-based on 2 variables:
  - m_{comb}: weighted average of calo- and track-based "top"-jet mass
  - τ_3/τ_2 N-subjettiness: # of sub-jets
  - expected ε_{top}=80%
- m_{ttbar} > 500 GeV

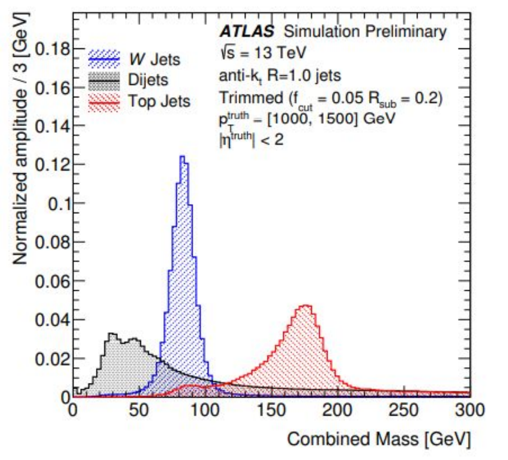

ATLAS-CONF-2017-064

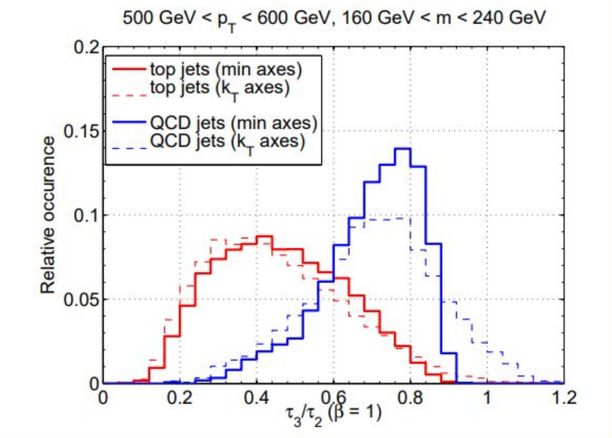

JHEP02(2012)093

see also ATLAS paper Eur. Phys. J. C (2019) 79: 375

Charge asymmetry: yields and backgrounds

- Signal and bkg from MC
  - except Multijet, data-driven [Matrix Method]
- [Fully Bayesian Unfolding]: unfolding through posterior likelihood marginalisation which includes bkg normalisations and systematic uncertainties as nuisance parameters

Process:	Resolved		Boosted	
	$1b$-excl.	$2b$-incl.	$1b$-excl	$2b$-incl.
$t\bar{t}$	1520000±120000	1840000±150000	50000± 7000	74000±10000
Single top	89000± 12000	49000± 8000	3600± 1200	3000± 1200
W + jets	200000± 23000	23000± 14000	10000± 5000	1800± 1000
$Z + VV + t\bar{t}X$	52000± 28000	15000± 8000	2600± 1300	1400± 800
Multijet	90000± 40000	47000± 23000	3000± 1500	2300± 1200
Total Prediction	1950000±200000	1980000±160000	69000±11000	83000±11000
Data (139 fb^{-1})	1945037	2009526	54710	66582

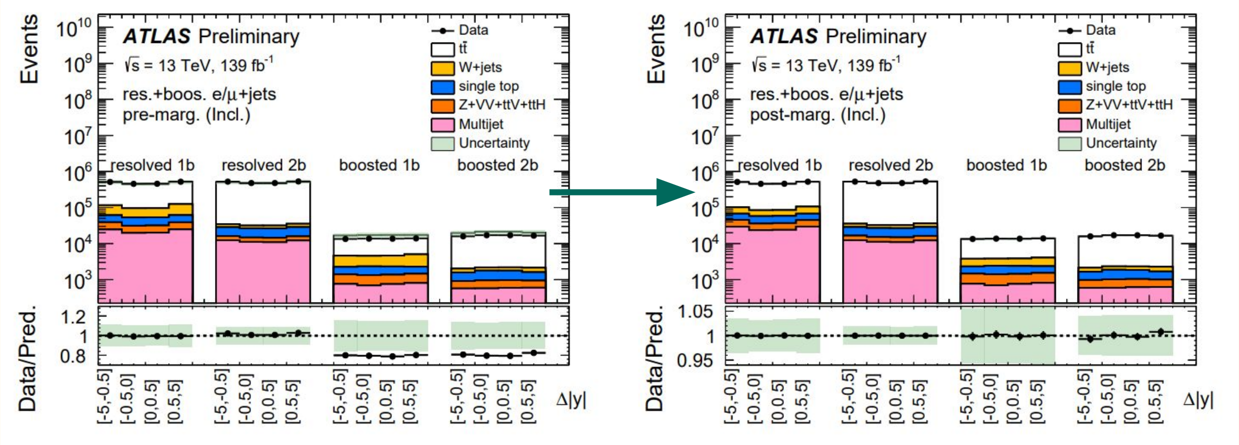

20% normalization disagreement in boosted (confirmed by [xsec measurements])
→ extra free floating normalisation parameter

Charge asymmetry: uncertainties

Most important uncertainties:

1. ISR modelling (variations of μ_F^{ISR}, μ_R^{ISR}, h_{damp})
2. W+jets μ_F, μ_R scales and normalizations
3. Detector uncertainties on E_T^{miss} and JES
4. PS+hadronization

Total syst. uncertainty on $A_C = \pm 0.0009$

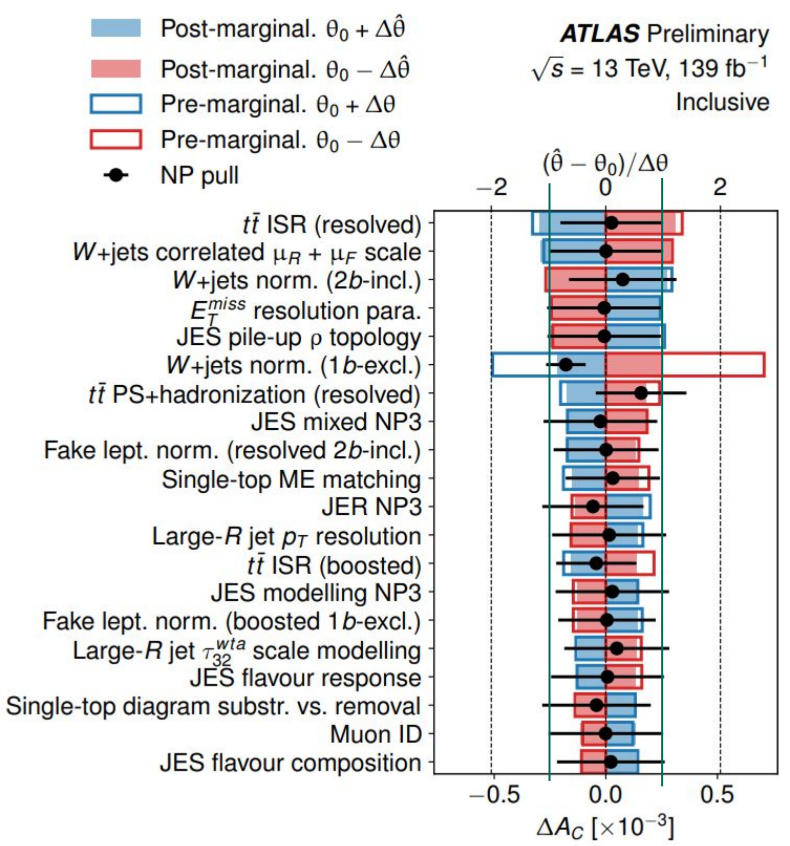

Charge asymmetry: results

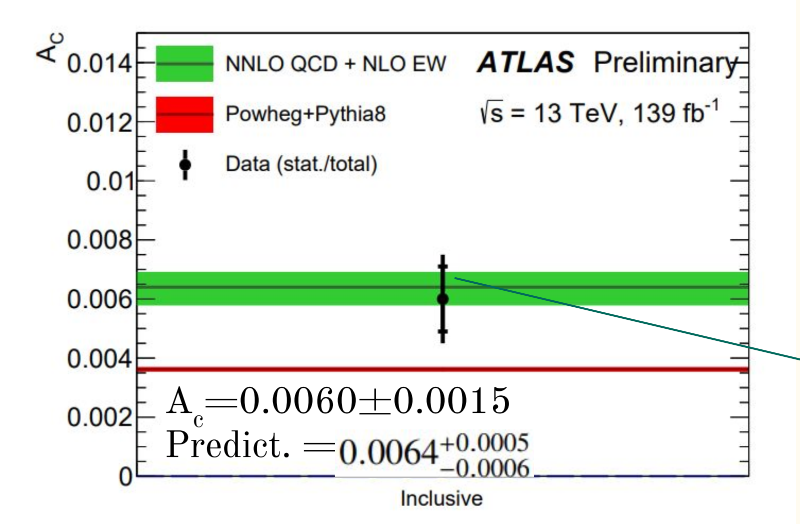

$A_c = 0.0060 \pm 0.0015$
Predict. $= 0.0064^{+0.0005}_{-0.0006}$

Stat.	Syst.	MC stat.	Bias	Total unc.
0.0011	0.0009	0.0005	0.0001	0.0015

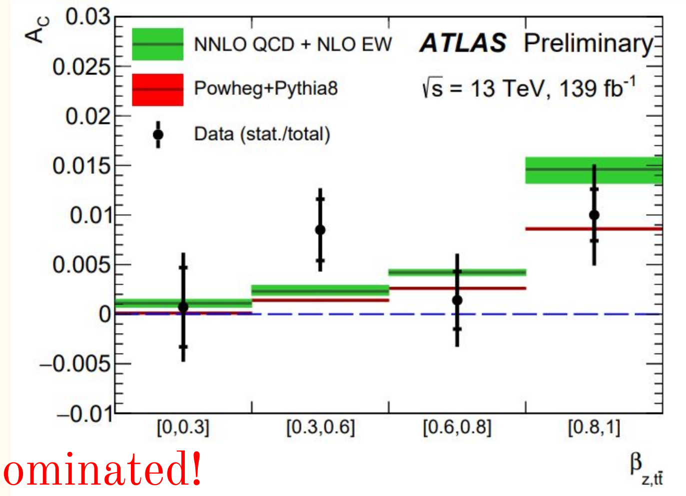

stat. dominated!

<u>Evidence of charge asymmetry @ 4σ!</u>

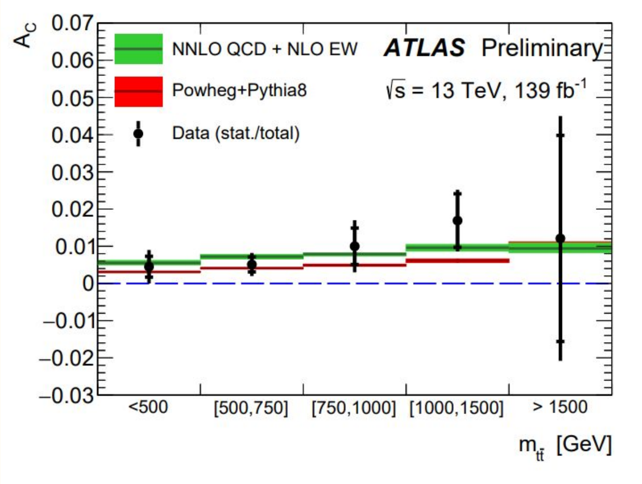

In the note presented also results for an EFT extension of the SM

Charge asymmetry vs state of the art

- ATLAS result, 139/fb @ 13 TeV: 0.0060±0.0015, still stat-limited
  - SM prediction : $0.0064^{+0.0005}_{-0.0006}$
- CMS result, 36/fb @ 13 TeV: 0.01±0.009
- ATLAS+CMS JHEP 04 (2018) 033
  - 7 TeV: 0.005±0.009
  - 8 TeV: 0.0055±0.0034

Comparison with Tevatron is a bit of apples with oranges

- A_{FB} can be used, effect is one order of magnitude bigger
- Combined D0+CDF: AFB=(12.8±2.5)% vs pred. (9.5±0.7)%
- BUT: very new CMS result also measured A_{FB} on 36/fb, qqbar/gg xsec model dependent, but can compare with Tevatron

Conclusion

- Inclusive cross section measured with 2.4% uncertainty at 13 TeV
  - uncertainty completely dominated by luminosity
  - differential cross section → input for ttbar modelling, can be used to measure m_t
- m_t measured with 0.78 GeV (0.45%) uncertainty exploiting B→μ decays
  - "alternative" methods now competitive with "standard" methods
  - "independent" cross-check, sensitive to different modelling effects, useful for combinations
  - LHC will need to attack on all fronts to break the 500 MeV barrier
  - will need crucial input from theory community
- Charge asymmetry: evidence at 4σ at LHC!
  - measurement stat-limited
  - simultaneous l+jets resolved AND boosted analysis → more powerful and fully self-consistent setup
  - reached a new domain of precision, currently very good agreement with state-of-the-art predictions

BACKUP

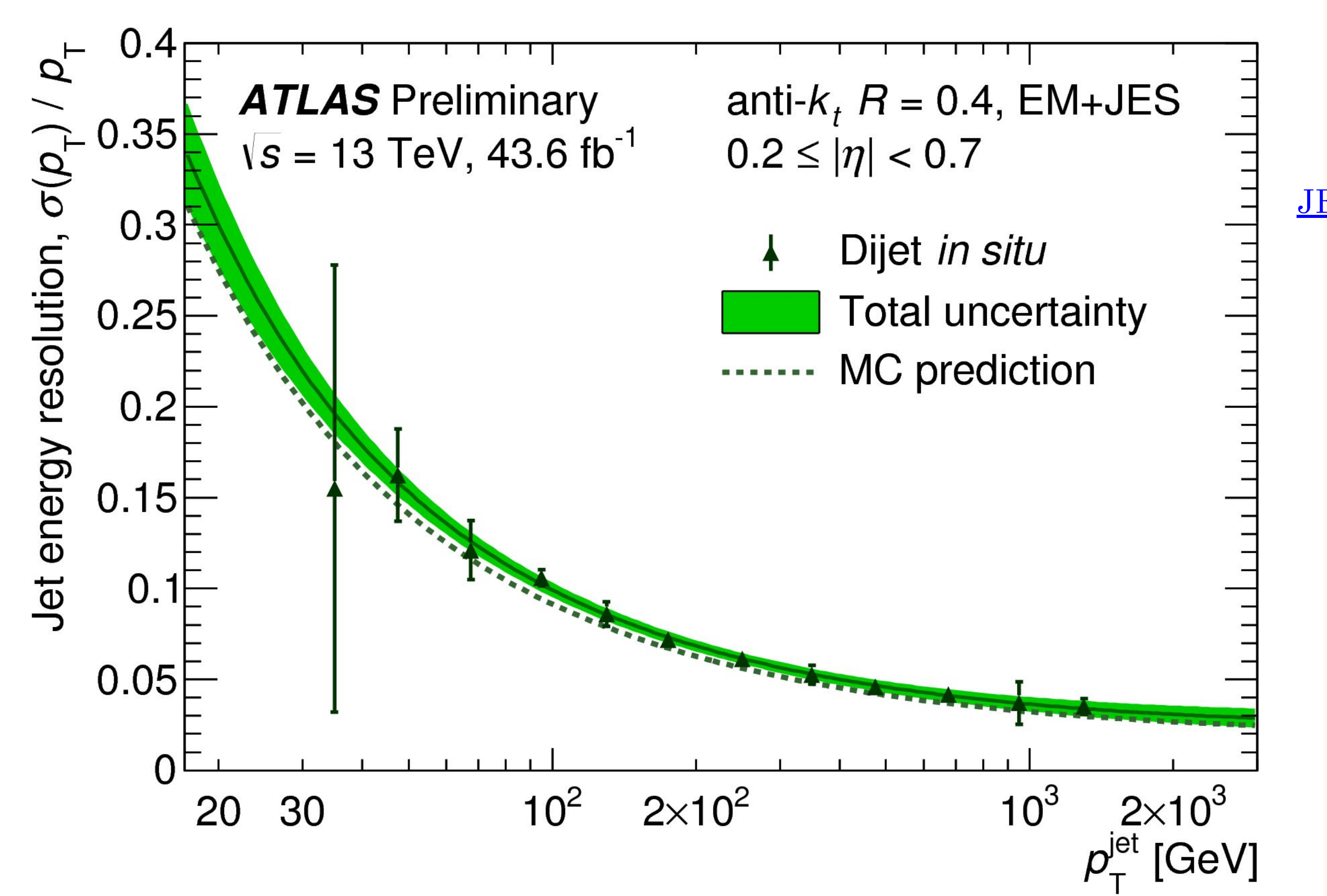

JETM-2018-005

Jet reconstruction in ATLAS

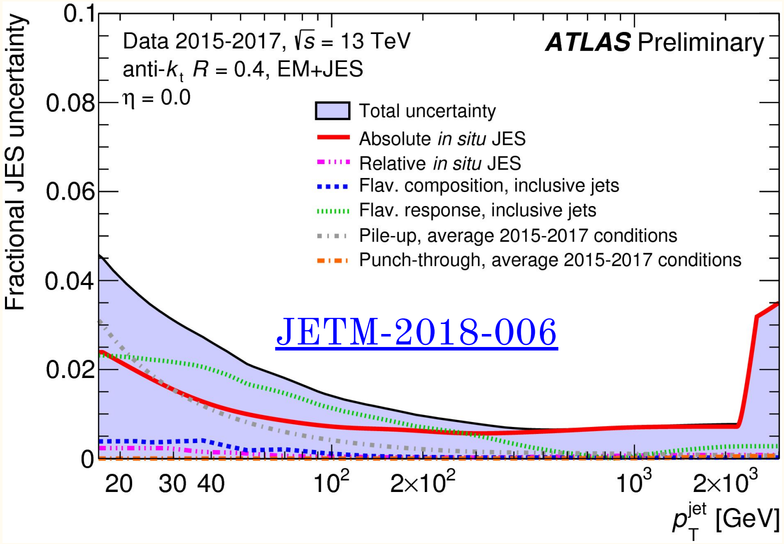

[JETM-2018-006]

boosted objects →

overlapping jets →

R=1.0 "Large" jets

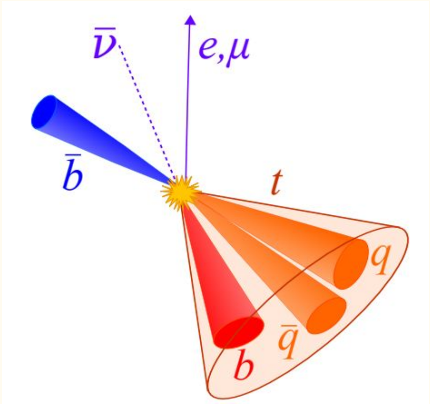

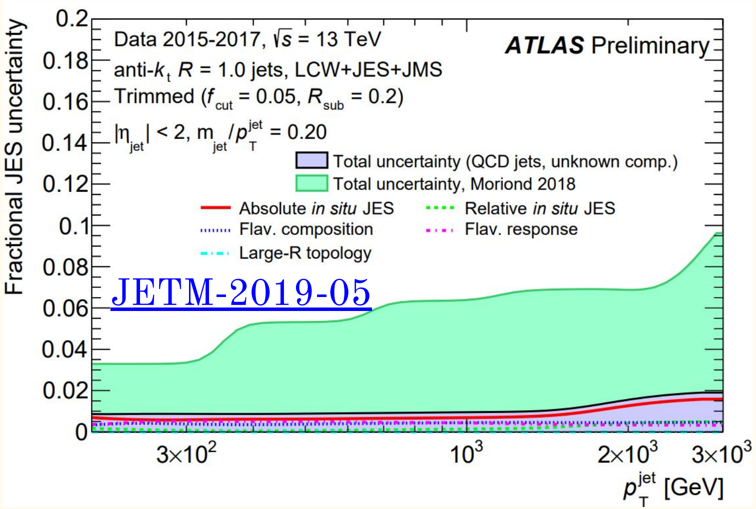

[JETM-2019-05]

Hadronic jets:

%-level unc. on jet energy scale (JES),

%-level resolution (JER)

b-jet identification in ATLAS

b→μ+X decays can also be used, see later in the talk

- Low-level taggers: secondary vert., impact parameter of tracks, kinematics…
- Several low-level taggers → (multivariate/neural network) → high-level taggers
- Performance calibrated in data
- E.g. MV2c10 working point with 70% efficiency on b-jets
  - rejection of factor 12 for c-jets, ~400 for light/gluon-jets

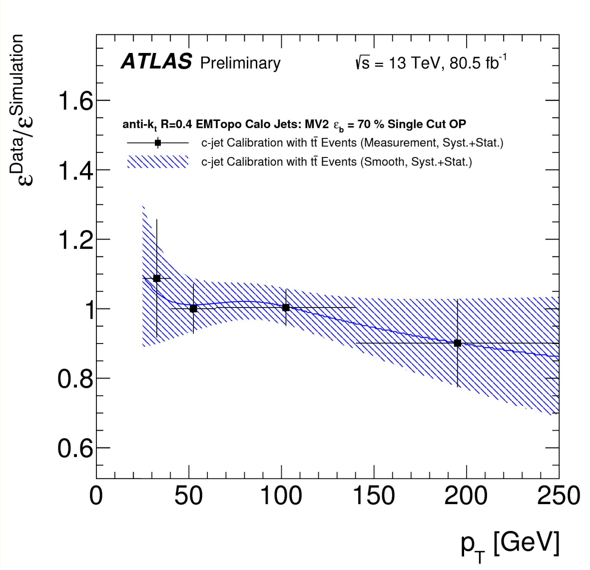

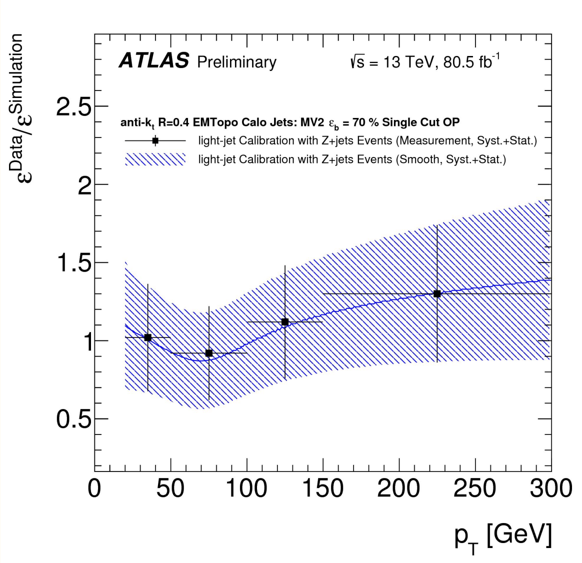

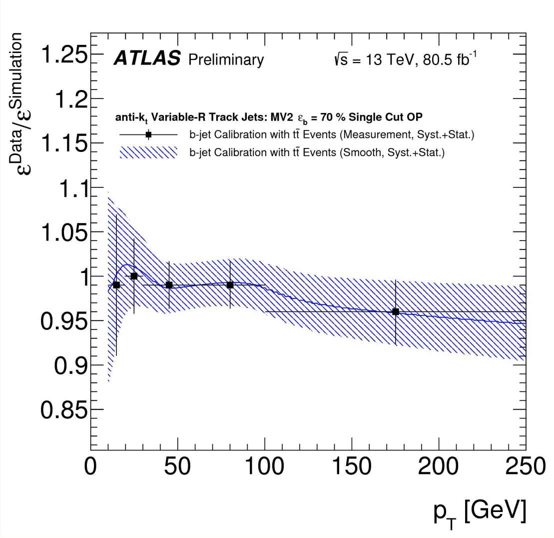

From FTAG-2019-0039-005

Electron triggers in ATLAS

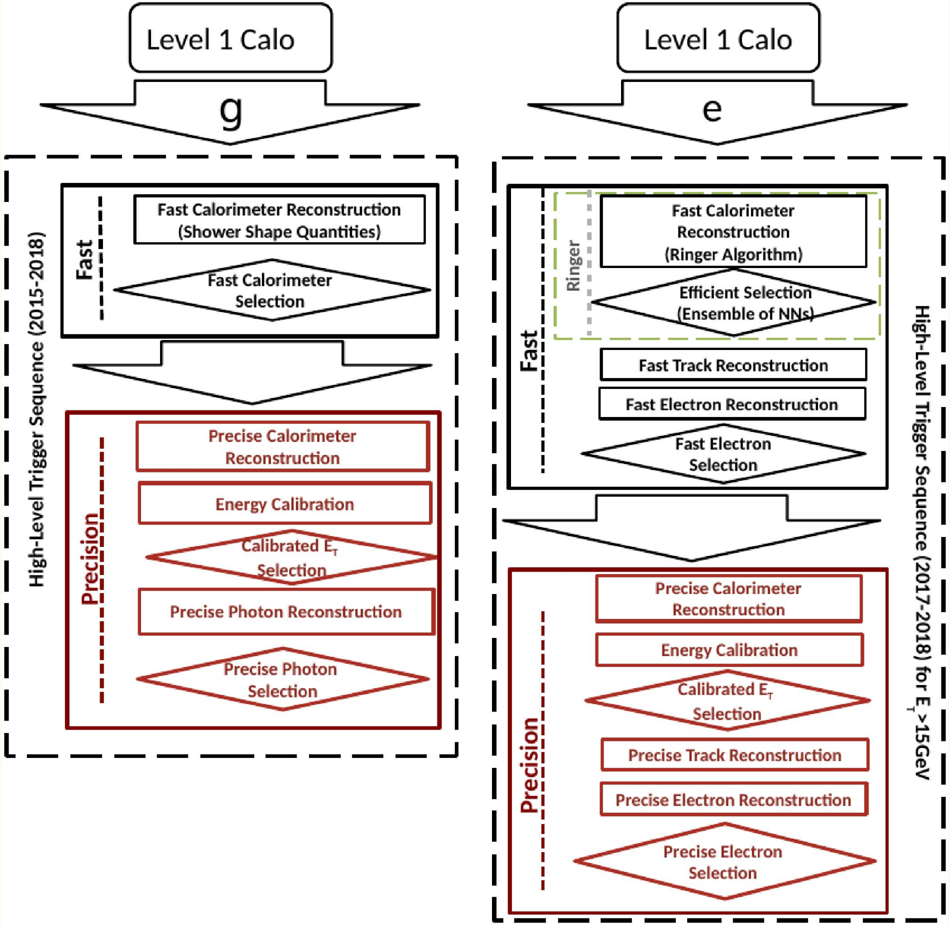

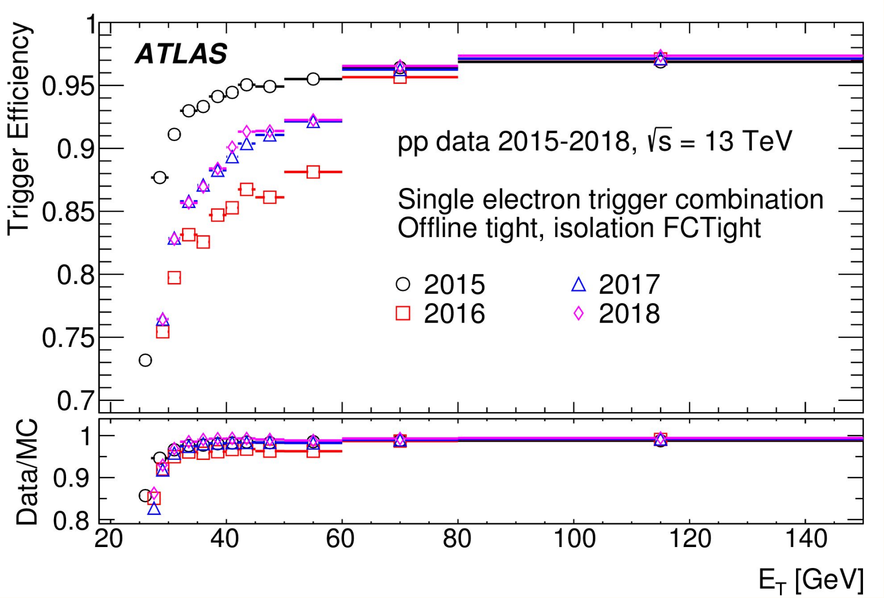

Plots from [arXiv:1909.00761](https://arxiv.org/abs/1909.00761)

Muon triggers in ATLAS

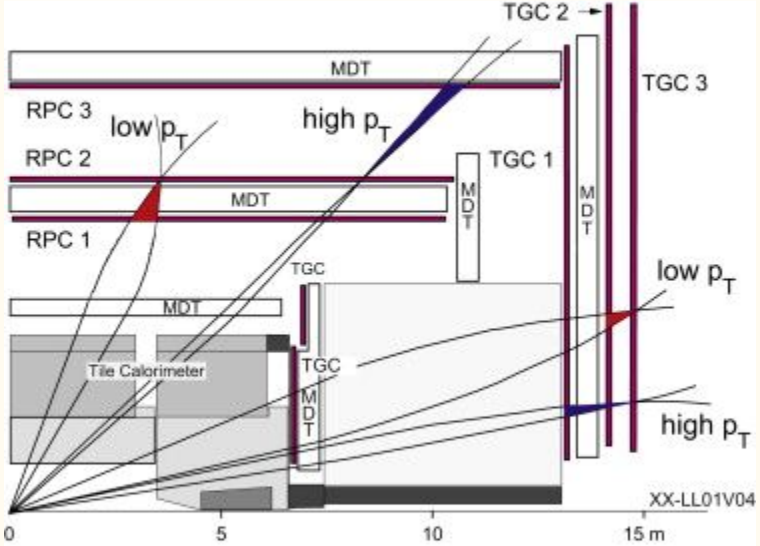

Trigger scheme from [here]()

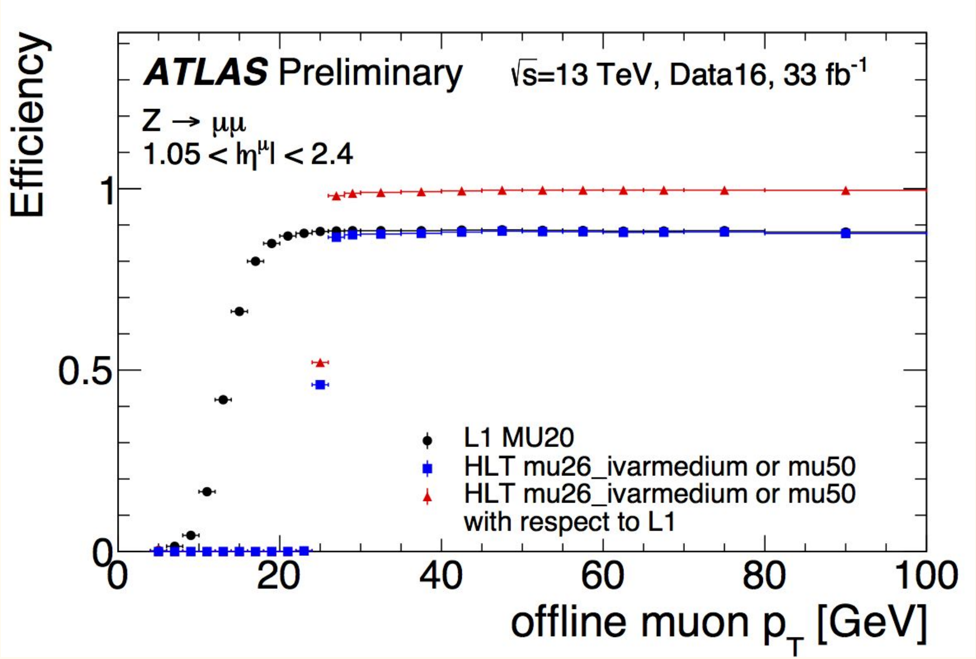

Plot from [here]()

Muon reconstruction in ATLAS

Very high reconstruction efficiency

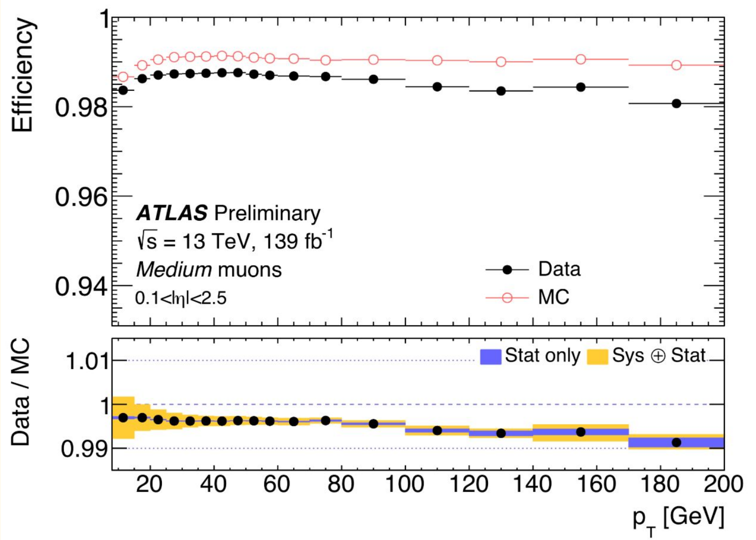

Momentum resolution at % level

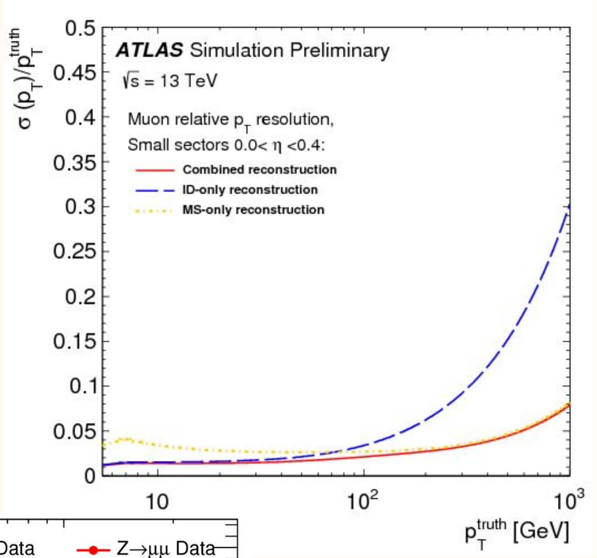

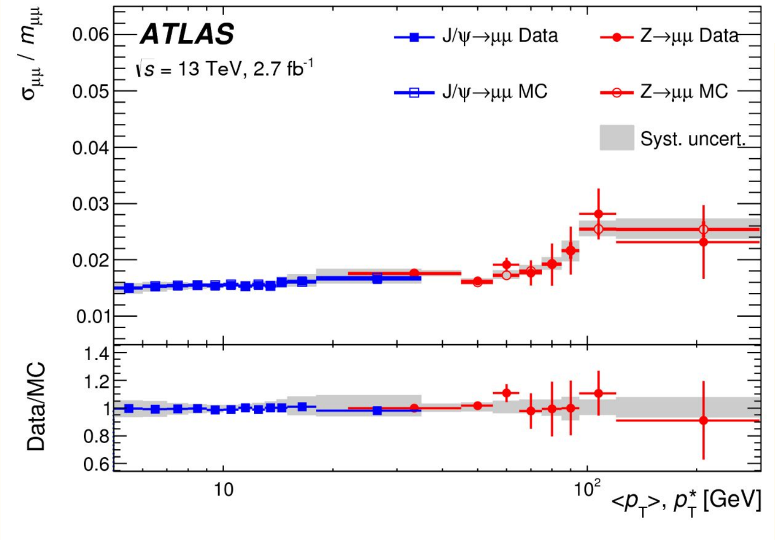

Plots from Eur. Phys. J. C 76 (2016) 292, MUON-2019-03 and MUON-2018-003

Electron reconstruction in ATLAS

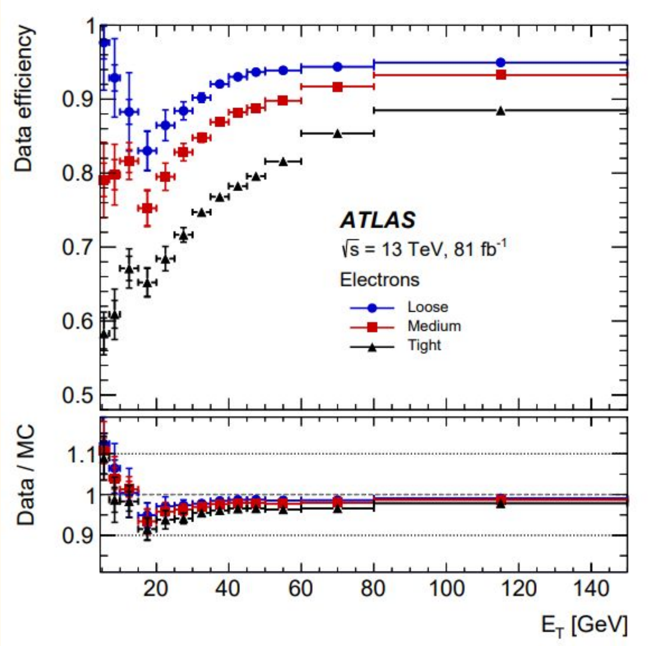

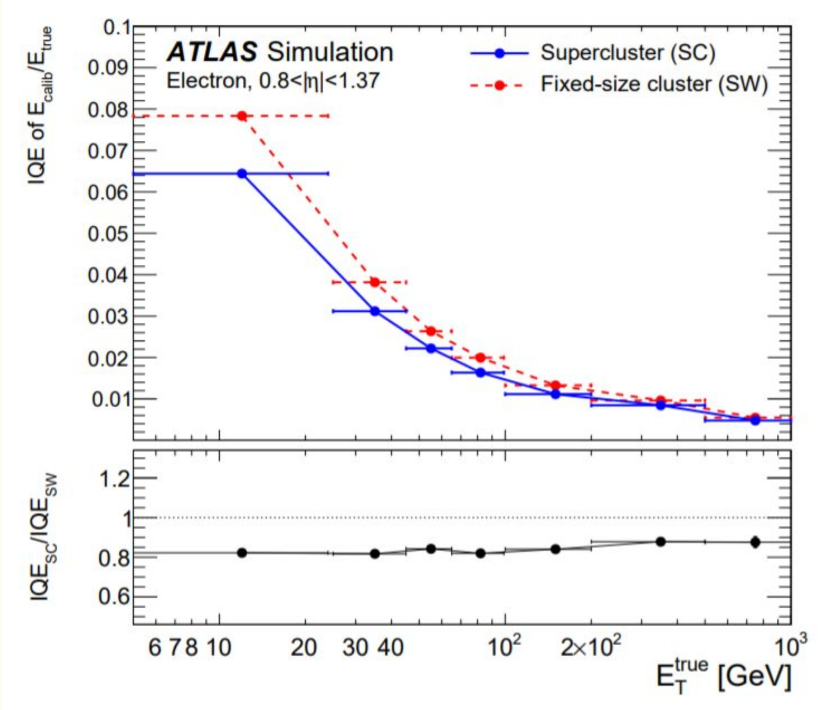

Efficiency at the 70-90% level

Energy resolution at few % level

Plots from [arXiv:1908.00005]

Variables used for b-tagging

https://arxiv.org/abs/1907.05120

Table 1: Input variables used by the MV2 and the DL1 algorithms. The JetFitter c-tagging variables are only used by the DL1 algorithm.

Input	Variable	Description
Kinematics	p_{T}	Jet p_{T}
	η	Jet $\lvert\eta\rvert$
IP2D/IP3D	$\log(P_b/P_{\mathrm{light}})$	Likelihood ratio between the b-jet and light-flavour jet hypotheses
	$\log(P_b/P_c)$	Likelihood ratio between the b- and c-jet hypotheses
	$\log(P_c/P_{\mathrm{light}})$	Likelihood ratio between the c-jet and light-flavour jet hypotheses
SV1	$m(\mathrm{SV})$	Invariant mass of tracks at the secondary vertex assuming pion mass
	$f_E(\mathrm{SV})$	Energy fraction of the tracks associated with the secondary vertex
	$N_{\mathrm{TrkAtVtx}}(\mathrm{SV})$	Number of tracks used in the secondary vertex
	$N_{\mathrm{2TrkVtx}}(\mathrm{SV})$	Number of two-track vertex candidates
	$L_{xy}(\mathrm{SV})$	Transverse distance between the primary and secondary vertex
	$L_{xyz}(\mathrm{SV})$	Distance between the primary and the secondary vertex
	$S_{xyz}(\mathrm{SV})$	Distance between the primary and the secondary vertex divided by its uncertainty
	$\Delta R(\vec{p}_{\mathrm{jet}}, \vec{p}_{\mathrm{vtx}})(\mathrm{SV})$	ΔR between the jet axis and the direction of the secondary vertex relative to the primary vertex.
JetFitter	$m(\mathrm{JF})$	Invariant mass of tracks from displaced vertices
	$f_E(\mathrm{JF})$	Energy fraction of the tracks associated with the displaced vertices
	$\Delta R(\vec{p}_{\mathrm{jet}}, \vec{p}_{\mathrm{vtx}})(\mathrm{JF})$	ΔR between jet axis and vectorial sum of momenta of all tracks attached to displaced vertices
	$S_{xyz}(\mathrm{JF})$	Significance of average distance between PV and displaced vertices
	$N_{\mathrm{TrkAtVtx}}(\mathrm{JF})$	Number of tracks from multi-prong displaced vertices
	$N_{\mathrm{2TrkVtx}}(\mathrm{JF})$	Number of two-track vertex candidates (prior to decay chain fit)
	$N_{\text{1-trk vertices}}(\mathrm{JF})$	Number of single-prong displaced vertices
	$N_{\geq\text{2-trk vertices}}(\mathrm{JF})$	Number of multi-prong displaced vertices
JetFitter c-tagging	$L_{xyz}(2^{\mathrm{nd}}/3^{\mathrm{rd}}\mathrm{vtx})(\mathrm{JF})$	Distance of 2^{nd} or 3^{rd} vertex from PV
	$L_{xy}(2^{\mathrm{nd}}/3^{\mathrm{rd}}\mathrm{vtx})(\mathrm{JF})$	Transverse displacement of the 2^{nd} or 3^{rd} vertex
	$m_{\mathrm{Trk}}(2^{\mathrm{nd}}/3^{\mathrm{rd}}\mathrm{vtx})(\mathrm{JF})$	Invariant mass of tracks associated with 2^{nd} or 3^{rd} vertex
	$E_{\mathrm{Trk}}(2^{\mathrm{nd}}/3^{\mathrm{rd}}\mathrm{vtx})(\mathrm{JF})$	Energy fraction of the tracks associated with 2^{nd} or 3^{rd} vertex
	$f_E(2^{\mathrm{nd}}/3^{\mathrm{rd}}\mathrm{vtx})(\mathrm{JF})$	Fraction of charged jet energy in 2^{nd} or 3^{rd} vertex
	$N_{\mathrm{TrkAtVtx}}(2^{\mathrm{nd}}/3^{\mathrm{rd}}\mathrm{vtx})(\mathrm{JF})$	Number of tracks associated with 2^{nd} or 3^{rd} vertex
	$Y_{\mathrm{trk}}^{\mathrm{min}}, Y_{\mathrm{trk}}^{\mathrm{max}}, Y_{\mathrm{trk}}^{\mathrm{avg}}(2^{\mathrm{nd}}/3^{\mathrm{rd}}\mathrm{vtx})(\mathrm{JF})$	Min., max. and avg. track rapidity of tracks at 2^{nd} or 3^{rd} vertex

Single-top production

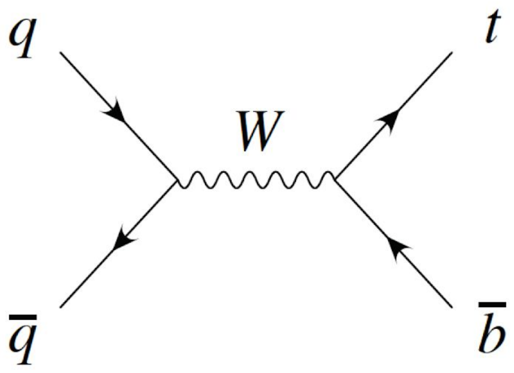

s-channel,
xsec @ 13 TeV=10 pb

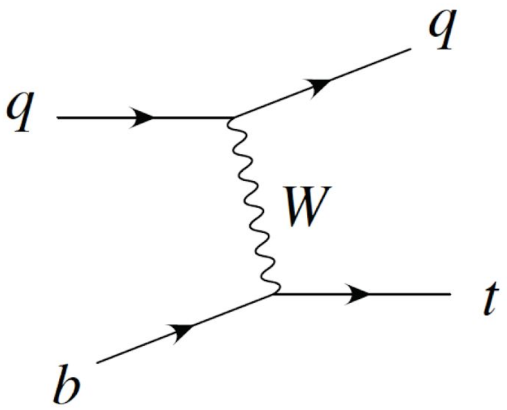

t-channel,
xsec @ 13 TeV=217 pb

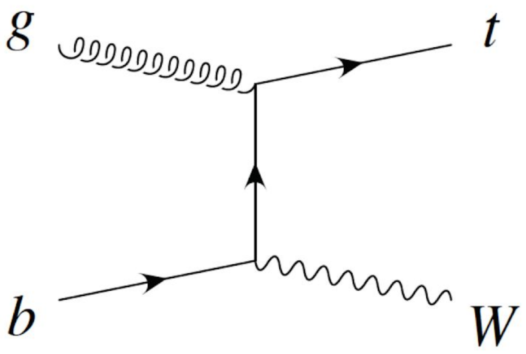

Wt-channel,
xsec @ 13 TeV=72 pb

ttbar cross section measurement in dilepton events with Run-2 data ATLAS-CONF-2019-041

Prescription

The calculations are performed for top-quark mass (mtop) values of 172.5 GeV and 173.2 GeV. The renormalisation and factorisation scales, muR and muF, are taken as: muR = muF = mtop. The following NNLO PDF sets are used: MSTW2008NNLO, CT10 NNLO, NNPDF2.3 NNLO. The midpoint of the envelope is used for the central prediction.

- **Scale uncertainty**: consider restricted scale variation (used also by Czakon, Fiedler and Mitov, arXiv:1303.6254):
    - Vary muR, muF independently by a factor of 2 while never allowing them to differ by more than a factor of 2 from each other.
    - The scale uncertainty is defined by taking the envelope of the resulting cross section values.
- **PDF+alphaS** uncertainty: PDF4LHC-style treatment to provide a combined PDF+alphaS uncertainty (**different approach** to arXiv:1303.6254):
    - Evaluate the 68% CL PDF uncertainties for the PDF sets mentioned above at the most similar alphaS values.
    - Evaluate the 68% CL alphaS uncertainty.
    - Take the envelope of the PDF+alphaS uncertainties.
- **Mass uncertainty**: assign a mtop variation of ± 1.0 GeV, following the latest top-quark mass combinations: mtop(Tevatron) = 173.20 +/- 0.87 GeV, mtop(LHC) = 173.29 +/- 0.95 GeV (ATLAS, CMS).

See link

Measuring dσ(ttbar)/dx: validation

$(1/\sigma)d\sigma/dx$ measured vs

- p_T^{ℓ}, $|\eta^{\ell}|$
- $p_T^{e\mu}$, $m^{e\mu}$, $|y^{e\mu}|$, $\Delta\phi^{e\mu}$
- $p_T^{e}+p_T^{\mu}$, E^e+E^{μ}
- $|\eta^{\ell}|\times m^{e\mu}$, $|y^{e\mu}|\times m^{e\mu}$, $|\Delta\phi^{\ell}|\times m^{e\mu}$

Bin-by-bin corrections,
no need for more sophisticated unfolding

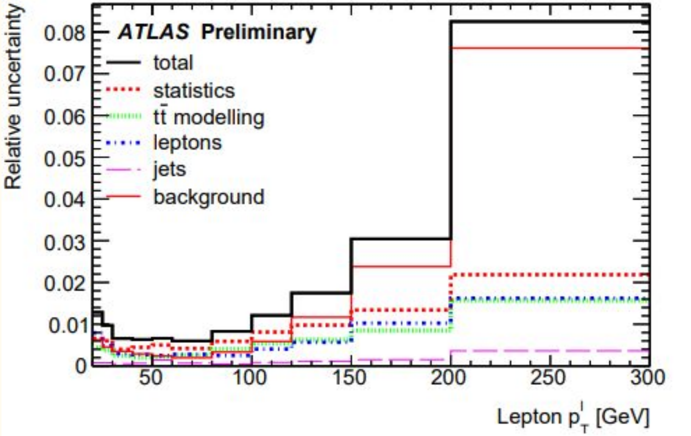

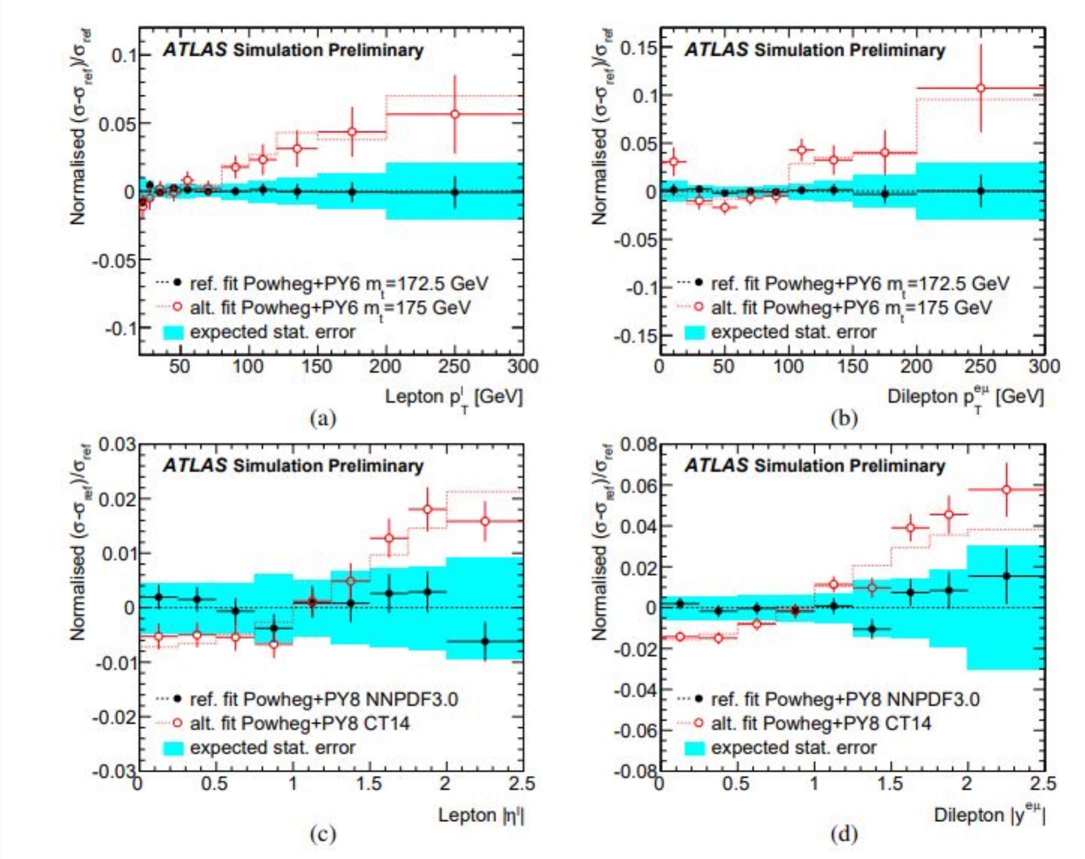

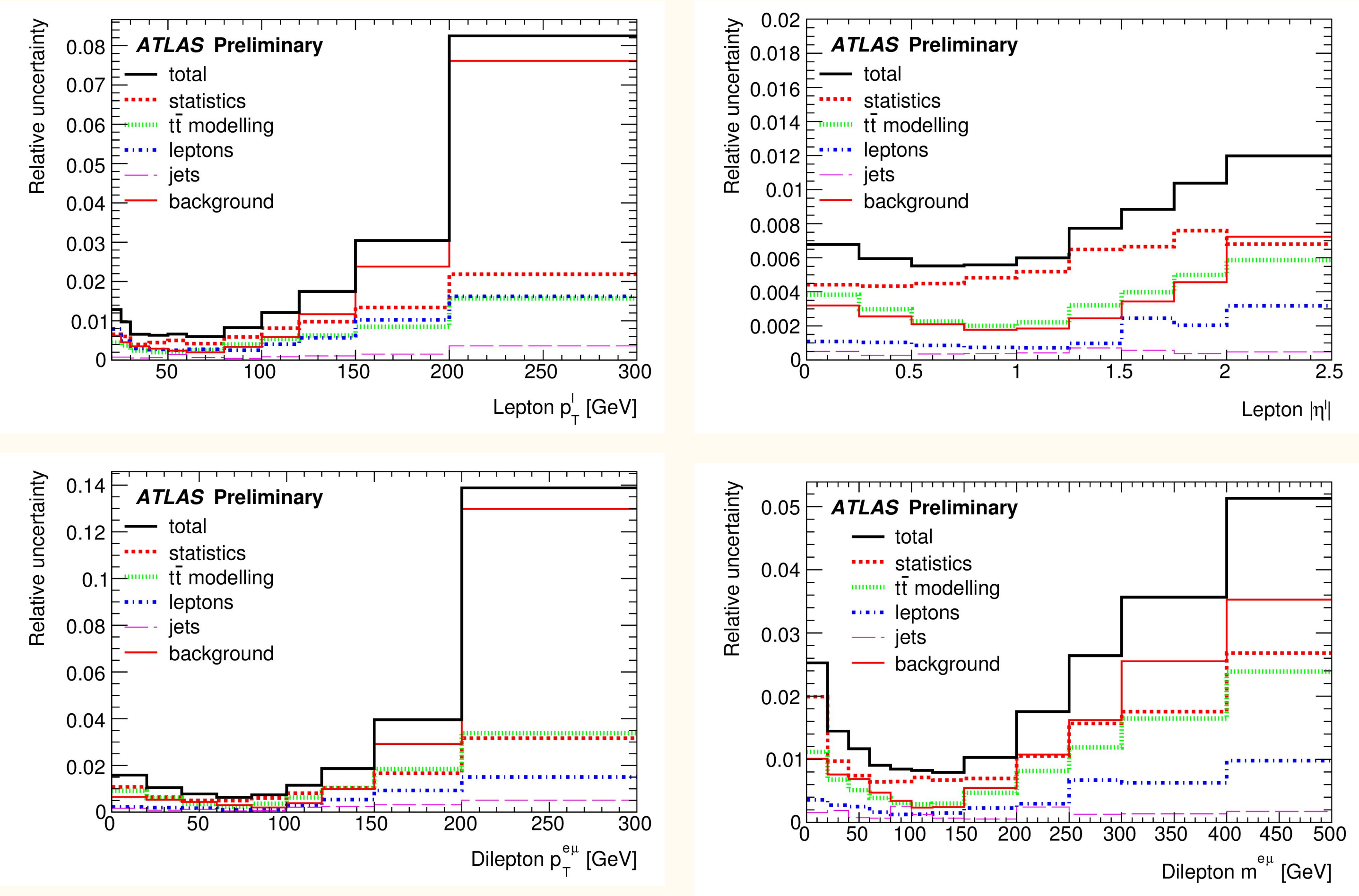
ATLAS Preliminary
total
statistics
$t\bar{t}$ modelling
leptons
jets
background
Relative uncertainty
Lepton p_T^l [GeV]
Lepton $|\eta^l|$
Dilepton $p_T^{e\mu}$ [GeV]
Dilepton $m^{e\mu}$ [GeV]

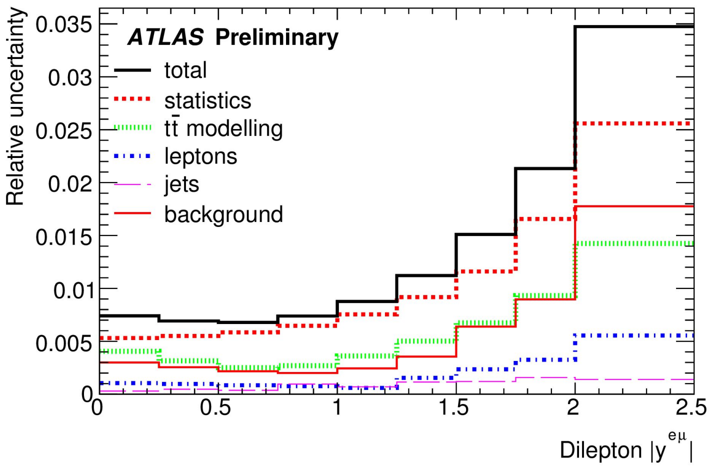
ATLAS Preliminary
total
statistics
$t\bar{t}$ modelling
leptons
jets
background
Relative uncertainty
Dilepton $|y^{e\mu}|$

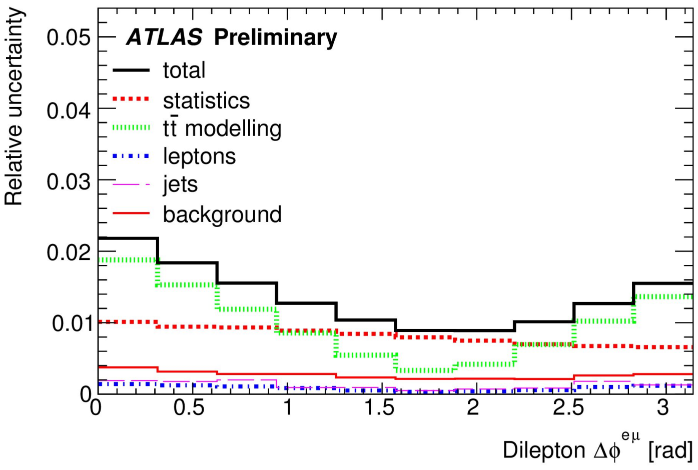
ATLAS Preliminary
total
statistics
$t\bar{t}$ modelling
leptons
jets
background
Relative uncertainty
Dilepton $\Delta\phi^{e\mu}$ [rad]

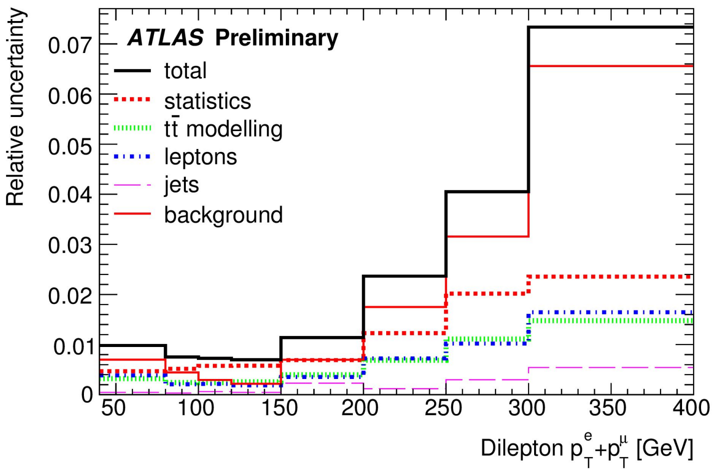
ATLAS Preliminary
total
statistics
$t\bar{t}$ modelling
leptons
jets
background
Relative uncertainty
Dilepton $p_T^e+p_T^\mu$ [GeV]

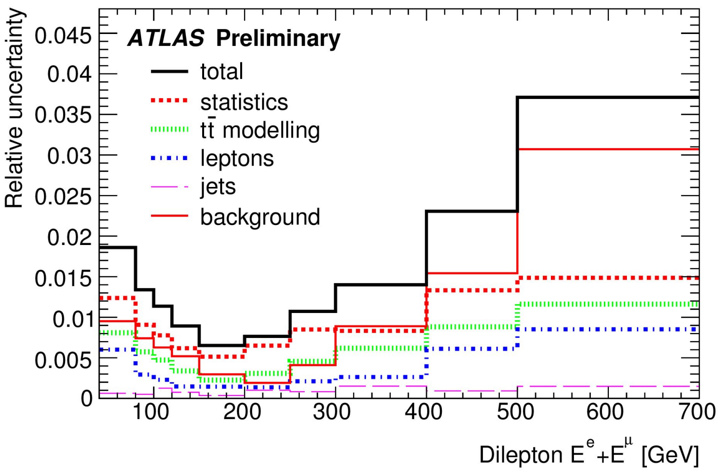
ATLAS Preliminary
total
statistics
$t\bar{t}$ modelling
leptons
jets
background
Relative uncertainty
Dilepton E^e+E^μ [GeV]

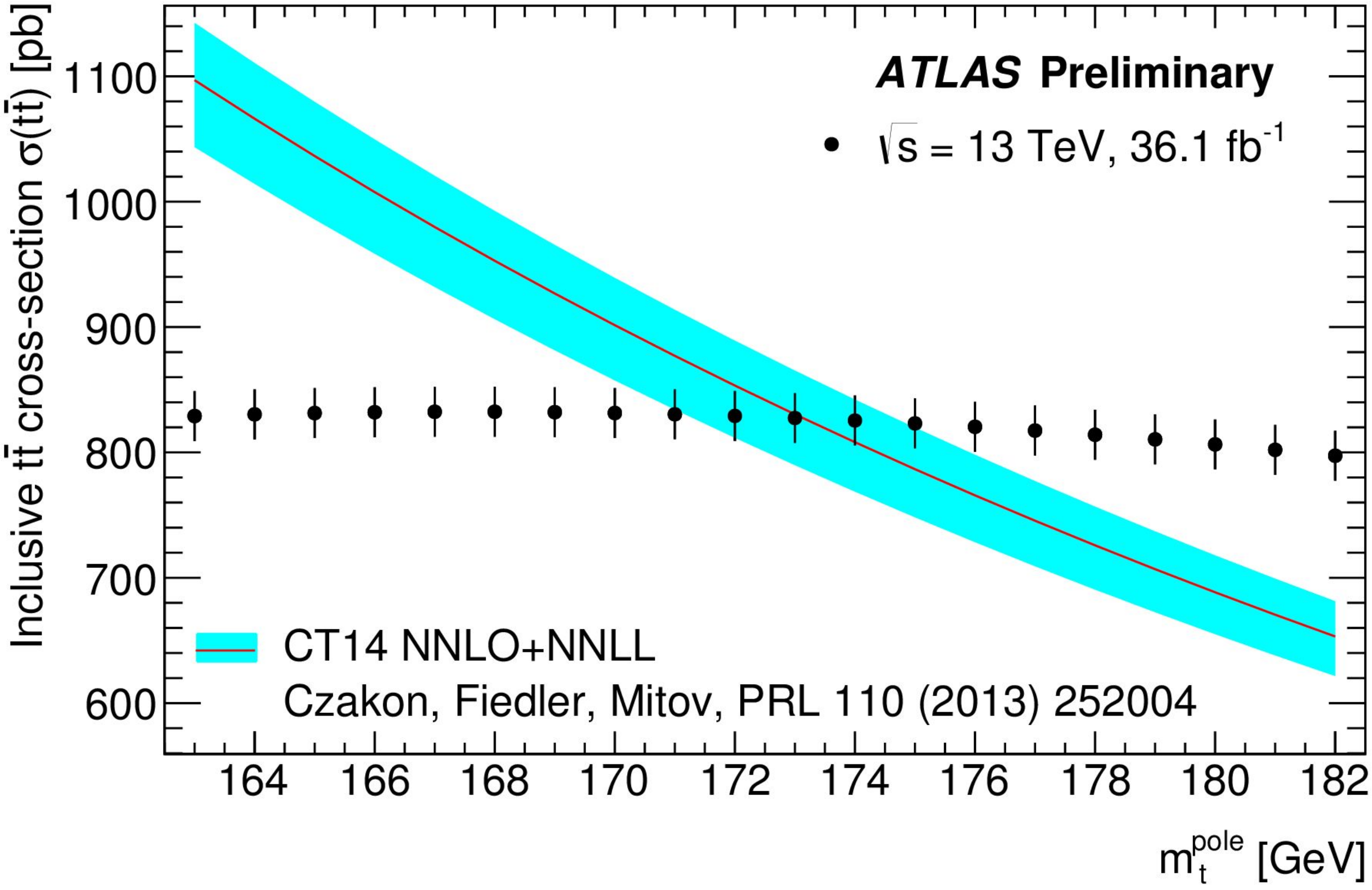
ATLAS Preliminary
√s = 13 TeV, 36.1 fb-1
CT14 NNLO+NNLL
Czakon, Fiedler, Mitov, PRL 110 (2013) 252004
Inclusive tt̄ cross-section σ(tt̄) [pb]
1100
1000
900
800
700
600
164
166
168
170
172
174
176
178
180
182
m_t^pole [GeV]

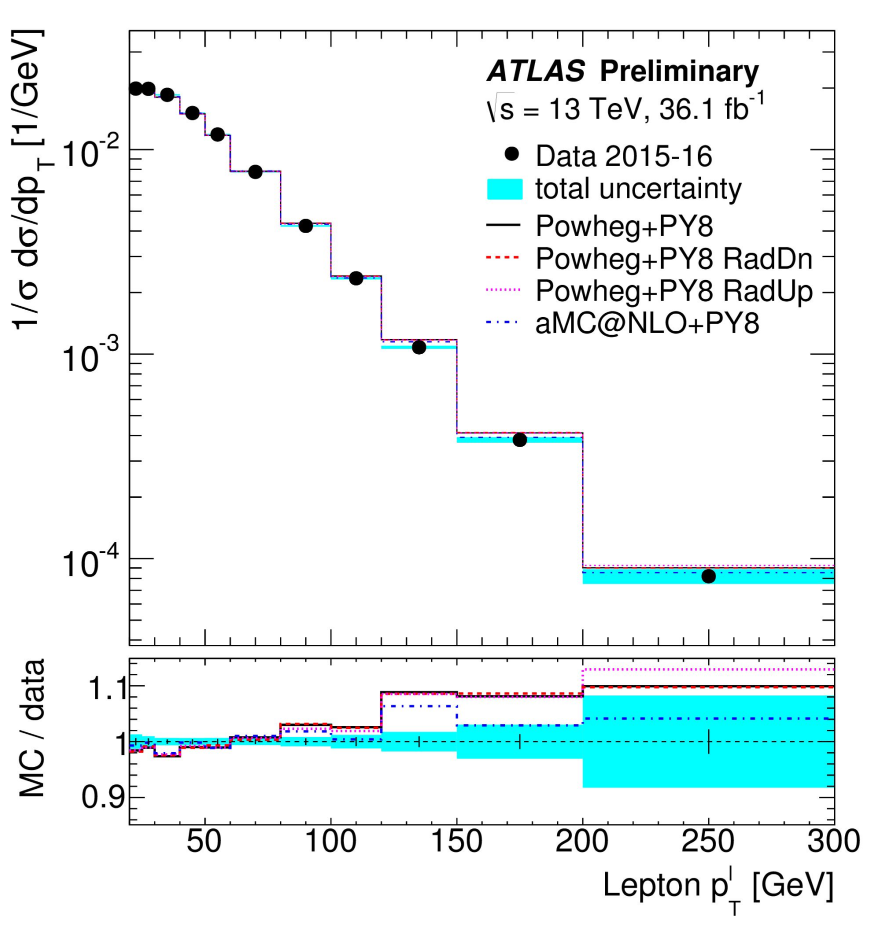
ATLAS Preliminary
√s = 13 TeV, 36.1 fb-1
Data 2015-16
total uncertainty
Powheg+PY8
Powheg+PY8 RadDn
Powheg+PY8 RadUp
aMC@NLO+PY8
1/σ dσ/dpT [1/GeV]
MC / data
Lepton pT^l [GeV]

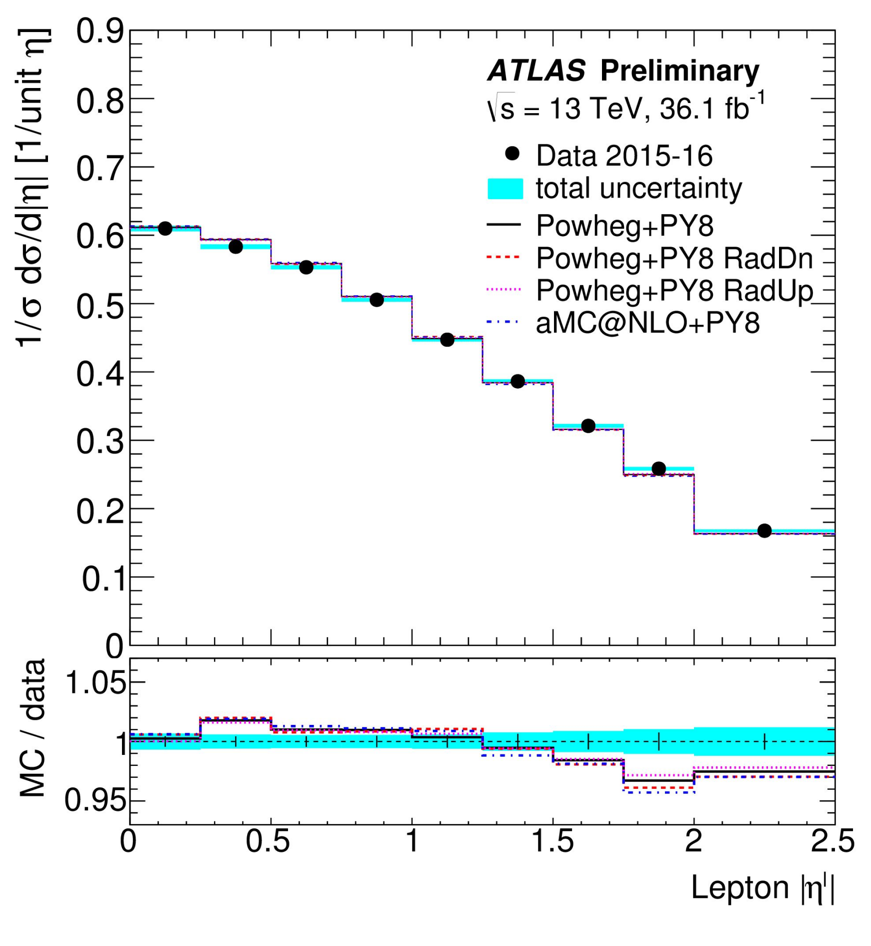
ATLAS Preliminary
√s = 13 TeV, 36.1 fb-1
Data 2015-16
total uncertainty
Powheg+PY8
Powheg+PY8 RadDn
Powheg+PY8 RadUp
aMC@NLO+PY8
1/σ dσ/d|η| [1/unit η]
MC / data
Lepton |η^l|

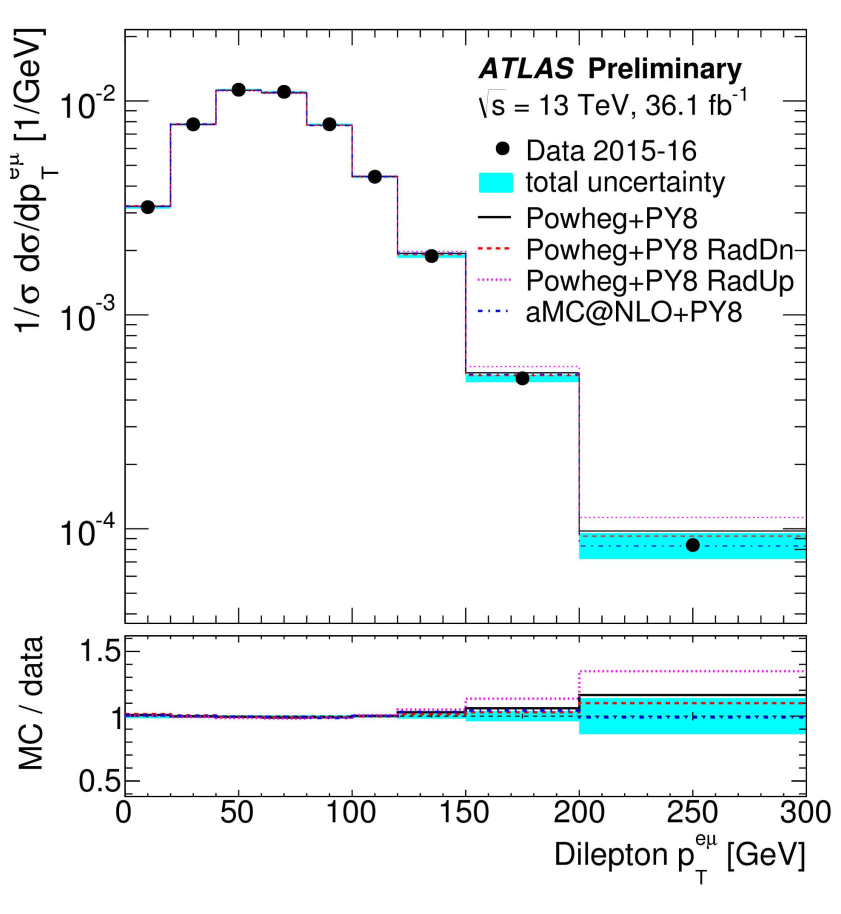
ATLAS Preliminary
$\sqrt{s}$ = 13 TeV, 36.1 fb^{-1}
Data 2015-16
total uncertainty
Powheg+PY8
Powheg+PY8 RadDn
Powheg+PY8 RadUp
aMC@NLO+PY8
$1/\sigma\ d\sigma/dp_T^{e\mu}$ [1/GeV]
MC / data
Dilepton $p_T^{e\mu}$ [GeV]

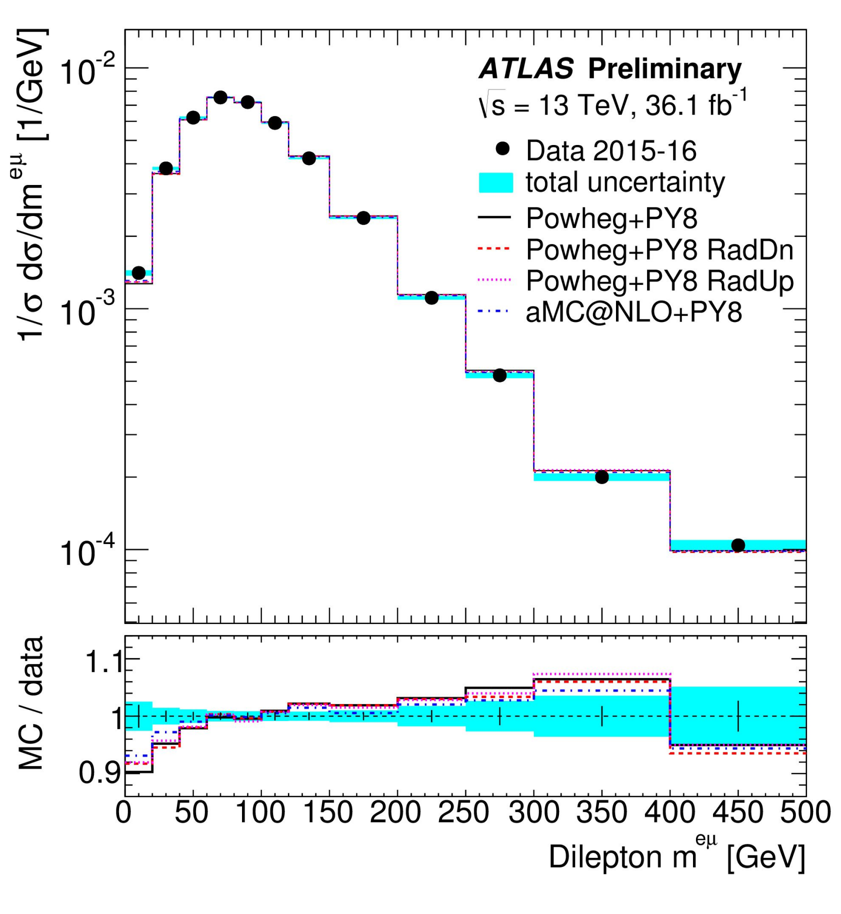
ATLAS Preliminary
$\sqrt{s}$ = 13 TeV, 36.1 fb^{-1}
Data 2015-16
total uncertainty
Powheg+PY8
Powheg+PY8 RadDn
Powheg+PY8 RadUp
aMC@NLO+PY8
$1/\sigma\ d\sigma/dm^{e\mu}$ [1/GeV]
MC / data
Dilepton $m^{e\mu}$ [GeV]

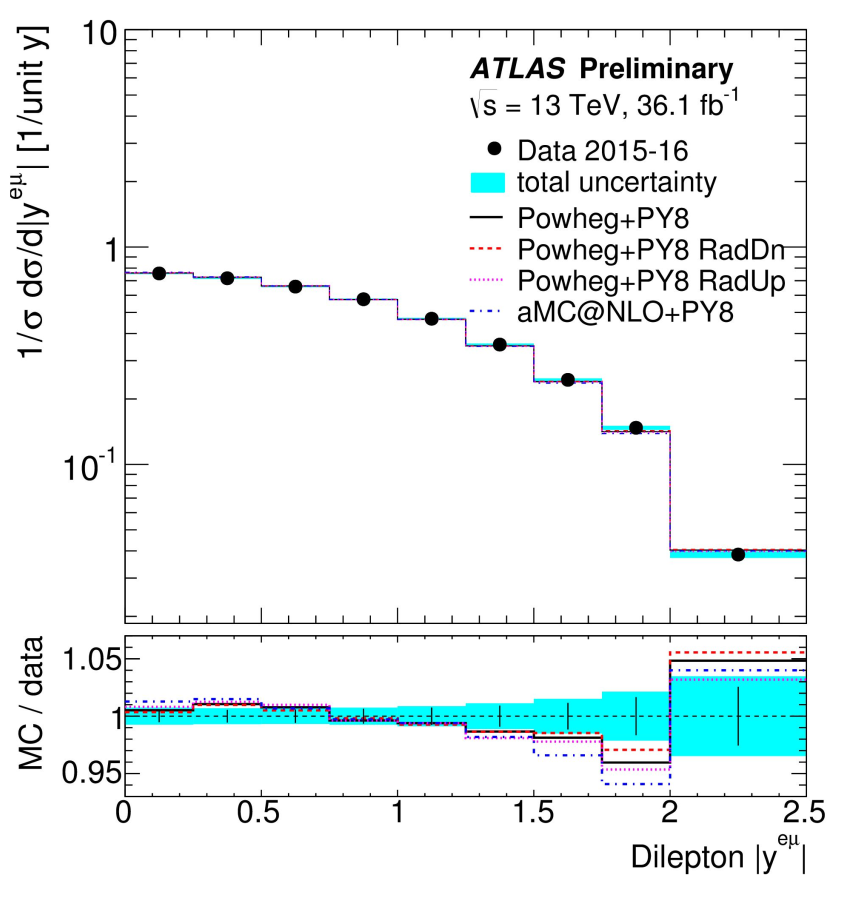
ATLAS Preliminary
√s = 13 TeV, 36.1 fb-1
Data 2015-16
total uncertainty
Powheg+PY8
Powheg+PY8 RadDn
Powheg+PY8 RadUp
aMC@NLO+PY8
1/σ dσ/d|y^eμ| [1/unit y]
MC / data
Dilepton |y^eμ|

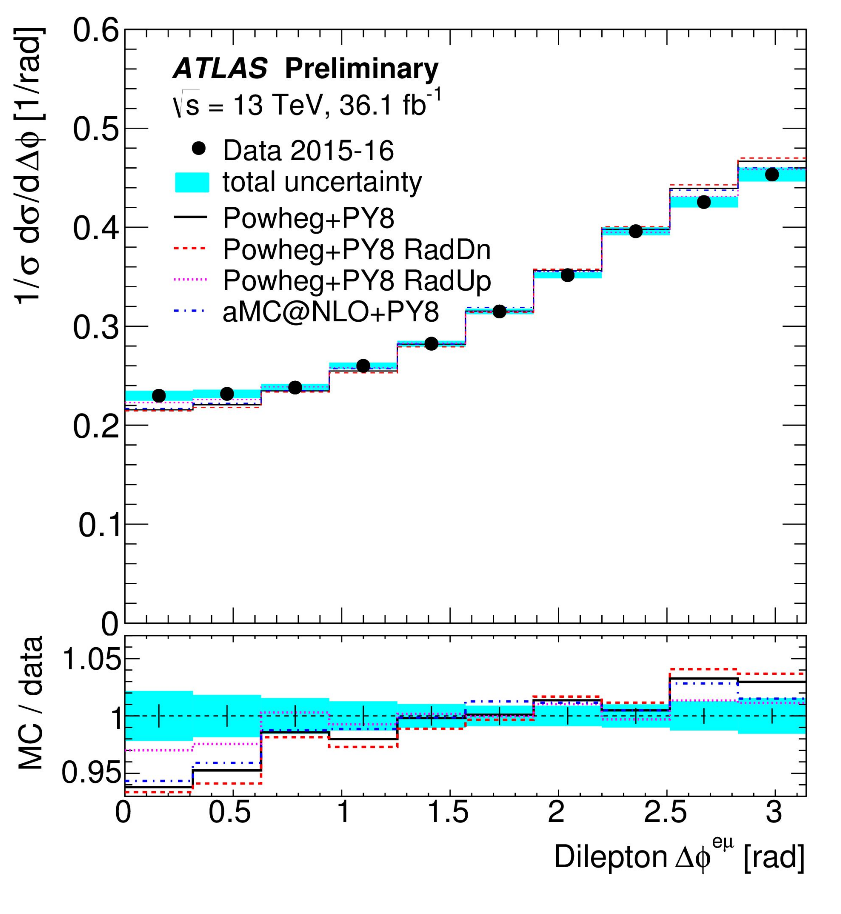
ATLAS Preliminary
√s = 13 TeV, 36.1 fb-1
Data 2015-16
total uncertainty
Powheg+PY8
Powheg+PY8 RadDn
Powheg+PY8 RadUp
aMC@NLO+PY8
1/σ dσ/dΔφ [1/rad]
MC / data
Dilepton Δφ^eμ [rad]

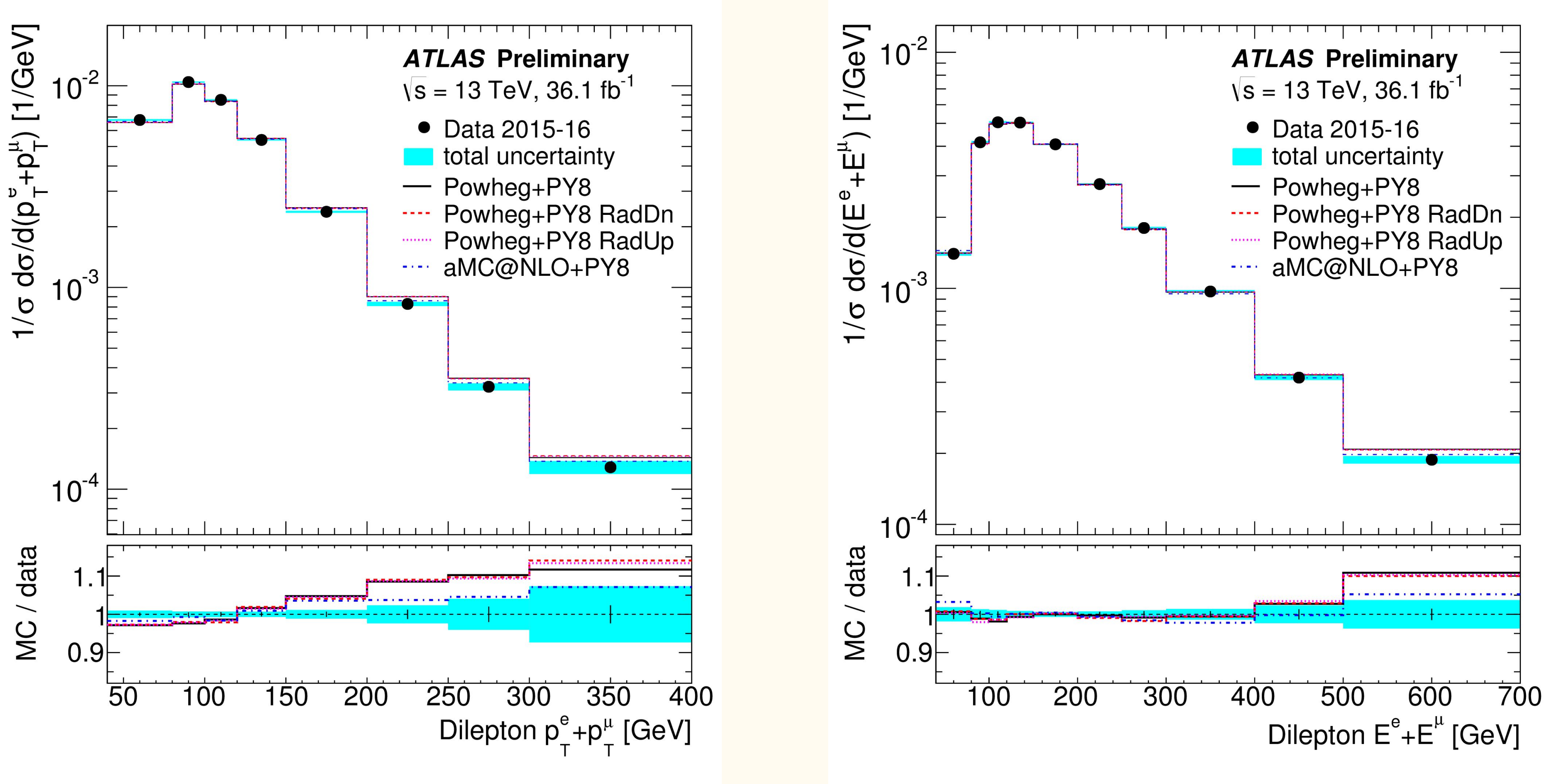

ATLAS Preliminary
√s = 13 TeV, 36.1 fb-1
Data 2015-16
total uncertainty
Powheg+PY8
Powheg+PY8 RadDn
Powheg+PY8 RadUp
aMC@NLO+PY8
1/σ dσ/d(pTe+pTμ) [1/GeV]
MC / data
Dilepton pTe+pTμ [GeV]
ATLAS Preliminary
√s = 13 TeV, 36.1 fb-1
Data 2015-16
total uncertainty
Powheg+PY8
Powheg+PY8 RadDn
Powheg+PY8 RadUp
aMC@NLO+PY8
1/σ dσ/d(Ee+Eμ) [1/GeV]
MC / data
Dilepton Ee+Eμ [GeV]

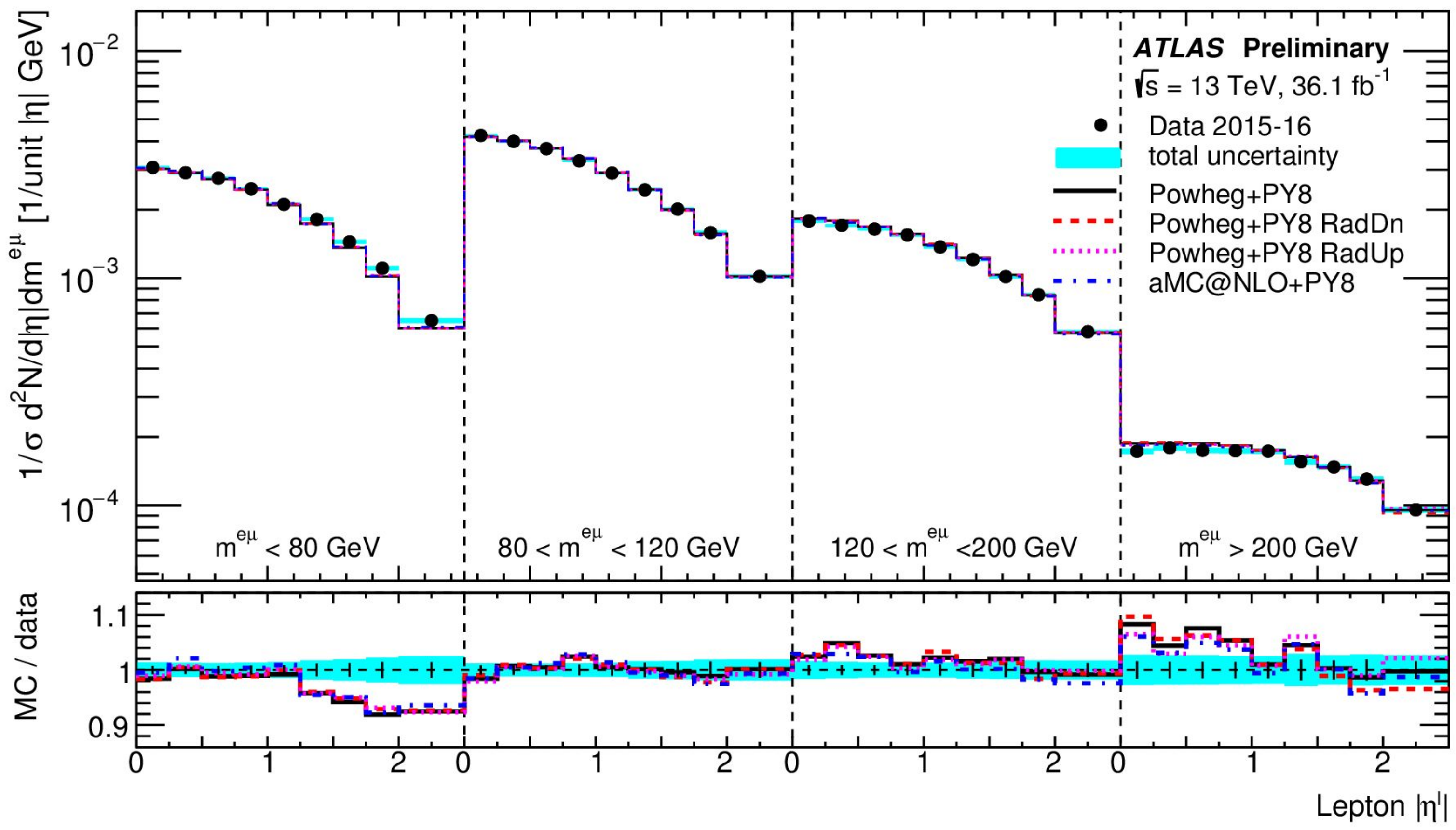

ATLAS Preliminary
√s = 13 TeV, 36.1 fb-1
Data 2015-16
total uncertainty
Powheg+PY8
Powheg+PY8 RadDn
Powheg+PY8 RadUp
aMC@NLO+PY8
1/σ d2N/d|η|dmeμ [1/unit |η| GeV]
m eμ < 80 GeV
80 < m eμ < 120 GeV
120 < m eμ <200 GeV
m eμ > 200 GeV
MC / data
Lepton |ηl|

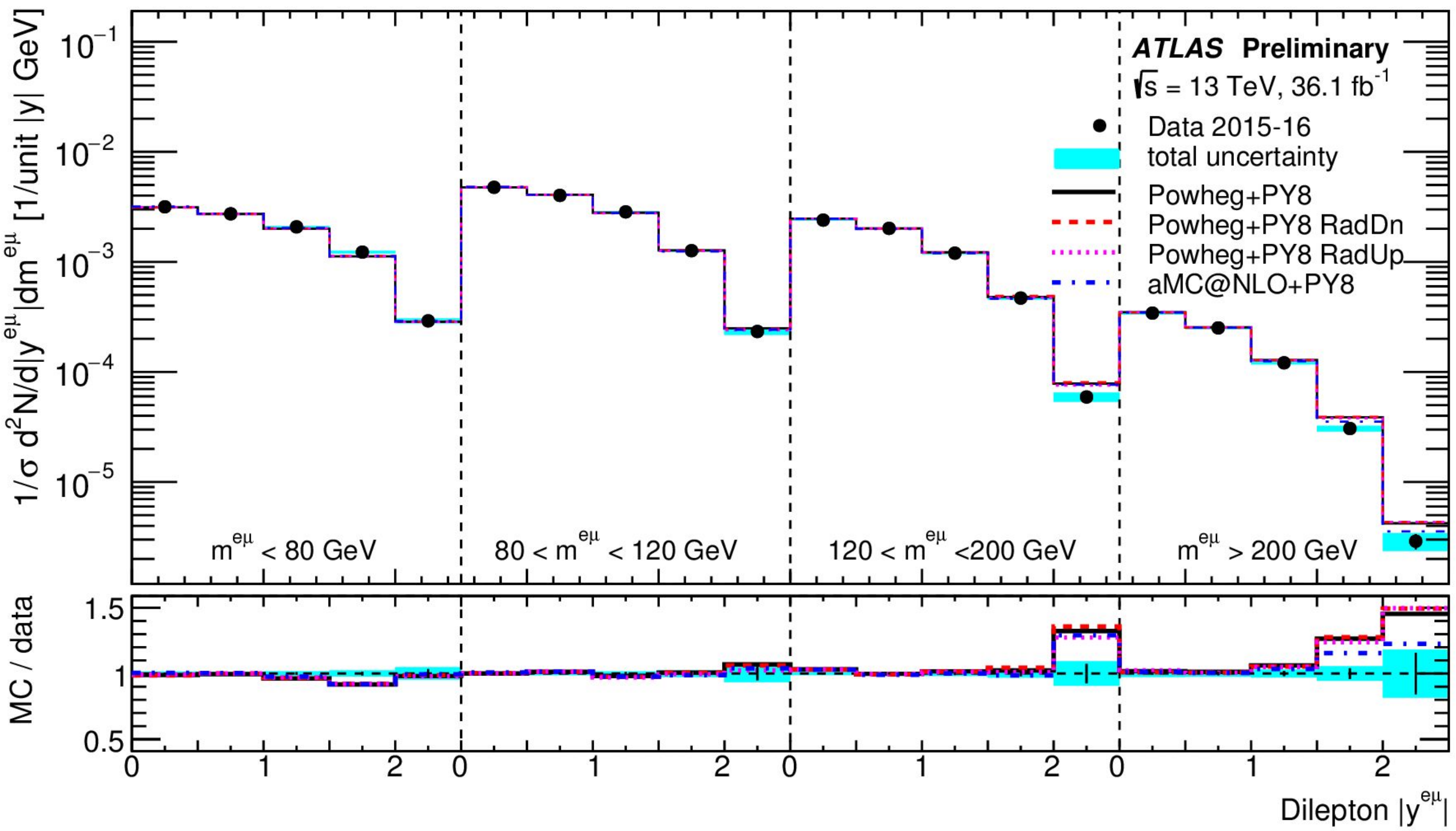

ATLAS Preliminary
√s = 13 TeV, 36.1 fb-1
Data 2015-16
total uncertainty
Powheg+PY8
Powheg+PY8 RadDn
Powheg+PY8 RadUp
aMC@NLO+PY8
1/σ d2N/d|yeμ|dmeμ [1/unit |y| GeV]
meμ < 80 GeV
80 < meμ < 120 GeV
120 < meμ <200 GeV
meμ > 200 GeV
MC / data
Dilepton |yeμ|

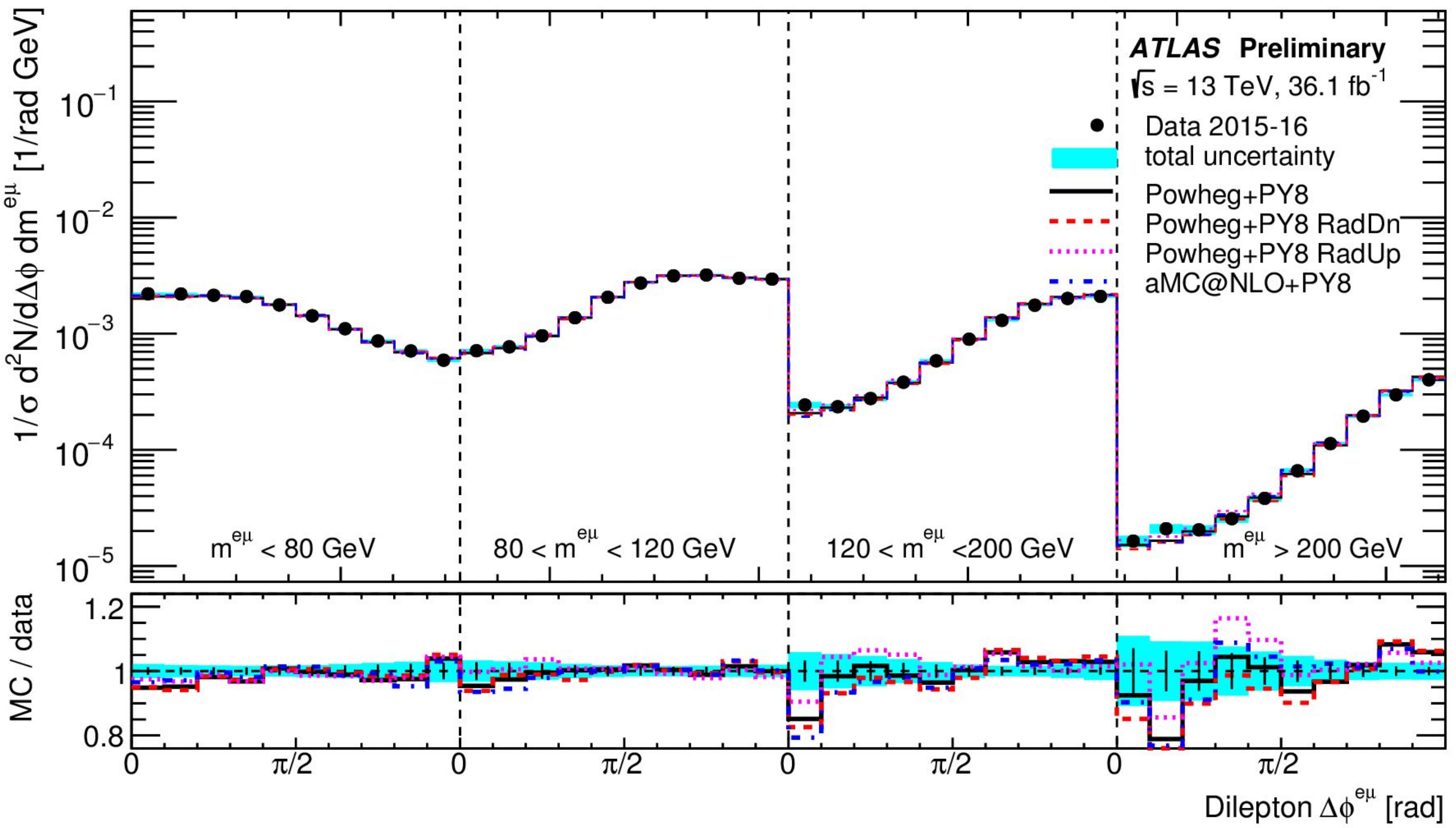

ATLAS Preliminary
$\sqrt{s}$ = 13 TeV, 36.1 fb^{-1}
Data 2015-16
total uncertainty
Powheg+PY8
Powheg+PY8 RadDn
Powheg+PY8 RadUp
aMC@NLO+PY8
$m^{e\mu}$ < 80 GeV
80 < $m^{e\mu}$ < 120 GeV
120 < $m^{e\mu}$ <200 GeV
$m^{e\mu}$ > 200 GeV
$1/\sigma\ d^2N/d\Delta\phi\ dm^{e\mu}$ [1/rad GeV]
MC / data
Dilepton $\Delta\phi^{e\mu}$ [rad]

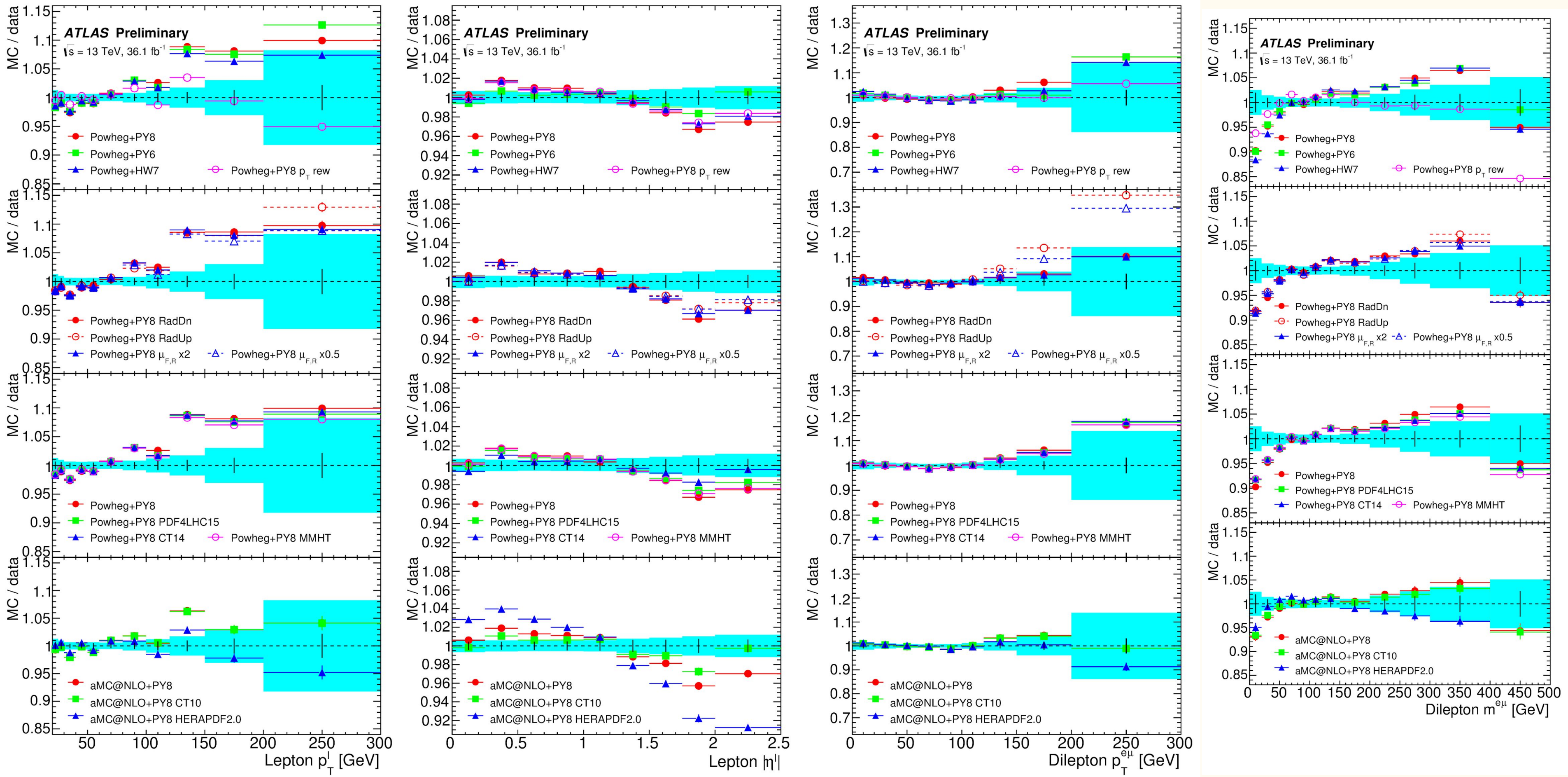
ATLAS Preliminary
$\sqrt{s}$ = 13 TeV, 36.1 fb^{-1}
MC / data
Powheg+PY8
Powheg+PY6
Powheg+HW7
Powheg+PY8 p_T rew
Powheg+PY8 RadDn
Powheg+PY8 RadUp
Powheg+PY8 $\mu_{F,R}$ x2
Powheg+PY8 $\mu_{F,R}$ x0.5
Powheg+PY8 PDF4LHC15
Powheg+PY8 CT14
Powheg+PY8 MMHT
aMC@NLO+PY8
aMC@NLO+PY8 CT10
aMC@NLO+PY8 HERAPDF2.0
Lepton p_T^l [GeV]
Lepton $|\eta^l|$
Dilepton $p_T^{e\mu}$ [GeV]
Dilepton $m^{e\mu}$ [GeV]

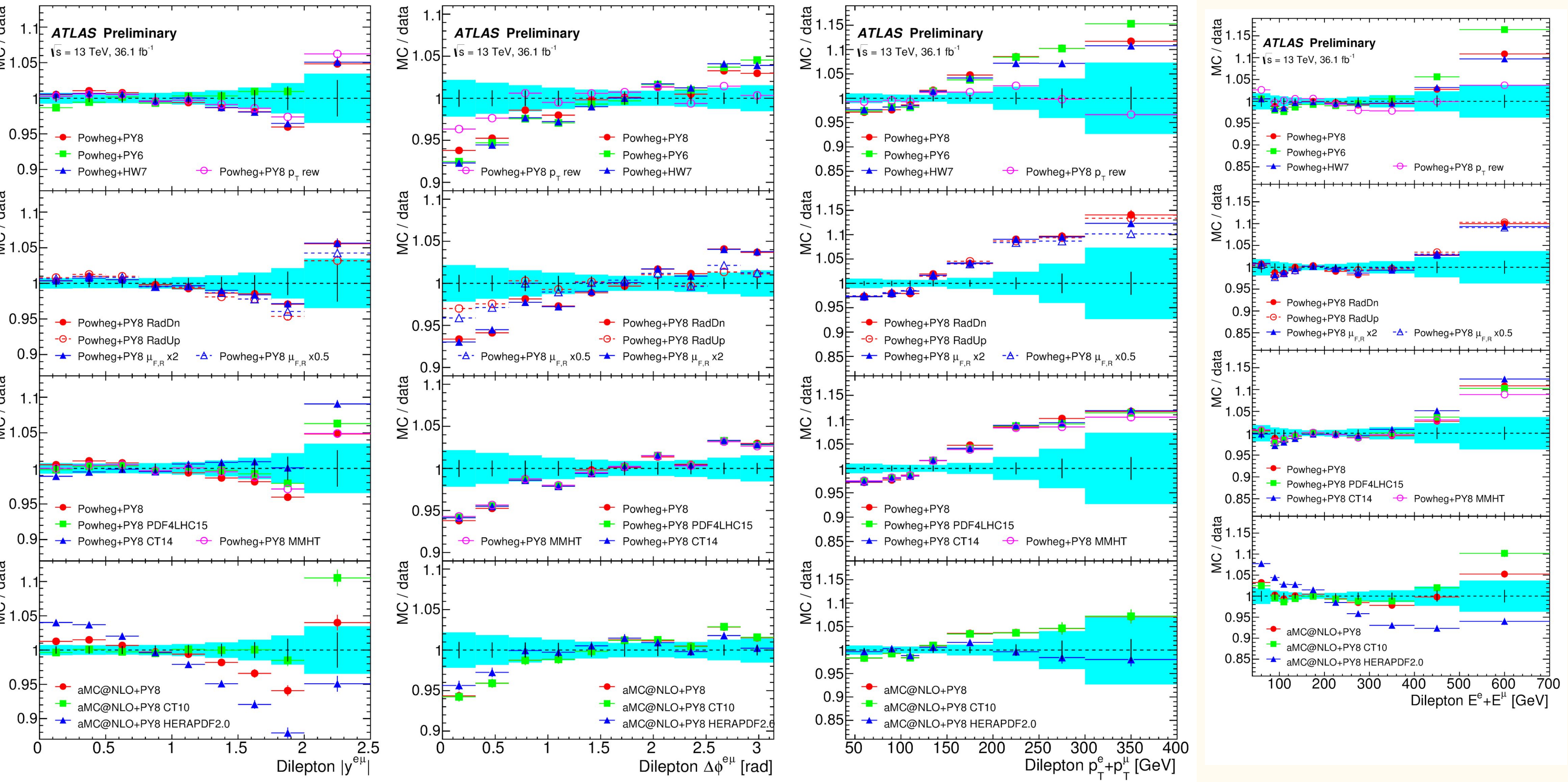

ATLAS Preliminary
√s = 13 TeV, 36.1 fb-1
MC / data
Powheg+PY8
Powheg+PY6
Powheg+HW7
Powheg+PY8 pT rew
Powheg+PY8 RadDn
Powheg+PY8 RadUp
Powheg+PY8 μF,R x2
Powheg+PY8 μF,R x0.5
Powheg+PY8 PDF4LHC15
Powheg+PY8 CT14
Powheg+PY8 MMHT
aMC@NLO+PY8
aMC@NLO+PY8 CT10
aMC@NLO+PY8 HERAPDF2.0
Dilepton |yeμ|
Dilepton Δφeμ [rad]
Dilepton pTe+pTμ [GeV]
Dilepton Ee+Eμ [GeV]

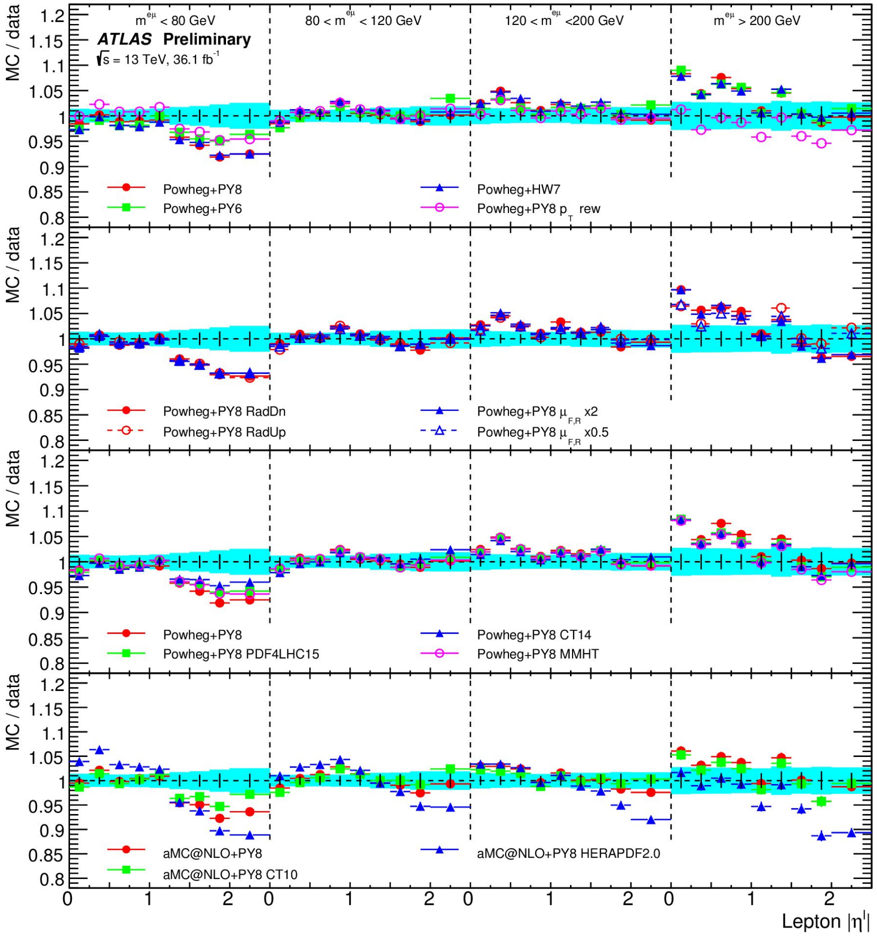

ATLAS Preliminary
$\sqrt{s}$ = 13 TeV, 36.1 fb^{-1}
$m^{e\mu}$ < 80 GeV
80 < $m^{e\mu}$ < 120 GeV
120 < $m^{e\mu}$ <200 GeV
$m^{e\mu}$ > 200 GeV
MC / data
Powheg+PY8
Powheg+PY6
Powheg+HW7
Powheg+PY8 p_T rew
Powheg+PY8 RadDn
Powheg+PY8 RadUp
Powheg+PY8 $\mu_{F,R}$ x2
Powheg+PY8 $\mu_{F,R}$ x0.5
Powheg+PY8 PDF4LHC15
Powheg+PY8 CT14
Powheg+PY8 MMHT
aMC@NLO+PY8
aMC@NLO+PY8 CT10
aMC@NLO+PY8 HERAPDF2.0
Lepton $|\eta^l|$

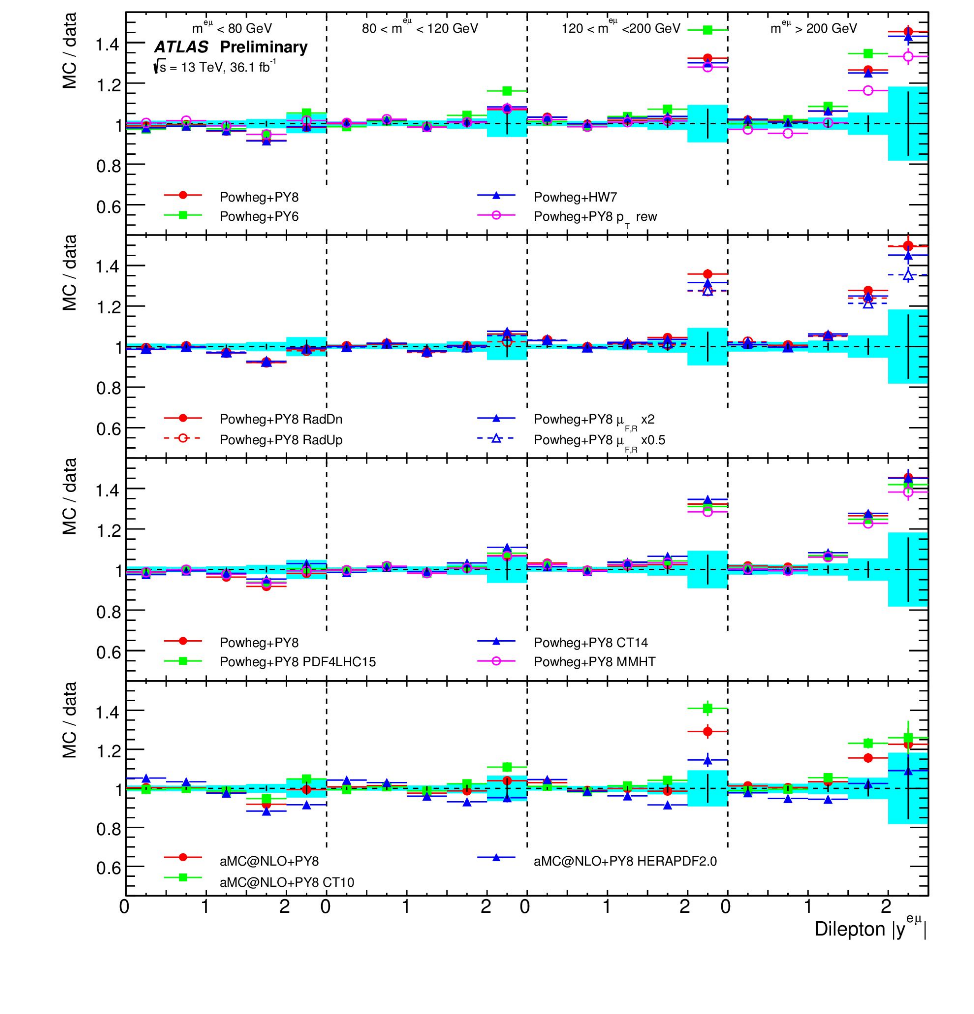
ATLAS Preliminary
$\sqrt{s}$ = 13 TeV, 36.1 fb^{-1}
$m^{e\mu}$ < 80 GeV
80 < $m^{e\mu}$ < 120 GeV
120 < $m^{e\mu}$ <200 GeV
$m^{e\mu}$ > 200 GeV
MC / data
Powheg+PY8
Powheg+PY6
Powheg+HW7
Powheg+PY8 p_T rew
Powheg+PY8 RadDn
Powheg+PY8 RadUp
Powheg+PY8 $\mu_{F,R}$ x2
Powheg+PY8 $\mu_{F,R}$ x0.5
Powheg+PY8 PDF4LHC15
Powheg+PY8 CT14
Powheg+PY8 MMHT
aMC@NLO+PY8
aMC@NLO+PY8 CT10
aMC@NLO+PY8 HERAPDF2.0
Dilepton $|y^{e\mu}|$

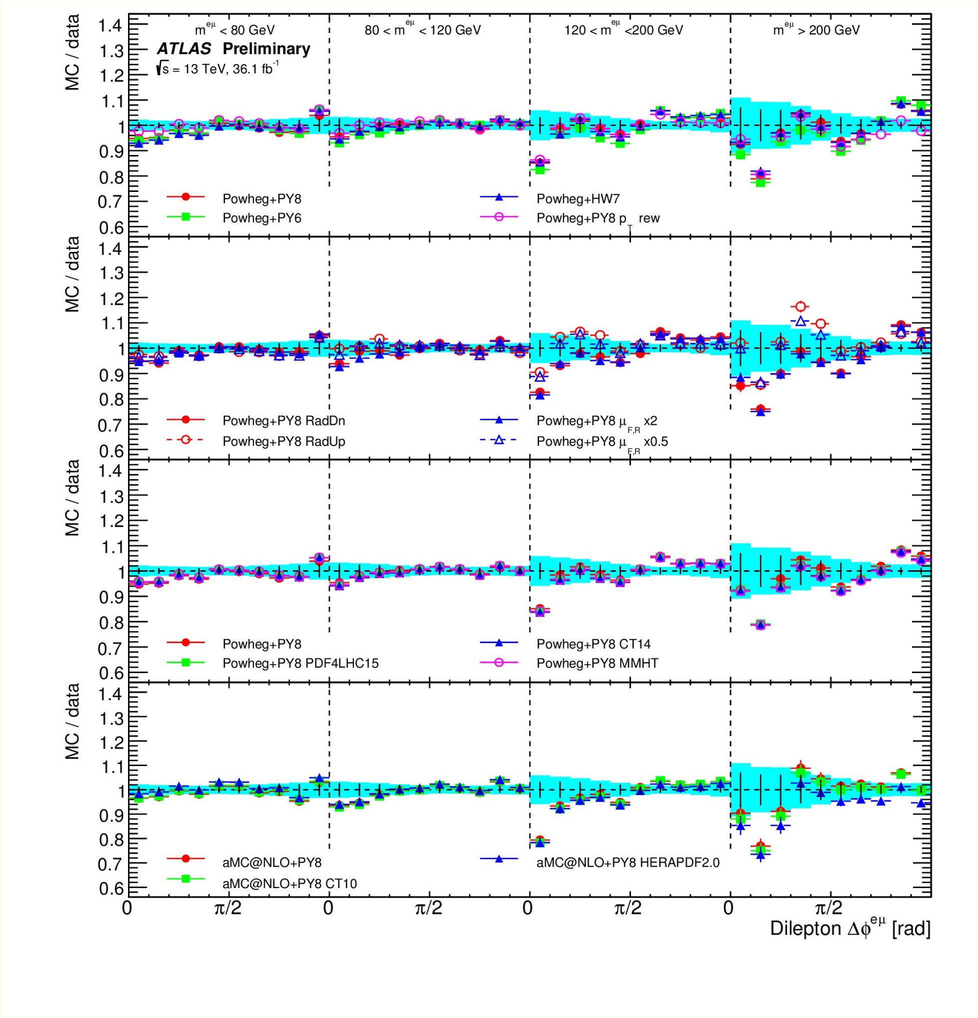

ATLAS Preliminary
$\sqrt{s}$ = 13 TeV, 36.1 fb^{-1}
$m^{e\mu}$ < 80 GeV
80 < $m^{e\mu}$ < 120 GeV
120 < $m^{e\mu}$ <200 GeV
$m^{e\mu}$ > 200 GeV
MC / data
Powheg+PY8
Powheg+PY6
Powheg+HW7
Powheg+PY8 p_T rew
Powheg+PY8 RadDn
Powheg+PY8 RadUp
Powheg+PY8 $\mu_{F,R}$ x2
Powheg+PY8 $\mu_{F,R}$ x0.5
Powheg+PY8
Powheg+PY8 PDF4LHC15
Powheg+PY8 CT14
Powheg+PY8 MMHT
aMC@NLO+PY8
aMC@NLO+PY8 CT10
aMC@NLO+PY8 HERAPDF2.0
Dilepton $\Delta\phi^{e\mu}$ [rad]

	Uncertainty source	$\Delta\epsilon_{e\mu}/\epsilon_{e\mu}$ (%)	$\Delta G_{e\mu}/G_{e\mu}$ (%)	$\Delta C_b/C_b$ (%)	$\Delta\sigma_{t\bar{t}}/\sigma_{t\bar{t}}$ (%)	$\Delta\sigma^{\rm fid}_{t\bar{t}}/\sigma^{\rm fid}_{t\bar{t}}$ (%)
	Data statistics				0.44	0.44
$t\bar{t}$ mod.	$t\bar{t}$ generator	0.38	0.05	0.05	0.43	0.10
	$t\bar{t}$ hadronisation	0.24	0.42	0.25	0.49	0.67
	Initial/final state radiation	0.30	0.26	0.16	0.45	0.41
	$t\bar{t}$ heavy-flavour production	0.01	0.01	0.26	0.26	0.26
	Parton distribution functions	0.44	0.05	-	0.45	0.07
	Simulation statistics	0.22	0.15	0.17	0.22	0.18
Lept.	Electron energy scale	0.06	0.06	-	0.06	0.06
	Electron energy resolution	0.01	0.01	-	0.01	0.01
	Electron identification	0.34	0.34	-	0.37	0.37
	Electron charge mis-id	0.09	0.09	-	0.10	0.10
	Electron isolation	0.22	0.22	-	0.24	0.24
	Muon momentum scale	0.03	0.03	-	0.03	0.03
	Muon momentum resolution	0.01	0.01	-	0.01	0.01
	Muon identification	0.28	0.28	-	0.30	0.30
	Muon isolation	0.16	0.16	-	0.18	0.18
	Lepton trigger	0.13	0.13	-	0.14	0.14
Jet/b	Jet energy scale	0.02	0.02	0.06	0.03	0.03
	Jet energy resolution	0.01	0.01	0.04	0.01	0.01
	Pileup jet veto	-	-	-	0.02	0.02
	b-tagging efficiency	-	-	0.04	0.20	0.20
	b-tag mistagging	-	-	0.06	0.06	0.06
Bkg.	Single top cross-section	-	-	-	0.52	0.52
	Single-top/$t\bar{t}$ interference	-	-	-	0.15	0.15
	Single top modelling	-	-	-	0.34	0.34
	Z+jets extrapolation	-	-	-	0.09	0.09
	Diboson cross-sections	-	-	-	0.02	0.02
	Diboson modelling	-	-	-	0.03	0.03
	Misidentified leptons	-	-	-	0.43	0.43
	Analysis systematics	0.91	0.75	0.44	1.39	1.31
$L/E_{\rm b}$	Integrated luminosity	-	-	-	1.90	1.90
	Beam energy	-	-	-	0.23	0.23
	Total uncertainty	0.91	0.75	0.44	2.40	2.36

Dataset	$\sigma_{t\bar{t}}$ [pb]	$\sigma_{t\bar{t}}^{\mathrm{fid}}$ [pb]
All data	$830.7 \pm 2.2 \pm 11.6 \pm 18.4 \pm 1.9\ (22.0)$	$14.14 \pm 0.04 \pm 0.19 \pm 0.31 \pm 0.03\ (0.37)$
2015 data	$820.9 \pm 6.9 \pm 11.9 \pm 18.4 \pm 1.9\ (23.1)$	$13.98 \pm 0.12 \pm 0.19 \pm 0.31 \pm 0.03\ (0.39)$
2016 data	$831.8 \pm 2.3 \pm 11.6 \pm 19.5 \pm 1.9\ (22.9)$	$14.16 \pm 0.04 \pm 0.19 \pm 0.33 \pm 0.03\ (0.39)$
Combination	$826.4 \pm 3.6 \pm 11.5 \pm 15.7 \pm 1.9\ (19.9)$	$14.07 \pm 0.06 \pm 0.18 \pm 0.27 \pm 0.03\ (0.33)$

	Matrix element	PDF	Parton shower/tune	Comments
1	Powheg	NNPDF3.0	Pythia8 A14	$h_{\mathrm{damp}} = \frac{3}{2}m_t$
	Powheg	CT10	Pythia6 P2012	$h_{\mathrm{damp}} = m_t$
	Powheg	NNPDF3.0	Herwig7 H7UE	$h_{\mathrm{damp}} = \frac{3}{2}m_t$
	Powheg	NNPDF3.0	Pythia8 A14	top quark p_{T} reweighted to [87]
2	Powheg	NNPDF3.0	Pythia8 A14v3cDo	$h_{\mathrm{damp}} = \frac{3}{2}m_t$, $2\mu_{\mathrm{F,R}}$ (RadDn)
	Powheg	NNPDF3.0	Pythia8 A14v3cUp	$h_{\mathrm{damp}} = 3m_t$, $\frac{1}{2}\mu_{\mathrm{F,R}}$ (RadUp)
	Powheg	NNPDF3.0	Pythia8 A14	$h_{\mathrm{damp}} = \frac{3}{2}m_t$, $2\mu_{\mathrm{F,R}}$
	Powheg	NNPDF3.0	Pythia8 A14	$h_{\mathrm{damp}} = \frac{3}{2}m_t$, $\frac{1}{2}\mu_{\mathrm{F,R}}$
3	Powheg	NNPDF3.0	Pythia8 A14	$h_{\mathrm{damp}} = \frac{3}{2}m_t$
	Powheg	PDF4LHC15	Pythia8 A14	$h_{\mathrm{damp}} = \frac{3}{2}m_t$
	Powheg	CT14	Pythia8 A14	$h_{\mathrm{damp}} = \frac{3}{2}m_t$
	Powheg	MMHT	Pythia8 A14	$h_{\mathrm{damp}} = \frac{3}{2}m_t$
4	aMC@NLO	NNPDF3.0	Pythia8 A14	
	aMC@NLO	CT10	Pythia8 A14	
	aMC@MLO	HERAPDF2.0	Pythia8 A14	

Generator	p_{T}^{ℓ}	$\lvert\eta^{\ell}\rvert$	$p_{\mathrm{T}}^{e\mu}$	$m^{e\mu}$	$\lvert y^{e\mu}\rvert$	$\Delta\phi^{e\mu}$	$p_{\mathrm{T}}^{e}+p_{\mathrm{T}}^{\mu}$	$E^{e}+E^{\mu}$
N_{dof}	10	8	8	11	8	9	7	9
Powheg + PY8	43.7	19.5	8.6	44.3	11.4	14.4	32.5	18.4
Powheg + PY6 CT10	36.1	7.9	9.3	33.0	16.2	16.2	21.9	30.5
Powheg + HW7	34.8	15.9	11.5	62.7	9.4	17.3	23.0	14.7
Powheg + PY8 p_{T} rew.	20.2	14.7	2.3	38.3	8.4	12.7	9.4	14.0
Powheg + PY8 RadDn	40.0	24.2	6.1	44.3	9.2	16.3	29.0	20.1
Powheg + PY8 RadUp	33.0	16.3	21.9	35.3	12.3	6.4	26.7	16.5
Powheg + PY8 $\mu_{\mathrm{F,R}}\times 2$	46.5	21.6	6.2	42.6	8.5	16.5	28.9	17.1
Powheg + PY8 $\mu_{\mathrm{F,R}}\times 0.5$	39.8	17.3	11.4	38.0	10.7	10.9	27.6	14.2
Powheg + PY8 PDF4LHC15	43.4	14.6	7.4	39.0	6.2	13.5	28.0	15.9
Powheg + PY8 CT14	44.1	9.3	7.6	37.0	8.2	13.5	28.5	18.2
Powheg + PY8 MMHT	41.2	17.7	6.9	39.0	6.3	13.2	26.3	14.3
aMC@NLO + PY8	26.2	25.7	11.4	19.7	16.7	13.2	12.5	14.0
aMC@NLO + PY8 CT10	24.9	11.7	10.6	16.9	10.0	13.4	12.0	19.0
aMC@NLO + PY8 HERA2	17.1	96.6	6.9	26.0	68.5	12.5	6.1	38.4
Powheg + PY8	$4\cdot10^{-6}$	0.012	0.37	$6\cdot10^{-6}$	0.18	0.11	$3\cdot10^{-5}$	0.030
Powheg + PY6 CT10	$8\cdot10^{-5}$	0.45	0.32	$5\cdot10^{-4}$	0.039	0.062	$3\cdot10^{-3}$	$4\cdot10^{-4}$
Powheg + HW7	$1\cdot10^{-4}$	0.043	0.18	$3\cdot10^{-9}$	0.31	0.045	$2\cdot10^{-3}$	0.098
Powheg + PY8 p_{T} rew.	0.028	0.065	0.97	$7\cdot10^{-5}$	0.39	0.18	0.23	0.12
Powheg + PY8 RadDn	$2\cdot10^{-5}$	$2\cdot10^{-3}$	0.64	$6\cdot10^{-6}$	0.32	0.060	$1\cdot10^{-4}$	0.017
Powheg + PY8 RadUp	$3\cdot10^{-4}$	0.038	$5\cdot10^{-3}$	$2\cdot10^{-4}$	0.14	0.70	$4\cdot10^{-4}$	0.057
Powheg + PY8 $\mu_{\mathrm{F,R}}\times 2$	$1\cdot10^{-6}$	$6\cdot10^{-3}$	0.62	$1\cdot10^{-5}$	0.39	0.056	$1\cdot10^{-4}$	0.048
Powheg + PY8 $\mu_{\mathrm{F,R}}\times 0.5$	$2\cdot10^{-5}$	0.027	0.18	$8\cdot10^{-5}$	0.22	0.28	$3\cdot10^{-4}$	0.12
Powheg + PY8 PDF4LHC15	$4\cdot10^{-6}$	0.067	0.49	$5\cdot10^{-5}$	0.62	0.14	$2\cdot10^{-4}$	0.068
Powheg + PY8 CT14	$3\cdot10^{-6}$	0.32	0.47	$1\cdot10^{-4}$	0.42	0.14	$2\cdot10^{-4}$	0.033
Powheg + PY8 MMHT	$1\cdot10^{-5}$	0.024	0.55	$5\cdot10^{-5}$	0.62	0.15	$5\cdot10^{-4}$	0.11
aMC@NLO + PY8	$3\cdot10^{-3}$	$1\cdot10^{-3}$	0.18	0.049	0.034	0.15	0.086	0.12
aMC@NLO + PY8 CT10	$5\cdot10^{-3}$	0.16	0.23	0.11	0.27	0.15	0.10	0.025
aMC@NLO + PY8 HERA2	0.073	0	0.54	$6\cdot10^{-3}$	0	0.19	0.53	$1\cdot10^{-5}$

Generator	$\lvert\eta^{\ell}\rvert \times m^{e\mu}$	$\lvert y^{e\mu}\rvert \times m^{e\mu}$	$\lvert\Delta\phi^{\ell}\rvert \times m^{e\mu}$
N_{dof}	35	19	39
POWHEG + PY8	53.1	72.3	65.4
POWHEG + PY6 CT10	45.9	92.9	79.5
POWHEG + HW7	49.3	67.4	63.7
POWHEG + PY8 p_{T} rew.	47.1	56.1	51.4
POWHEG + PY8 RadDn	57.1	74.2	69.9
POWHEG + PY8 RadUp	50.6	62.5	51.7
POWHEG + PY8 $\mu_{\mathrm{F,R}} \times 2$	60.7	68.4	71.1
POWHEG + PY8 $\mu_{\mathrm{F,R}} \times 0.5$	50.3	60.0	52.0
POWHEG + PY8 PDF4LHC15	51.5	61.5	59.7
POWHEG + PY8 CT14	50.6	67.3	60.0
POWHEG + PY8 MMHT	53.7	57.9	58.7
aMC@NLO + PY8	55.0	45.9	58.2
aMC@NLO + PY8 CT10	43.7	50.6	59.5
aMC@NLO + PY8 HERA2	130.3	97.6	58.0
POWHEG + PY8	0.026	$4 \cdot 10^{-8}$	$5 \cdot 10^{-3}$
POWHEG + PY6 CT10	0.10	0	$1 \cdot 10^{-4}$
POWHEG + HW7	0.055	$2 \cdot 10^{-7}$	$8 \cdot 10^{-3}$
POWHEG + PY8 p_{T} rew.	0.084	$2 \cdot 10^{-5}$	0.088
POWHEG + PY8 RadDn	0.011	$2 \cdot 10^{-8}$	$2 \cdot 10^{-3}$
POWHEG + PY8 RadUp	0.042	$2 \cdot 10^{-6}$	0.083
POWHEG + PY8 $\mu_{\mathrm{F,R}} \times 2$	$5 \cdot 10^{-3}$	$2 \cdot 10^{-7}$	$1 \cdot 10^{-3}$
POWHEG + PY8 $\mu_{\mathrm{F,R}} \times 0.5$	0.045	$4 \cdot 10^{-6}$	0.079
POWHEG + PY8 PDF4LHC15	0.036	$2 \cdot 10^{-6}$	0.018
POWHEG + PY8 CT14	0.042	$3 \cdot 10^{-7}$	0.017
POWHEG + PY8 MMHT	0.023	$8 \cdot 10^{-6}$	0.022
aMC@NLO + PY8	0.017	$5 \cdot 10^{-4}$	0.024
aMC@NLO + PY8 CT10	0.15	$1 \cdot 10^{-4}$	0.019
aMC@NLO + PY8 HERA2	0	0	0.026

Generator	p_{T}^{ℓ}, $p_{\mathrm{T}}^{e}+p_{\mathrm{T}}^{\mu}$	$p_{\mathrm{T}}^{e\mu}$, $m^{e\mu}$, $p_{\mathrm{T}}^{e}+p_{\mathrm{T}}^{\mu}$	$\lvert\eta^{\ell}\rvert$, $\lvert y^{e\mu}\rvert$	$\lvert\eta^{\ell}\rvert$, $\lvert y^{e\mu}\rvert$, $E^{e}+E^{\mu}$	All 8 dists.
N_{dof}	17	26	16	25	70
Powheg + PY8	52.2	92.8	31.2	51.5	176.5
Powheg + PY6 CT10	42.9	87.9	31.0	58.0	176.6
Powheg + HW7	42.5	97.4	25.7	41.6	169.8
Powheg + PY8 p_{T} rew.	27.5	57.4	25.4	36.5	137.6
Powheg + PY8 RadDn	49.7	110.8	37.8	58.3	193.9
Powheg + PY8 RadUp	42.9	71.8	25.5	44.2	151.8
Powheg + PY8 $\mu_{\mathrm{F,R}} \times 2$	54.5	111.1	35.6	54.4	195.0
Powheg + PY8 $\mu_{\mathrm{F,R}} \times 0.5$	50.5	71.3	26.3	42.8	160.4
Powheg + PY8 PDF4LHC15	52.2	89.7	26.7	44.1	167.1
Powheg + PY8 CT14	52.9	91.5	26.6	44.8	170.2
Powheg + PY8 MMHT	49.9	89.4	28.7	44.8	167.6
aMC@NLO + PY8	33.2	46.3	37.1	49.6	131.9
aMC@NLO + PY8 CT10	31.6	46.7	26.2	43.0	122.9
aMC@NLO + PY8 HERA2	23.1	51.5	119.0	132.8	229.8
Powheg + PY8	$2 \cdot 10^{-5}$	$2 \cdot 10^{-9}$	0.013	$1 \cdot 10^{-3}$	0
Powheg + PY6 CT10	$5 \cdot 10^{-4}$	$1 \cdot 10^{-8}$	0.014	$2 \cdot 10^{-4}$	0
Powheg + HW7	$6 \cdot 10^{-4}$	$3 \cdot 10^{-10}$	0.058	0.020	$3 \cdot 10^{-10}$
Powheg + PY8 p_{T} rew.	0.052	$4 \cdot 10^{-4}$	0.062	0.064	$3 \cdot 10^{-6}$
Powheg + PY8 RadDn	$5 \cdot 10^{-5}$	0	$2 \cdot 10^{-3}$	$2 \cdot 10^{-4}$	0
Powheg + PY8 RadUp	$5 \cdot 10^{-4}$	$4 \cdot 10^{-6}$	0.062	0.010	$6 \cdot 10^{-8}$
Powheg + PY8 $\mu_{\mathrm{F,R}} \times 2$	$8 \cdot 10^{-6}$	0	$3 \cdot 10^{-3}$	$6 \cdot 10^{-4}$	0
Powheg + PY8 $\mu_{\mathrm{F,R}} \times 0.5$	$4 \cdot 10^{-5}$	$4 \cdot 10^{-6}$	0.049	0.015	$5 \cdot 10^{-9}$
Powheg + PY8 PDF4LHC15	$2 \cdot 10^{-5}$	$6 \cdot 10^{-9}$	0.045	0.011	$7 \cdot 10^{-10}$
Powheg + PY8 CT14	$2 \cdot 10^{-5}$	$3 \cdot 10^{-9}$	0.046	$9 \cdot 10^{-3}$	$3 \cdot 10^{-10}$
Powheg + PY8 MMHT	$4 \cdot 10^{-5}$	$7 \cdot 10^{-9}$	0.026	$9 \cdot 10^{-3}$	$6 \cdot 10^{-10}$
aMC@NLO + PY8	0.011	$9 \cdot 10^{-3}$	$2 \cdot 10^{-3}$	$2 \cdot 10^{-3}$	$1 \cdot 10^{-5}$
aMC@NLO + PY8 CT10	0.017	$8 \cdot 10^{-3}$	0.051	0.014	$1 \cdot 10^{-4}$
aMC@NLO + PY8 HERA2	0.14	$2 \cdot 10^{-3}$	0	0	0

Measurement of the top quark mass using a dileptonic invariant mass in pp collisions at $\sqrt{s} = 13$ TeV with the ATLAS detector

ATLAS-CONF-2019-046

36/fb @ 13 TeV

Matrix Method

ATLAS-CONF-2014-058

$$
\begin{aligned}
N^{\mathrm{l}} &= N^{\mathrm{l}}_{\mathrm{r}} + N^{\mathrm{l}}_{\mathrm{f}}, \\
N^{\mathrm{t}} &= \varepsilon_{\mathrm{r}} N^{\mathrm{l}}_{\mathrm{r}} + \varepsilon_{\mathrm{f}} N^{\mathrm{l}}_{\mathrm{f}},
\end{aligned}
$$

$$
N^{\mathrm{t}}_{\mathrm{f}} = \frac{\varepsilon_{\mathrm{f}}}{\varepsilon_{\mathrm{r}} - \varepsilon_{\mathrm{f}}} \left(\varepsilon_{\mathrm{r}} N^{\mathrm{l}} - N^{\mathrm{t}} \right)
$$

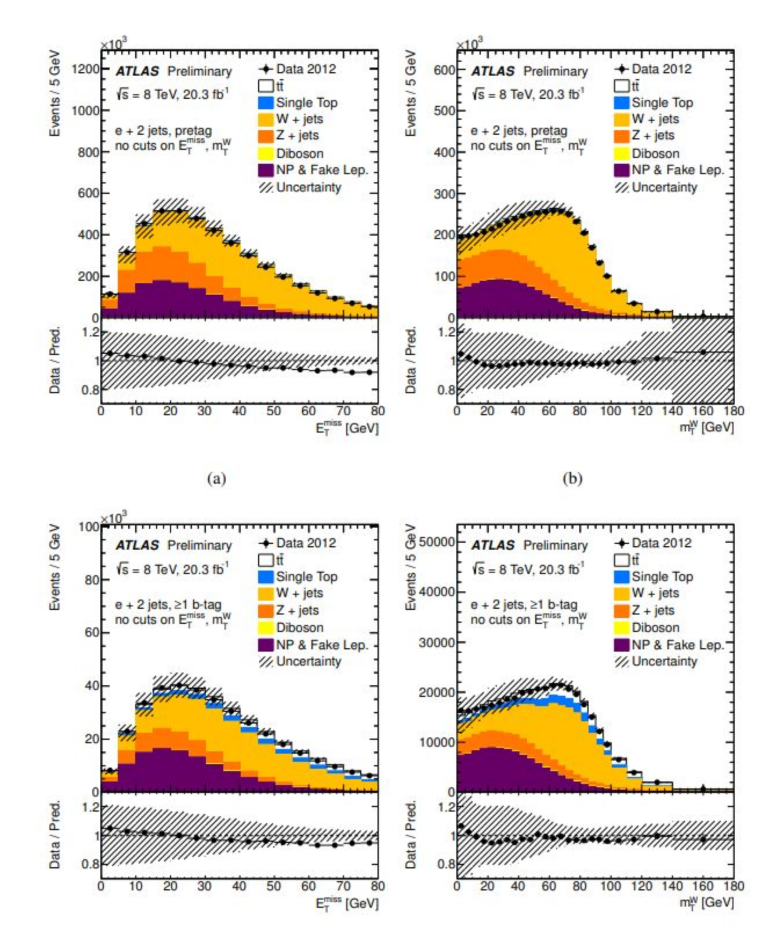

W+jets background measurement

Explained in detail in [this paper]

$$N_{W^+} + N_{W^-} = \left(\frac{r_{\mathrm{MC}} + 1}{r_{\mathrm{MC}} - 1}\right)(D_+ - D_-)$$

data yields

W^+/W^- xsec ratio

Wb/Wc/Wcc/Wlight composition estimated in data control sample with exactly two jets

Source	Unc. on m_t [GeV]	Stat. precision [GeV]
Data statistics	0.40	
Signal and background model statistics	0.16	
Monte Carlo generator	0.04	± 0.07
Parton shower and hadronisation	0.07	± 0.07
Initial-state QCD radiation	0.17	± 0.07
Parton shower α_S^{FSR}	0.09	± 0.04
b-quark fragmentation	0.19	± 0.02
HF-hadron production fractions	0.11	± 0.01
HF-hadron decay modelling	0.39	± 0.01
Underlying event	< 0.01	± 0.02
Colour reconnection	< 0.01	± 0.02
Choice of PDFs	0.06	± 0.01
W/Z+jets modelling	0.17	± 0.01
Single top modelling	0.01	± 0.01
Fake lepton modelling ($t \to W \to \ell$)	0.06	± 0.02
Soft muon fake modelling	0.15	± 0.03
Jet energy scale	0.12	± 0.02
Soft muon jet $\mathrm{p_T}$ calibration	< 0.01	± 0.01
Jet energy resolution	0.07	± 0.05
Jet vertex tagger	< 0.01	± 0.01
b-tagging	0.10	± 0.01
Leptons	0.12	± 0.00
Missing transverse momentum modelling	0.15	± 0.01
Pile-up	0.20	± 0.05
Luminosity	< 0.01	± 0.01
Total systematic uncertainty	0.67	± 0.04
Total uncertainty	0.78	± 0.03

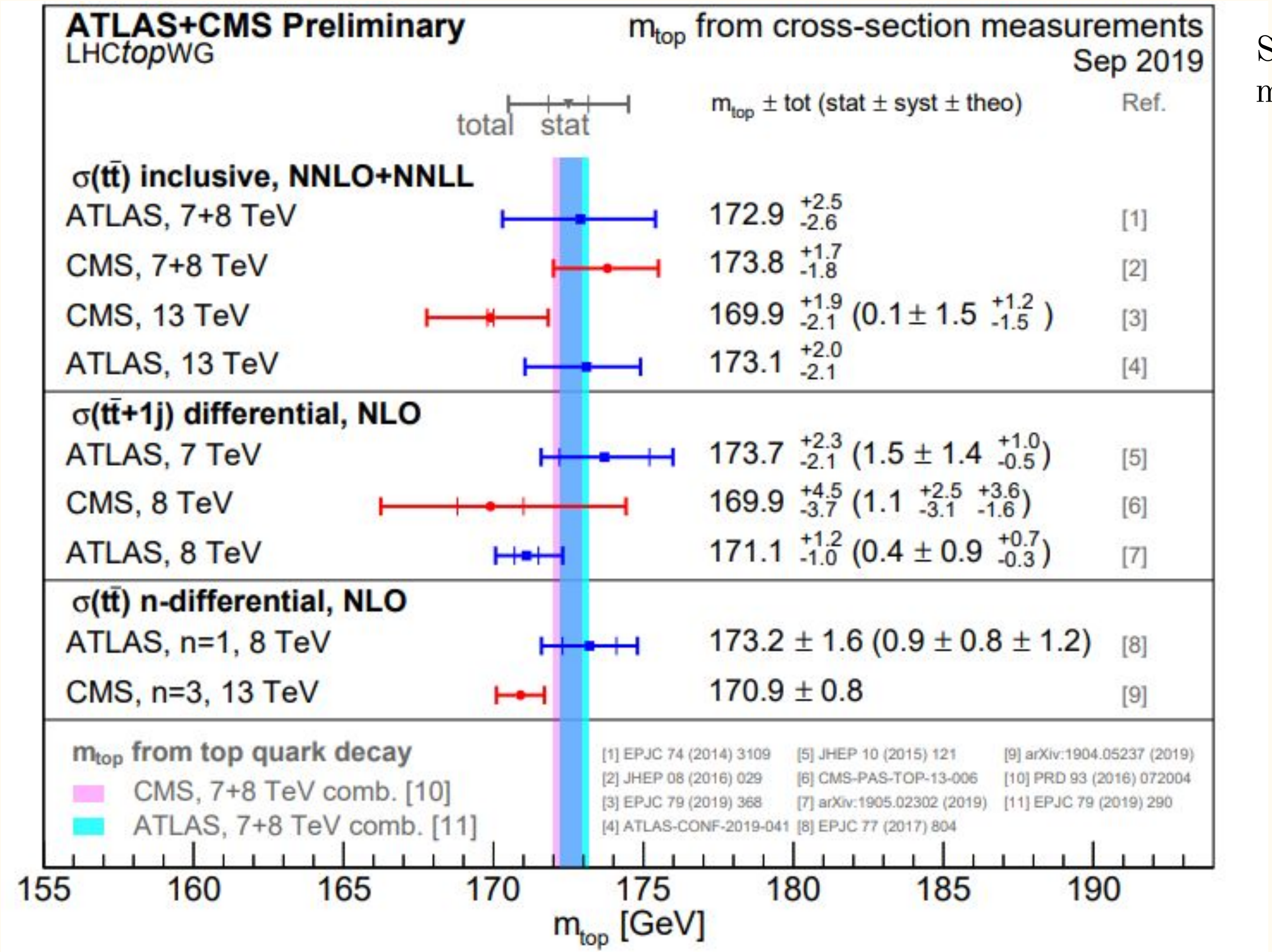

Summary of “indirect” top mass measurements

ℓ+jets channel: ATLAS 8 TeV

- 1 high-pt isolated e/mu, >=4 jets, =2 b-jets
- Topology reconstruction: KLFitter
  $L(m_t^{reco})$ maximised to assign jets to partons
- observables:
  - m_{top}^{reco}
  - m_W^{reco} → Jet Energy Scale
  - $R_{bq}^{reco} = (p_T^{b\text{-}lep} + p_T^{b\text{-}had}) / (p_T^{q1} + p_T^{q2})$ → b-Jet Energy Scale
- selection on BDT score
  - kinematics used against wrong topological reconstruction

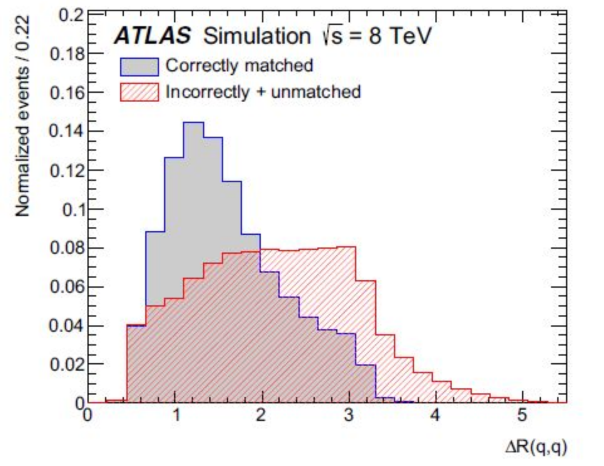

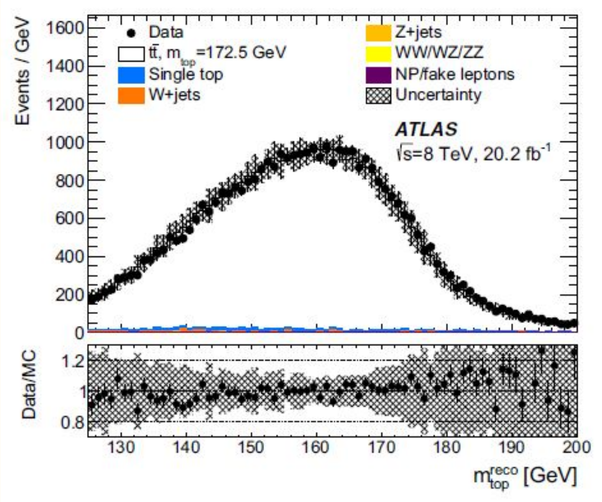

Eur. Phys. J. C79 (2019) 290

ℓ+jets channel: ATLAS 8 TeV

Eur. Phys. J. C79 (2019) 290

- 3-dimensional template fit to the 3 observables, templates as a function of m_t^{MC}

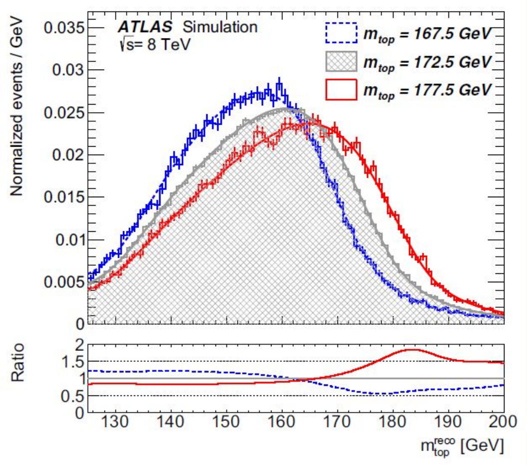

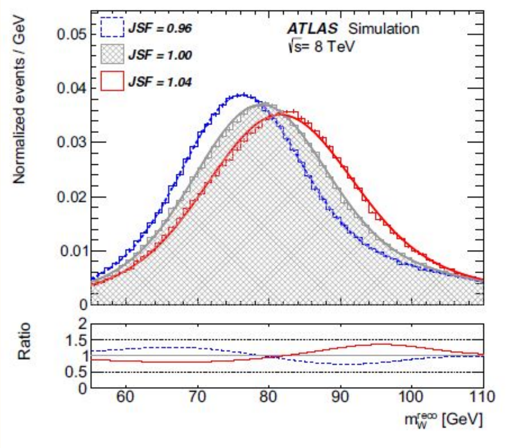

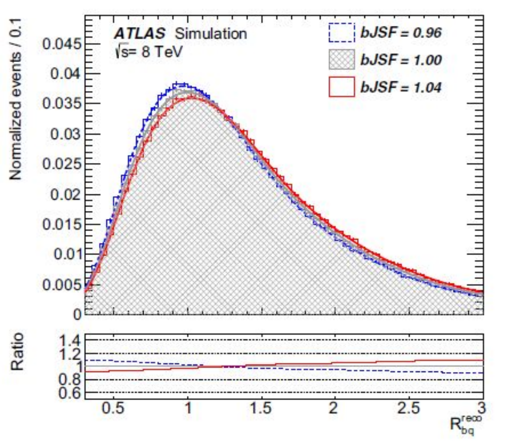

$$m_{\text{top}} = 172.08 \pm 0.39\,(\text{stat})\ \text{GeV},$$
$$\text{JSF} = 1.005 \quad \pm 0.001\,(\text{stat}), \quad \text{and}$$
$$\text{bJSF} = 1.008 \quad \pm 0.005\,(\text{stat}).$$

$$m_{\text{top}} = 172.08 \pm 0.39\,(\text{stat}) \pm 0.82\,(\text{syst})\ \text{GeV}$$

Dominant systematics:

- Jet Energy Scale: 0.58 GeV
- b-tagging: 0.38 GeV

ℓ+jets channel: ATLAS 8 TeV

Eur. Phys. J. C79 (2019) 290

Anti-correlation of systematics in different analyses -> combination!

Dominant uncertainties after the combination:

- ME generator: 0.12 GeV
  - aMC@NLO vs Powheg
- Jet Energy Scale: 0.22 GeV
- b-Jet Energy Scale: 0.17 GeV
- b-tagging: 0.17 GeV

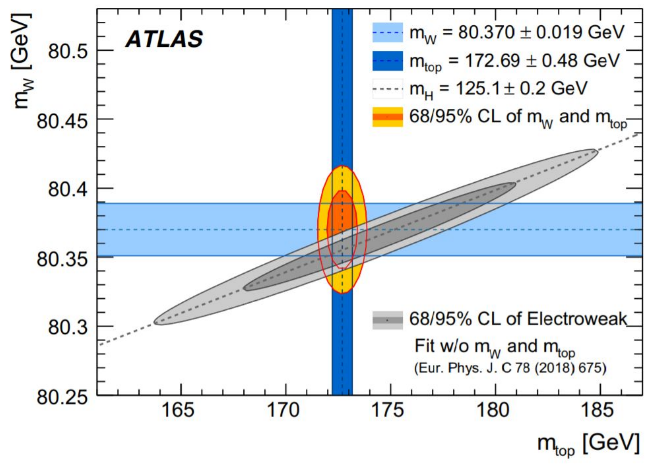

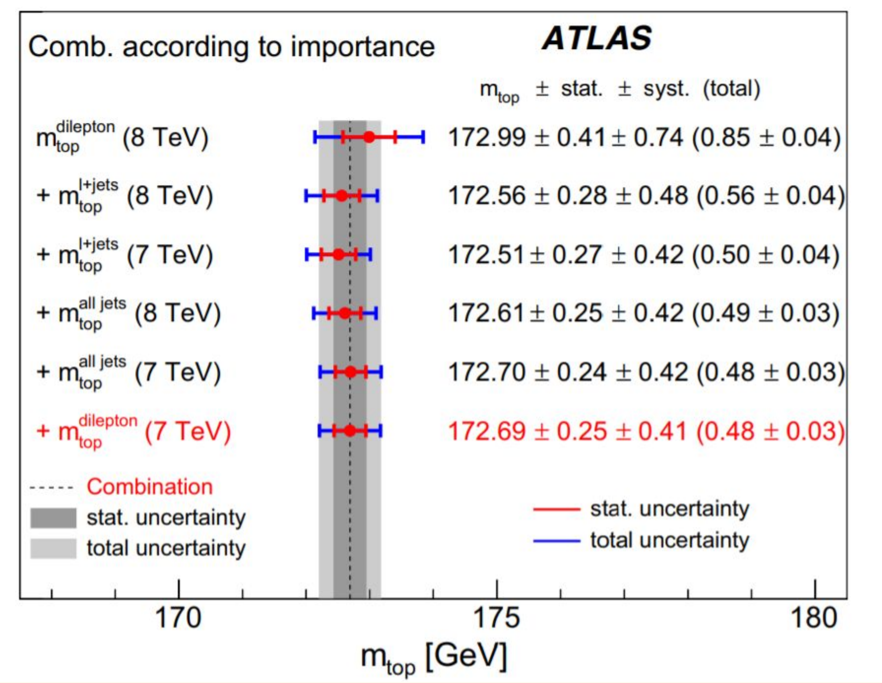

Inclusive and differential measurement of the charge asymmetry in ttbar events ATLAS-CONF-2019-026

139/fb @ 13 TeV

Track assisted mass and combined mass

Calo-based mass

$$m^{\mathrm{calo}} = \sqrt{\left(\sum_{i\in J} E_i\right)^2 - \left(\sum_{i\in J} \vec{p}_i\right)^2}$$

Track-assisted mass

$$m^{\mathrm{TA}} = m^{\mathrm{track}} \times \frac{p_{\mathrm{T}}^{\mathrm{calo}}}{p_{\mathrm{T}}^{\mathrm{track}}}$$

Helps at high-p_T, where calo granularity becomes a limit for m^{calo}

Combined mass: average weighted by relative resolutions

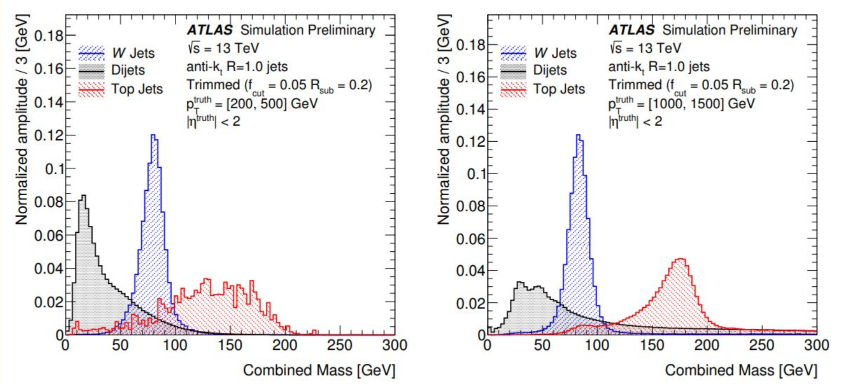

ATLAS-CONF-2017-064

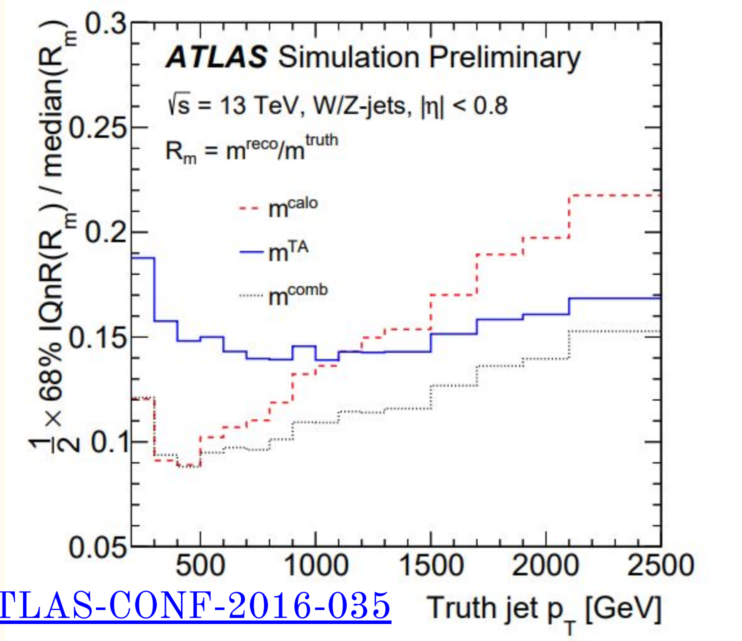

ATLAS-CONF-2016-035

Top Tagging

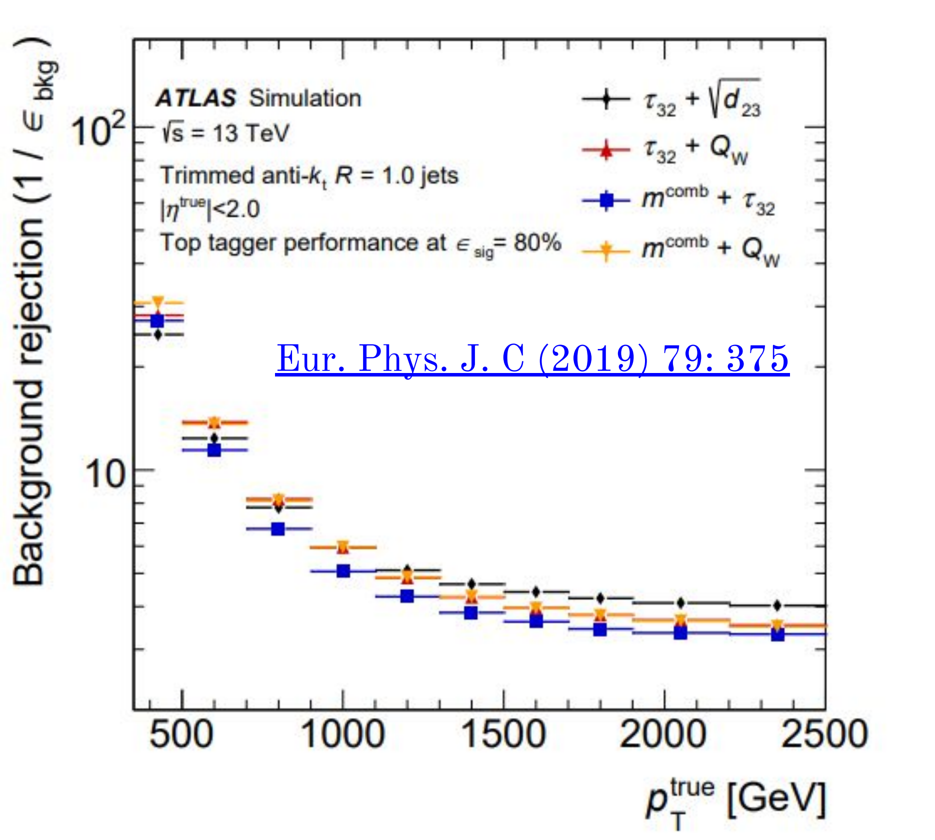

[Eur. Phys. J. C (2019) 79: 375]

Charge asymmetry: resolved selection

- $>=4$ small-R jets $p_T>25$ GeV
- MV2c10 tagging @ 77% ε_b
  - events divided into $N_{b\text{-tag}}=1$ or 2
- topology reconstruction: need to assign jets to corresponding partons
- Boosted Decision Tree used
  - uses KLFitter, likelihood based topology reconstruction algorithm, as one of the inputs
  - tries all permutations of $<=5$ jets
  - trained on ttbar MC
- Highest BDT-score permutation used
- $BDT_{score}>0.3$ cut applied
  - S/B improves factor 2
  - 75% ttbar events correctly assign.

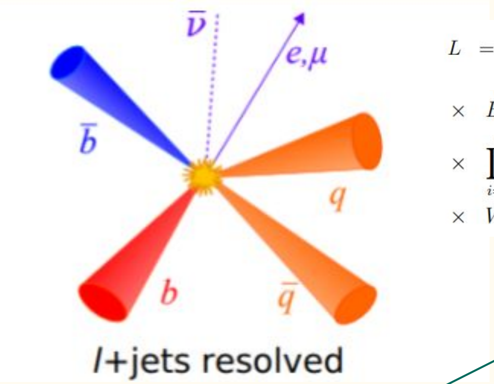

$$
\begin{aligned}
L \;=\; & B(m_{q_1q_2q_3}|m_{\text{top}},\Gamma_{\text{top}}) \cdot \exp\left(-4\cdot\ln 2\cdot\frac{(m_{q_1q_2}-m_{\text{W}})^2}{\Gamma_{\text{W}}^2}\right) \\
\times\; & B(m_{q_4\ell\nu}|m_{\text{top}},\Gamma_{\text{top}}) \cdot B(m_{\ell\nu}|m_{\text{W}},\Gamma_{\text{W}}) \\
\times\; & \prod_{i=1}^{4} W_{\text{jet}}(E^{\text{meas}}_{\text{jet},i}|E_{\text{jet},i}) \cdot W_{\ell}(E^{\text{meas}}_{\ell}|E_{\ell}) \\
\times\; & W_{\text{miss}}(E^{\text{miss}}_{x}|p^{\nu}_{x}) \cdot W_{\text{miss}}(E^{\text{miss}}_{y}|p^{\nu}_{y}) \,,
\end{aligned}
$$

- m^{reco}(had. top)
- $\ln(L_{KLFitter})$
- m^{reco}(had. W)
- b-tagging info jets assigned to lep./had. top
- light-jet from hadronic W
- m^{reco}(lep. top)
- ΔR(b-jet of lep. top,lepton)
- ΔR(light jets from W)
- p_T of lepton and b-jet from lep. top
- N_{jets}
- η had. top
- ΔR(b-jets)

Charge asymmetry: the method

- Signal and bkg from MC
  - except Multijet, measured with a data-driven Matrix Method
- Fully Bayesian Unfolding (FBU)

Process:	Resolved		Boosted	
	$1b$-excl.	$2b$-incl.	$1b$-excl	$2b$-incl.
$t\bar{t}$	1520000±120000	1840000±150000	50000± 7000	74000±10000
Single top	89000± 12000	49000± 8000	3600± 1200	3000± 1200
W + jets	200000± 23000	23000± 14000	10000± 5000	1800± 1000
$Z + VV + t\bar{t}X$	52000± 28000	15000± 8000	2600± 1300	1400± 800
Multijet	90000± 40000	47000± 23000	3000± 1500	2300± 1200
Total Prediction	1950000±200000	1980000±160000	69000±11000	83000±11000
Data (139 fb^{-1})	1945037	2009526	54710	66582

uniform prior is employed

$$p(\boldsymbol{T}|\boldsymbol{D},\mathcal{M}) \propto \mathcal{L}(\boldsymbol{D}|\boldsymbol{T},\mathcal{M}) \cdot \pi(\boldsymbol{T})$$

$$p(A_C|\boldsymbol{D}) = \int \delta(A_C - A_C(\boldsymbol{T}))\, p(\boldsymbol{T}|\boldsymbol{D},\mathcal{M})\, d\boldsymbol{T}$$

true distribution

observed data

response matrix, from MC

Systematics included as Nuisance Parameters in the Likelihood

$$\mathcal{L}(\boldsymbol{D}|\boldsymbol{T}) = \int \mathcal{L}(\boldsymbol{D}|\boldsymbol{T},\boldsymbol{\theta}) \cdot \mathcal{N}(\boldsymbol{\theta})\, d\boldsymbol{\theta}$$

marginalised likelihod

Different regions are combined simply by:

$$\mathcal{L}(\{\boldsymbol{D}_1 \cdots \boldsymbol{D}_{N_{ch}}\}|\boldsymbol{T}) = \int \prod_{i=1}^{N_{ch}} \mathcal{L}(\boldsymbol{D}_i|\boldsymbol{T};\boldsymbol{\theta}) \cdot \mathcal{N}(\boldsymbol{\theta})\, d\boldsymbol{\theta}$$

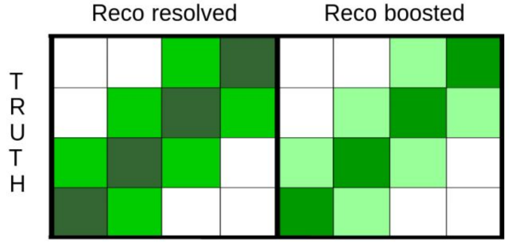

Charge asymmetry: differential measurement

Differential measurement performed vs $\beta_{ttbar,z}$ and vs m_{ttbar}

Post-marginalization plots are shown here

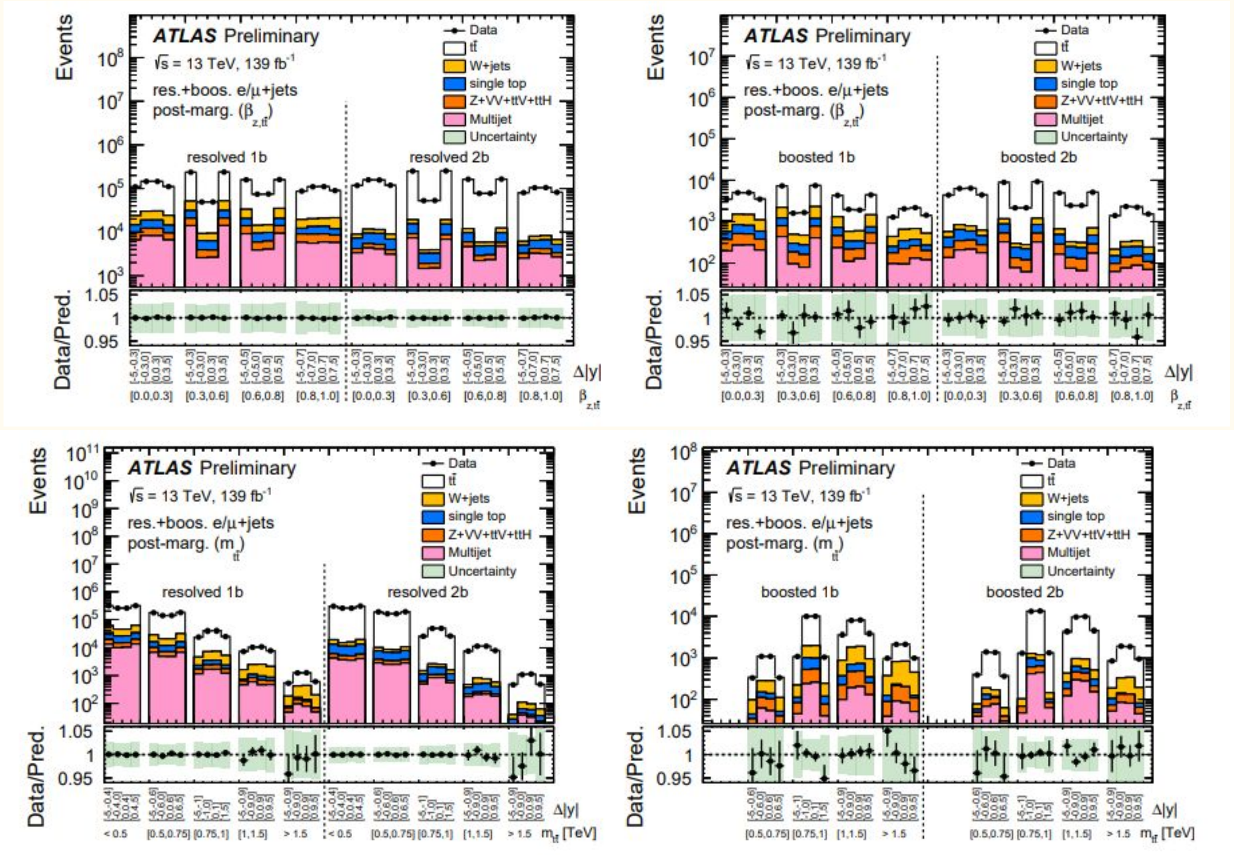

		Data 139 fb^{-1}						SM prediction
		A_C	Stat.	Syst.	MC stat.	Bias	Total unc.	
Inclusive		0.0060	0.0011	0.0009	0.0005	0.0001	0.0015	$0.0064^{+0.0005}_{-0.0006}$
$m_{t\bar{t}}$	< 500 GeV	0.0045	0.0028	0.0034	0.0013	0.0001	0.0045	$0.0055^{+0.0007}_{-0.0005}$
	500-750 GeV	0.0051	0.0020	0.0021	0.0009	<0.0001	0.0031	$0.0072^{+0.0006}_{-0.0006}$
	750-1000 GeV	0.0100	0.0049	0.0046	0.0021	0.0001	0.0070	$0.0079^{+0.0003}_{-0.0005}$
	1000-1500 GeV	0.0169	0.0072	0.0027	0.0029	0.0004	0.0083	$0.0096^{+0.0009}_{-0.0009}$
	> 1500 GeV	0.0121	0.0277	0.0150	0.0092	0.0005	0.0329	$0.0094^{+0.0015}_{-0.0011}$
$\beta_{z,t\bar{t}}$	0-0.3	0.0007	0.0040	0.0032	0.0020	0.0001	0.0055	$0.0011^{+0.0004}_{-0.0004}$
	0.3-0.6	0.0085	0.0031	0.0025	0.0013	0.0003	0.0042	$0.0023^{+0.0006}_{-0.0004}$
	0.6-0.8	0.0014	0.0029	0.0033	0.0015	0.0004	0.0047	$0.0042^{+0.0003}_{-0.0003}$
	0.8-1.0	0.0100	0.0026	0.0042	0.0013	0.0007	0.0051	$0.0146^{+0.0012}_{-0.0014}$

Table 2: Results with statistical and systematic uncertainties, including the uncertainty due to limited number of MC events (MC stat. column), uncertainty due to the unfolding bias and the total uncertainty, for the inclusive and differential A_C measurements. The total uncertainty is the sum-in-quadrature of the aforementioned uncertainties. The SM predictions are calculated at NNLO in QCD and NLO in electroweak theory [133].

Charge asymmetry: EFT interpretation

$$\mathcal{L}_{eff} = \mathcal{L}_{SM} + \frac{1}{\Lambda^2}\sum_i C_i O_i + O\left(\Lambda^{-4}\right)$$

- Dimension-6 operator with a new physics scale Λ

Phys.Rev.D83:034006,2011

$$C_u^1 = C_{qq}^{(8,1)} + C_{qq}^{(8,3)} + C_{ut}^{(8)}$$
$$C_u^2 = C_{qu}^{(1)} + C_{qt}^{(1)}$$
$$C_d^1 = C_{qq}^{(8,1)} - C_{qq}^{(8,3)} + C_{dt}^{(8)}$$
$$C_d^2 = C_{qd}^{(1)} + C_{qt}^{(1)}$$

Then

$$C_u^1 = C_d^1 = C^1$$
$$C_u^2 = C_d^2 = C^2$$

$C^+ = C^1 + C^2$ → affects cross section

$C^- = C^1 - C^2$ → affects asymmetry

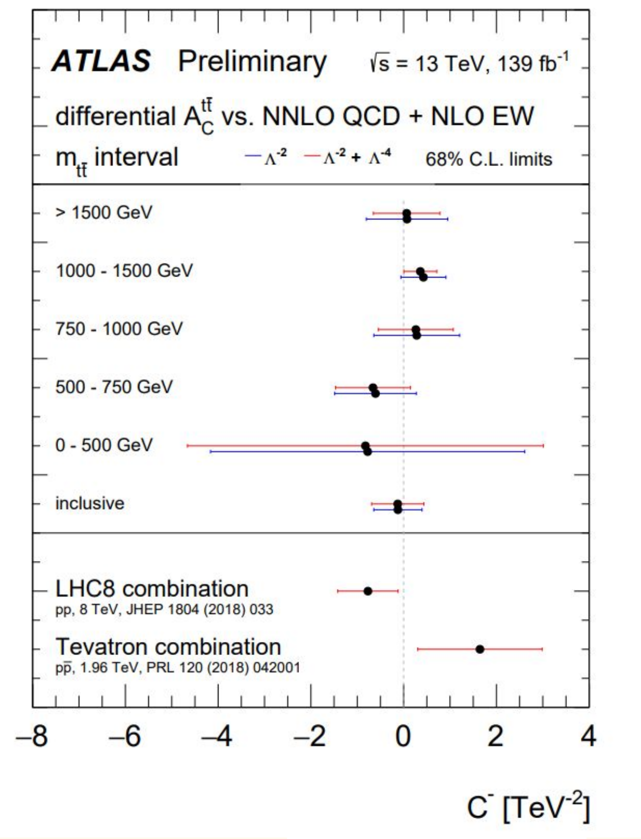

Limits on C^- can be recasted, e.g. for axigluons $C^-/\Lambda^2 = -4g_s^2/m_A^2$

Phys.Rev.D83:034006,2011

only the following four-quark operators contribute to the $u\bar{u}, d\bar{d} \to t\bar{t}$ reaction:

$$
\begin{aligned}
O_{qq}^{(8,1)} &= \tfrac{1}{4}(\bar{q}^i\gamma_\mu\lambda^A q^j)(\bar{q}\gamma^\mu\lambda^A q) & O_{qq}^{(8,3)} &= \tfrac{1}{4}(\bar{q}^i\gamma_\mu\tau^I\lambda^A q^j)(\bar{q}\gamma^\mu\tau^I\lambda^A q) \\
O_{ut}^{(8)} &= \tfrac{1}{4}(\bar{u}^i\gamma_\mu\lambda^A u^j)(\bar{t}\gamma^\mu\lambda^A t) & O_{dt}^{(8)} &= \tfrac{1}{4}(\bar{d}^i\gamma_\mu\lambda^A d^j)(\bar{t}\gamma^\mu\lambda^A t) \\
O_{qu}^{(1)} &= (\bar{q}u^i)(\bar{u}^j q) & O_{qd}^{(1)} &= (\bar{q}d^i)(\bar{d}^j q) \\
O_{qt}^{(1)} &= (\bar{q}^i t)(\bar{t}q^j)
\end{aligned}
$$

$$
\sigma_{\bar{u}u,\bar{d}d\to\bar{t}t} = \frac{g_s^4}{108\pi s}\beta(3-\beta^2) + \mathrm{Re}C_{tG}\frac{\sqrt{2}g_s^3 v}{9\pi\Lambda^2\sqrt{s}}\beta\sqrt{1-\beta^2} + (C_{u,d}^1 + C_{u,d}^2)\frac{g_s^2}{216\pi\Lambda^2}\beta(3-\beta^2)
$$

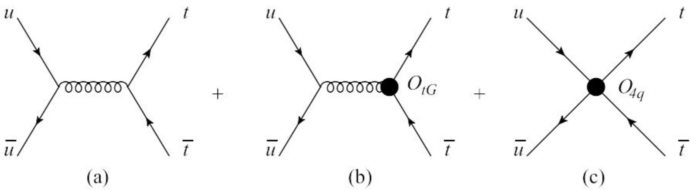

Figure 12: The Feynman diagrams for $u\bar{u} \to t\bar{t}$ process. (a) is the SM amplitude, (b) is the correction on gtt coupling induced by O_{tG}, and (c) is the four-fermion interactions. The $d\bar{d} \to t\bar{t}$ process has the same diagrams.

$$
\begin{aligned}
A_{FB}^t &= \frac{N(\cos\theta > 0) - N(\cos\theta < 0)}{N(\cos\theta > 0) + N(\cos\theta < 0)} \\
&= (C_{u,d}^1 - C_{u,d}^2)\frac{3s\beta}{4g_s^2\Lambda^2(3-\beta^2)}
\end{aligned}
$$